

SAFETY LIFE CYCLE ASSESSMENT PROGRAM

TASK 6 RAILROAD STRUCTURAL INTEGRITY CRITERIA ANALYSIS

Final Report

Prepared by
THE AEROSPACE CORPORATION
Eastern Technical Division
Development Programs Directorate
Washington, D.C.

October 1978

Prepared for
U.S. DEPARTMENT OF TRANSPORTATION
Federal Railroad Administration
Office of Rail Safety Research
Washington, D.C.

Contract No. F04701-77-C-0078

Aerospace Report No.
ATR-78(4847-11)-1ND

SAFETY LIFE CYCLE ASSESSMENT PROGRAM

TASK 6
RAILROAD STRUCTURAL
INTEGRITY CRITERIA
ANALYSIS

FINAL REPORT

Prepared by
THE AEROSPACE CORPORATION
Eastern Technical Division
Development Programs Directorate
Washington, D. C.

October 1978

Prepared for
U.S. DEPARTMENT OF TRANSPORTATION
Federal Railroad Administration
Office of Rail Safety Research
Washington, D. C.

Contract No. FO4701-77-C-0078

Report No.
ATR-78(4847-11)-1ND

SAFETY LIFE CYCLE ASSESSMENT PROGRAM

TASK 6
RAILROAD STRUCTURAL
INTEGRITY CRITERIA
ANALYSIS

Prepared by:

L. Raymond
Staff Scientist

J. D. Buch
Member Technical Staff

C. H. Zilliacus
Staff Assistant

Approved by:



W. D. Pittman
Principle Director
Development Programs Directorate



J. Meltzer
General Manager
Eastern Technical Division

FOREWORD

This report was prepared for the U.S. Department of Transportation, Federal Railroad Administration, Office of Rail Safety Research, Washington, D. C. Work was performed under Contract Number F04-701-77-C-0078 by The Aerospace Corporation in response to the requirement in the Statement of Work, Paragraph II of Modification 2 of the Safety Life-Cycle Assessment Program.

The purpose of the overall program is to perform an assessment for the applicability of current safe-life technology to railroad vehicle systems and components. The effort is divided into six primary tasks. Task 1 involves the assessment of railroad industry use of safe-life concepts. Task 2 is concerned with the development of a safety life-cycle methodology applicable to rail vehicle systems. Task 3 assesses the applicability of the Facility for Accelerated Service Testing (FAST) to the safety life-cycle program. Task 4 assesses the feasibility of a rail vehicle system validation/qualification program to improve railroad safety. Task 5 provides for project management and engineering direction of technical projects in support of overall program goals. Task 6 involves performing an analysis to develop structural integrity criteria for the safety life-cycle of rail vehicle components that are critical to safe operation.

Presented in this report is an evaluation of the structural integrity criteria for those railcar components critical to the safe service life of rolling stock. Current railroad design, testing, manufacturing, quality control, and service performance (inspection and maintenance) practices have been reviewed and compared with safe service life concepts extracted from the practices of other industries. A result of this effort is an analytical approach to the preparation of safety life-cycle prediction guidelines for side frames. The cooperation of the many railroad people contacted in generating this report is gratefully acknowledged. Special recognition is addressed to the following:

Abex Corporation, Mahwah, New Jersey

American Steel Foundries, Chicago, Illinois

Berwind Railway Service Co., Wilmington, California

Railway Educational Bureau, Omaha, Nebraska

CONTENTS

	<u>Page</u>
FOREWORD	v
1. INTRODUCTION	1-1
2. ELEMENTS OF A STRUCTURAL INTEGRITY PROGRAM	2-1
2.1 Identification of Critical Components	2-1
2.2 Design and Prototype Testing	2-5
2.3 Material Quality Control, Manufacturing, and Process Control	2-7
2.4 Service Performance	2-8
3. CURRENT RAILROAD STRUCTURAL INTEGRITY PRACTICES	3-1
3.1 Materials - General	3-1
3.2 Side Frames	3-3
3.3 Truck Bolsters	3-7
3.4 Couplers	3-11
3.5 Axles	3-14
3.6 Wheels	3-20
4. DAMAGE TOLERANCE AND FAILURE MODE ANALYSIS	4-1
4.1 Materials - General	4-1
4.2 Side Frames/Bolsters/Couplers	4-13
4.3 Axles/Springs/Center Pins	4-20
4.4 Wheels	4-22
5. SAFETY LIFE-CYCLE PREDICTION TECHNIQUES	5-1
5.1 Conventional Fatigue Analysis	5-2
5.2 Constant Amplitude SLC Analysis	5-3
5.3 Random Load Effects	5-6
6. APPLICATION OF RANDOM LOAD ANALYSIS TO A SIDE FRAME	6-1
6.1 Spectrum of Cyclic Stresses in a Side Frame	6-1
6.2 Significant Loading Parameters for Steel Castings Used for Side Frame Material	6-2
6.3 Side Frame Life Estimates	6-4
6.4 Allowable Flaw Size Requirements and Safe-Life Estimates	6-4

CONTENTS (Continued)

	<u>Page</u>
6.5 Side Frames in Test Machines	6-13
6.6 Safety Factors and Sensitivity Analysis	6-19
7. DISCUSSION	7-1
7.1 Recommended Activities	7-1
7.2 Limitations of Proposed SLC Crack Prediction Model	7-6
8. SUMMARY	8-1
8.1 Current Railroad Practices	8-1
8.2 Damage Tolerance and Failure Modes	8-2
8.3 Safety Life-Cycle Prediction	8-4
8.4 Conclusions Based on Side Frame Analysis	8-6
9. REFERENCES	9-1
APPENDIX A RANDOM LOAD DISTRIBUTION FUNCTIONS	A-1
APPENDIX B EVALUATION OF A RELATED THEORETICAL MODEL	B-1
APPENDIX C GLOSSARY OF ABBREVIATIONS AND TERMS	C-1

ILLUSTRATIONS

<u>Figure</u>		<u>Page</u>
2-1	Structural Integrity Program Elements	2-3
2-2	Components of Freight Car Truck System	2-4
2-3	Schematic Showing Relation Between "Initiation" Life and "Propagation" Life	2-9
2-4	Annual Failure Rates of Selected Components Causing Derailments From 1965 to 1974	2-10
3-1	Carbon Content of Freight Car Components	3-4
3-2	Sample FRA Periodic Inspection Checklist	3-8
4-1	Relative Location of Various Rail Vehicle Components on the Ratio Analysis Diagram	4-8
4-2	Effect of Carbon Content on Strength and Toughness of Railroad Steel Components	4-10
4-3	Potential Failure Modes of Freight Car Components at Room Temperature	4-12
4-4	Location of Railroad Steels Relative to the Fracture Toughness Technology Limit	4-12
4-5	Relative Location of Grades B and C Castings (Bolsters and Side Frames) on the Ratio Analysis Diagram at Various Temperatures	4-14
4-6	Damage Tolerance of Casting Steel Grades at Room Temperature	4-16
4-7	Relative Locations of Grades C and E Castings (Couplers) on the Ratio Analysis Diagram at Various Temperatures	4-18
4-8	Damage Tolerance of Axles, Center Pins, and Springs at Room Temperature	4-21
4-9	Relative Location of Classes, U, A, B, and C Wheel Rims on the Ratio Analysis Diagram at Various Temperatures	4-23
4-10	Damage Tolerance of Wheel Rims at Room Temperature .	4-24
5-1	Typical Fatigue Life S-N Curve Separated into Crack Initiation and Crack Propagation	5-4
5-2	Fatigue Crack Growth Data and Interpretations	5-7
5-3	Truck Bounce Load Spectra	5-17
5-4	Apparent Dependence of Load Parameter on Car Velocity for Loaded Hopper Car	5-18

ILLUSTRATIONS (Continued)

<u>Figure</u>		<u>Page</u>
5-5	Life Prediction Chart - Case I	5-23
5-6	Life Prediction Chart - Case II	5-23
5-7	Life Prediction Chart - Case III	5-24
5-8	Life Prediction Chart - Case IV	5-24
5-9	Life Prediction Chart - Case V	5-25
5-10	Life Prediction Chart - Case VI	5-25
6-1	Johnson's (1974) Side Frame Crack Growth Data versus Low Alloy Structural Steel Data	6-3
6-2	Relationships Between Initial Crack Size, Load Cycles, and Rail Miles for Nominal Toughness Conditions . . .	6-6
6-3	Relationship Between Initial Crack Size, Load Cycles, and Rail Miles for Reduced Toughness Conditions . .	6-7
6-4	Lower-Bound Probability of Detection of Failure Cracks as a Function of Crack Size	6-10
6-5	Visual Examination Limits for Crack Detection and Associated Safe Life Under Nominal Toughness Conditions	6-11
6-6	Visual Examination Limits for Crack Detection and Associated Safe Life Under Reduced Toughness Conditions	6-12
6-7	Crack Growth Response (growth to 0.5 in.) in ASF Fatigue Test for Varying Degrees of Design Conservatism	6-16
6-8	Crack Growth Response in ASF Fatigue Test for Varying Degrees of Design Conservatism	6-18
7-1	Effect of Internal Defects on Fatigue Life of an Aluminum Alloy Forged Plate	7-2

ILLUSTRATIONS (Continued)

<u>Table</u>		<u>Page</u>
2-1	Structural Integrity Documents Reviewed	2-2
3-1	Steels Used in Freight Car Components	3-2
3-2	Summary of Manufacturers' Inspection and Testing Practices for Side Frames	3-6
3-3	Summary of Manufacturers' Inspection and Testing Practices for Bolsters	3-10
3-4	Summary of Manufacturers' Inspection and Testing Practices for Couplers	3-13
3-5	Summary of Manufacturers' Inspection and Testing Practices for Axles	3-16
3-6	Test Flaw Diameters (in.) for 1-in. -Deep Flat Bottom Holes	3-17
3-7	Damage Tolerance Limits on Flaws Found in Newly Manufactured Axles, According to AAR Standard M-101	3-18
3-8	FRA and AAR Periodic Inspection Criteria for Axles . . .	3-19
3-9	Summary of Manufacturers' Inspection and Testing Practices of Wheels	3-21
3-10	Nondestructive Inspection Practices for New Wheels . . .	3-23
3-11	FRA and AAR Inspection Criteria for Wheels	3-24
4-1	Yield-Strength and Fracture-Toughness Values for Bolsters and Side Frames at Various Temperatures . .	4-3
4-2	Yield-Strength and Fracture-Toughness Values for Couplers at Various Temperatures	4-4
4-3	Yield-Strength and Fracture-Toughness Values for Wheels at Various Temperatures	4-5
4-4	Yield-Strength and Fracture-Toughness Values for Wheel Rims at Various Temperatures	4-6
5-1	Hopper Car Load Distribution Parameters	5-17
5-2	Crack Propagation Variables for Life Estimation	5-20
5-3	Structure of Variables in Life Prediction Charts	5-22
5-4	Systematic Variation of Life Prediction Factors	5-22
6-1	Estimates of Side Frame Loading	6-5
6-2	Side Frame Classifications	6-15
6-3	ASF Fatigue Test Compatibility Limits Compared to 20-Year Service Requirements	6-17

1. INTRODUCTION

The purpose of this report is to evaluate the structural integrity criteria for critical railcar components. Although the railroads do not have a formal structural integrity program like that specified by the Air Force for military aircraft (Military Standard 1530A), structural integrity criteria do exist and can be inferred from railroad practice. The railroad industry follows the standards recommended by the Association of American Railroads (AAR) for design, manufacture, materials, testing, inspection, and repair of rail vehicles. These standards extensively cover freight cars.

For this study, existing AAR documents and practices have been reviewed giving special attention to safe service life parameters such as design safety margins, damage tolerance, durability limits, component strength, and toughness. The implementation of these standards by designers, manufacturers, and inspection shops has been surveyed along with the additional safety and quality assurance practices which have evolved through years of manufacturing experience. These current railroad structural integrity practices are described in Section 3.

Safe service life concepts and practices of other industries have also been reviewed for comparison with railroad structural integrity criteria. Subjects of study were aircraft, space vehicles, wind tunnels, offshore structures, bridges, and ship hulls. Elements common to their structural integrity programs are extracted in Section 2.

The terms used in this report to describe safe-life criteria for railcar components are consistent with those applied in general industry. They have been refined to incorporate life-cycle predictions based on manufacturing, testing, and nondestructive inspection procedures. The combined inputs of Sections 2 and 3 are analyzed in Section 4 to identify testing procedures and material changes that would advance railroad structural integrity practices with respect to failure mode analysis and damage tolerance based on strength and toughness parameters.

Section 5 details an analytical approach to generate safe-life prediction guidelines that couple the degree of inspection and nondestructive test results with the remaining life-cycles for a randomly loaded structural component. Side frames are selected as a specimen example from which additional test requirements are specified to (1) obtain necessary information for safe-life predictions and (2) establish the validity of the prediction methodology.

In essence, it is concluded from this study that the railroad industry has evolved a structural integrity program that provides a relatively safe mode of transportation for freight. In many cases throughout this report, results based on fracture toughness correlations and analysis have reinforced the use of existing fracture mode and safety life-cycle criteria. The fact that the analysis is consistent with existing practice gives credence to the predicting capability of fracture mechanics technology. Now, new streamlined, lightweight, high performance design concepts can be implemented by the railroad industry without the expense and hazards of progressing through a learning curve and without any sacrifice in safety and reliability.

2. ELEMENTS OF A STRUCTURAL INTEGRITY PROGRAM

The purpose of any structural integrity program (SIP) is to ensure that the structure will perform its design function safely under various loading and environmental conditions for its expected design life. Two major considerations are (1) how will the structure respond to the failure of a component (i. e., failure mode analysis) and (2) how long will the structure continue to perform safely (i. e., safety life-cycle analysis). In order to compare the safe-life concepts of the rail industry with the structural integrity practices of other industries, design and verification documents (Table 2-1) for aircraft, space vehicles, wind tunnels, and off-shore structures were reviewed, and elements important to structural integrity analysis were extracted.

The elements of a structural integrity program can be divided into four categories:

- Critical component identification;
- Design and prototype testing;
- Materials and quality control testing combined with manufacturing and process control and component testing; and
- Service performance including periodic inspection, maintenance, and failure analysis.

A summary of the elements for a rail vehicle under each of these categories is shown for two critical systems in Figure 2-1.

2.1 IDENTIFICATION OF CRITICAL COMPONENTS

Two critical groups of freight car components are the suspension system (truck, wheels, and axles) and the draft system. (See column 1 of Figure 2-1.) The suspension system is of particular importance because its components statistically cause more failures than the car body, underframes, and draft system. The components of the suspension system are included in Figure 2-2.

Table 2-1. Structural Integrity Documents Reviewed

Reference Source	Title	Date of Publication	Other Relevant Data
U. S. Air Force	Aircraft Structural Integrity Program	August 1977	AFR 80-13/AFSC/AFLC Sup. 1
Rockwell International Space Division	Fracture Control Methods for Space Vehicles	January 1977	SD73-SH-0171-1
Journal of Engineering Materials Technology	A Procedure for Verifying the Structural Integrity of an Existing Pressurized Wind Tunnel	October 1977	NASA
Aerospace Report No. ATR-77(7627-01)-2	Verification of Structural Integrity of Existing Offshore Structure	1977	
American Bureau of Shipping	Material Guidelines to Reduce the Risk of Structural Failure in Offshore Mobile Drill Units	1978	
DET NORSKE VERITAS	Rules for the Design, Construction and Inspection of Offshore Structures	1975	
Advisory Group for Aerospace Research and Development	USAF Durability and Damage Tolerance Assessment of the F-5E/F Aircraft	September 1976	
Engineering Fracture Mechanics, V. 7	AASHTO Fracture-Toughness Requirements for Bridge Steels	1975	
Naval Engineers Journal	Structural Integrity Criteria for New Hull Materials	October 1976	

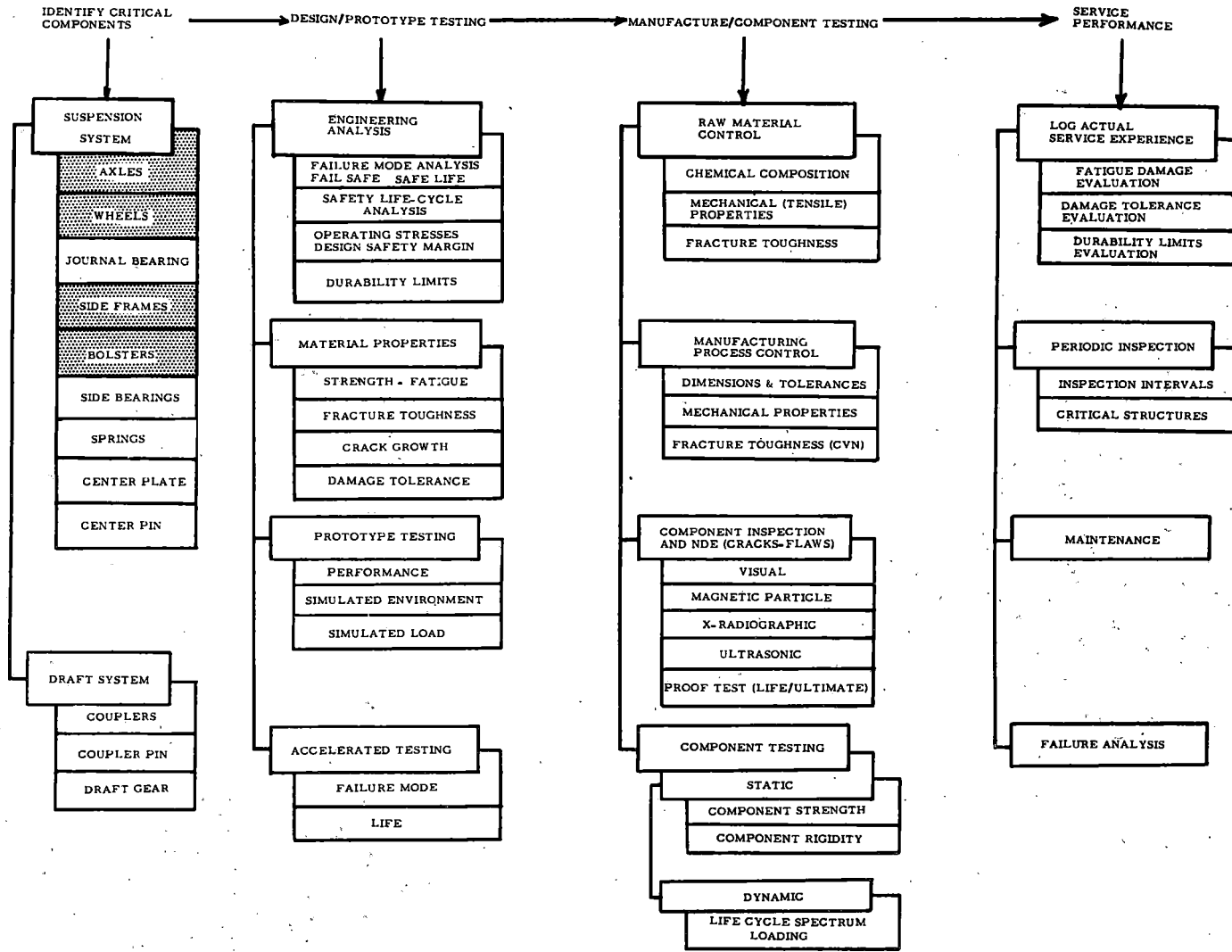
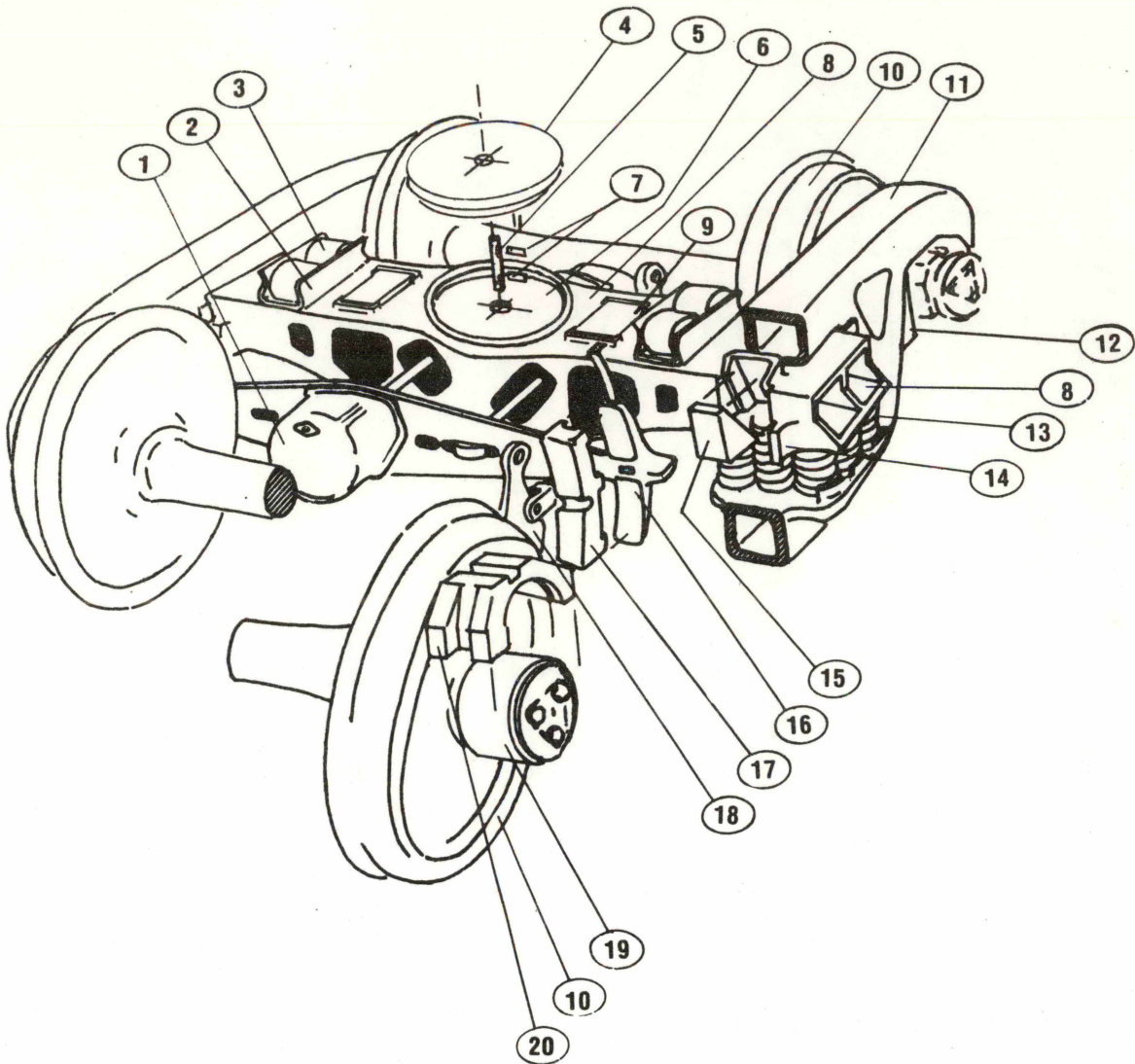


Figure 2-1. Structural Integrity Program Elements



- | | |
|------------------------------------|--|
| 1. BRAKE CYLINDER | 11. SIDE FRAME |
| 2. TRUCK SIDE BEARING ROLLER GUIDE | 12. SIDE FRAME PEDESTAL LEG |
| 3. TRUCK SIDE BEARING ROLLER | 13. DUAL RATE NESTED LOAD SPRINGS AND CUPS |
| 4. BODY CENTER PLATE | 14. SIDES FRAME GUIDE |
| 5. CENTER PIN | 15. FRICTION WEDGE |
| 6. BOLSTER BOWL | 16. BRAKE BEAM AND BRAKE SHOE LOCKING KEY |
| 7. CENTER PIN CROSS KEYS | 17. BRAKE SHOE |
| 8. BOLSTER | 18. HAND BRAKE LEVER |
| 9. CENTER PLATE EXTENSION PADS | 19. ROLLER BEARING |
| 10. WHEEL | 20. ROLLER BEARING ADAPTER |

Source: Railway Educational Bureau

Figure 2-2. Components of Freight Car Truck System

Four components of the suspension system--side frames, bolsters, wheels, and axles--are structurally critical because their failure could cause derailment. These nonredundant, primary, load carrying, safe-life structures have been selected for further discussion. Safe-life is determined by translating the number of loading cycles into time or miles for an initial defect of known size to grow to a size capable of causing a fracture. Thus, the failure prevention of these components must be controlled by inspection and maintenance at appropriate intervals.

2.2 DESIGN AND PROTOTYPE TESTING

A structural integrity program requires prototype testing and accelerated testing. A prototype design incorporates structural integrity by considering the anticipated service loads, the material response to these loads, and the consequences of partial or complete component failure. Prototype testing verifies the structural integrity of a new design by subjecting it to a real or simulated service environment. Accelerated testing involves exposing the design to loads more frequently than would be encountered in normal service. This testing technique is often applied in an effort to empirically determine useful life or eventual failure modes.

In order to be sure that a structure will perform its design function for its expected design life, it is necessary to know either the safe-life of the structure and its components or the extent of damage to the performance of the vehicle that a failure of the component would cause. These two design approaches are known as safe life and fail safe, respectively.

2.2.1 Safe-Life Design

Safe-life design is based on predicting a finite life or a specified number of applied load cycles prior to failure. The accuracy of the

analysis increases as the stresses are more accurately characterized. Reliability of the analysis is strongly dependent on the reliability of finding flaws by conventional nondestructive inspection techniques. Exact characterization of stresses and materials response is necessary to make the safe-life approach economically feasible in designing high performance structures.

The critical railroad truck components must be classified as safe-life components; in some cases the technology of safety life-cycle analysis may be a necessity as opposed to an aid to operations. Another alternative is drastic design modification that would alter these components so as to function in a fail-safe mode. The latter subject is outside the scope of this study, but should be addressed in the future.

2.2.2 Fail-Safe Design

In the fail-safe design concept, the structure is designed to last beyond the intended service life and the appropriate safeguards are incorporated into the design of the structure so that failure of a component will not endanger the remaining structure (i. e., catastrophic failure of the system does not result). Thus, the component can be replaced or repaired in an orderly manner. Redundant structures or parallel load-carrying members are considered to be fail safe when the load transfer is not severe enough to result in overload and immediate failure of the other members and subsequent failure of the system. An example of this type of design in railroad vehicles is the multiple truck spring nests.

Crack arresters are often considered an approach to fail-safe design because excessive crack growth, even initiating from a brittle fracture, is arrested before the structure fails. This technique is practical

by using side stakes in the wall studding of freight cars. When load transfer is the basis for crack arrest, the associated analysis is similar to that used for bridges, offshore platforms, pipelines, and ship hulls. Noncritical components under current design practices may not benefit significantly from safety life-cycle analysis and may best be addressed via fail-safe design concepts that utilize selective components designed to fail to prevent overload.

2.3 MATERIAL QUALITY CONTROL, MANUFACTURING, AND PROCESS CONTROL

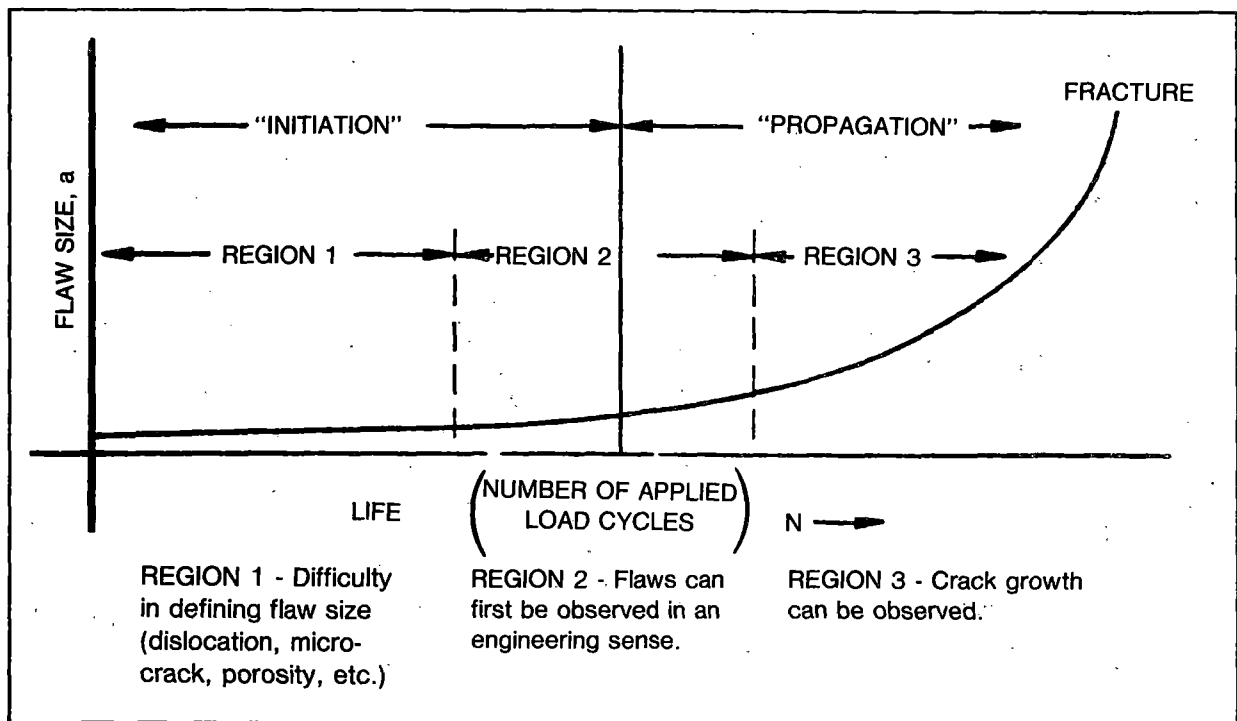
The next step in ensuring structural integrity is the control of materials and processing. The goal is to consistently guarantee that the manufactured component performs up to the expectations of the design analysis qualified by testing. Raw materials may be checked by chemical analysis and sometimes by testing the mechanical and fracture properties. The final product is measured to verify design dimensions within a predefined tolerance. The quality of the manufacturing process may also be checked by testing the mechanical properties and fracture toughness of the final product material. Final product inspection may include visual and magnetic particle inspection for surface defects, x-ray and ultrasonic inspection for internal defects, or any number of other nondestructive inspection procedures. Proof testing is performed to guarantee that cracks do not exceed a well-defined maximum initial crack size and location in the structure or component. The test consists of loading the component to the stress at which that desired maximum flaw becomes of critical size. Full-scale component testing includes static loading to ensure sufficient component strength and rigidity or dynamic loading to ensure a minimum number of loading cycles (i. e., safe life).

2.4 SERVICE PERFORMANCE

Service performance is that part of a structural integrity program that includes periodic inspection, service experience (i. e. , data tagging logistics), maintenance, and failure analysis. When safety life-cycle analysis is part of the design phase of a structural integrity program, it is typical to follow up the life-cycle prediction with periodic inspections before the predicted life is expected to expire in order to control the risk of premature failure. A measure of the safe life--often a factor of 3 or 4--is chosen as some fraction of the total calculated life. This means that a component designed (by safety life-cycle practices) to last 20 years would be inspected every 5 or 6 years. Currently, Federal Railroad Administration (FRA) periodic inspection intervals are 8 years for new freight cars and every 4 years thereafter. Such practice is consistent with normal flaw or crack behavior in engineering structures. During the initiation stage, a flaw or crack grows at a much slower rate than during the propagation stage (where flaws are large enough to be detected). Figure 2-3 schematically illustrates the delineation of the two stages.

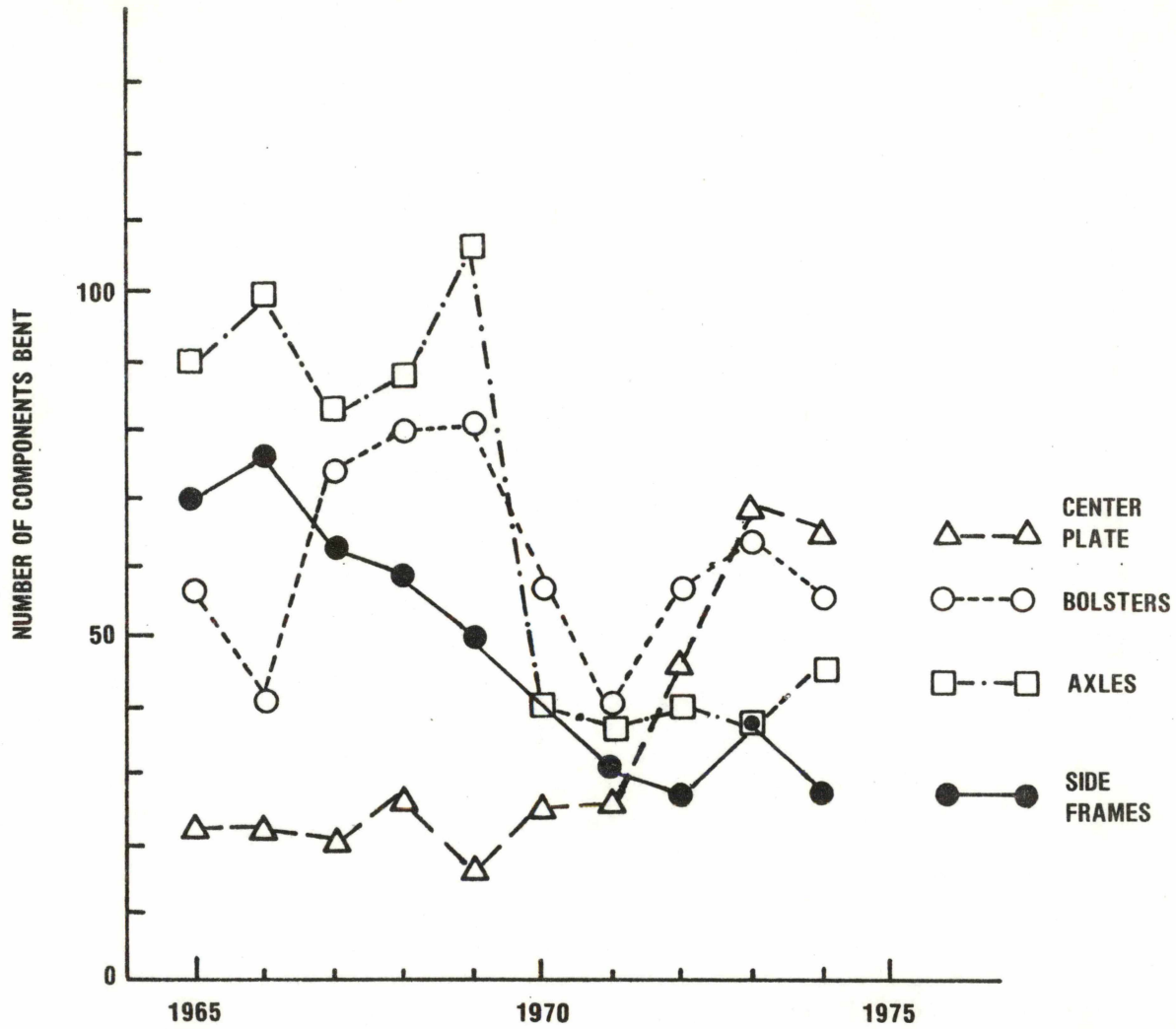
Logging service experience and failure analysis helps identify or verify deficiencies in the initial design analysis. A summary of the trends in failure rates of various freight car components during the 1965 to 1974 period is shown in Figure 2-4. Observed is the essentially constant decrease in the failure rate for side frames. This could be a result of the inclusion of a fatigue acceptance test into the specification. The bolster failure rate is erratic but can be considered constant with a large degree of scatter. Axles show an overall downward trend since the beginning of the reporting period, which could have been influenced by the incorporation of results from studies on the effect of surface finish on fatigue. The upswing in the failure rate of center plates since 1972 is notable. An attempt

should be made to understand the significance of these shifts with regard to concurrent changes in Association of American Railroad Specifications (AAR, 1976).



Source: Rolfe-Barsom, 1977.

Figure 2-3. Schematic Showing Relation Between "Initiation" Life and "Propagation" Life



Source: FRA Accident Bulletin #134-143 DOT FRA, ORS

Figure 2-4. Number of Failures of Selected Components Causing Derailments from 1965 to 1974 (approximately 3×10^9 freight car miles per year)

3. CURRENT RAILROAD STRUCTURAL INTEGRITY PRACTICES

The Association of American Railroads (AAR) is the organization primarily responsible for standardization of railroad structural integrity practices in materials selection, design, component verification testing, manufacturing, and processing controls, and service performance (including logging actual service experience, field inspection, maintenance, and failure data. In this section, current practices are reviewed for the purpose of identifying those related to the structural integrity program elements identified in Figure 2-1. Critical components of the suspension system are the main area of concentration. Structural integrity practices for couplers are included for comparison because they are a data source for casting Grade C steel which is also used for bolsters and side frames.

Rather than include a "Materials" section for each component, Section 3.1 deals with the subject of railcar steels in general--their carbon content, heat treatment, and forming methods. Sections 3.2 through 3.6 detail structural integrity practices for the critical components of the suspension system (and couplers) under the headings of Design Prototype Testing, Component Testing, Manufacturing and Processing Quality Control and Service Performance/Inspection:

3.1 MATERIALS - GENERAL

The freight car suspension system and draft system use only a limited number of the available grades of steels described in the AAR Standards. Table 3-1 summarizes the steels currently in use for each of the components. They are plain carbon steels (strength and hardness essentially increase with increasing carbon content). Each component is composed of a different grade of steel except for side frames, bolsters, and couplers, which use casting grade C. Wheels may also be cast but they are composed of higher carbon steels.

Table 3-1. Steels Used in Freight Car Components

STEEL COMPONENT	RAILWAY FORGING AAR STEEL GRADES														A X L E	AAR STEEL WHEEL CLASSES				CASTING STEEL AAR GRADE					M 1 1 8	A S T M A 36	M 1 1 4	A I S I 1020
	CARBON							ALLOY								U	U	A	B	C	L	A	B	C				
A	B	C	D	E	F	G	H	A	B	C	D	E	F	U	U										A	B	C	L
AXLES						2								1														
WHEELS															1			3										
BOLSTERS																			1	3								
SIDE FRAMES																			1	3								
COUPLER BODY AND KNUCKLE																				1			3					
COUPLER PINS																												
BODY CENTER PLATE																												
SPRINGS																												
CENTER PINS																												

- 1 - USED IN FREIGHT CARS UP TO 70-TON CAPACITY
- 2 - USED IN HIGH CAPACITY FREIGHT CARS (100 ton and greater)
- 3 - USED IN HIGH CAPACITY FREIGHT CARS ON CUSTOMER REQUEST

In Figure 3-1, the components have been rearranged according to their increasing carbon content. The general classification shows the low-carbon steels (less than 0.25 w/o) for body center plates and center pins; the 0.25 to 0.35 w/o C steels for castings in bolsters, side frames, and couplers; the 0.40 to 0.60 w/o C steels for forged axles and coupler pins; the 0.6 to 0.85 w/o C cast or wrought grade steels for wheels (with the exception of U-1 class which is about 1.0 w/o C); and the high-carbon, extruded 0.9⁺ w/o C steels used for springs. The hardness can be further increased by heat treatments, as in the case of wheels, where the microstructure is transformed to martensite by quenching. As the strength and carbon content increase, the fracture resistance or toughness generally decreases.

3.2 SIDE FRAMES

3.2.1 Design/Prototype Testing

Design and prototype testing of side frames is left essentially to the manufacturer; the only requirements are for specific dimensions and an acceptance test of the finished component. The dimensional restrictions are such that the side frame can interface with the remainder of the truck (AAR Manual of Standards and Recommended Practices, 1977, Sec. D.).

In order for side frames to be interchangeable, the manufacturer must perform not only a static design analysis as previously described (The Aerospace Corporation, 1977) but also a dynamic analysis. In addition to being loaded vertically as a three-point member, the side frame is loaded dynamically such that it experiences lateral (transverse) and longitudinal loads. Dynamic longitudinal loads are delivered to the side frame columns by the bolster and to the pedestal from the journal bearing adapter. Lateral load is applied between the side frame columns

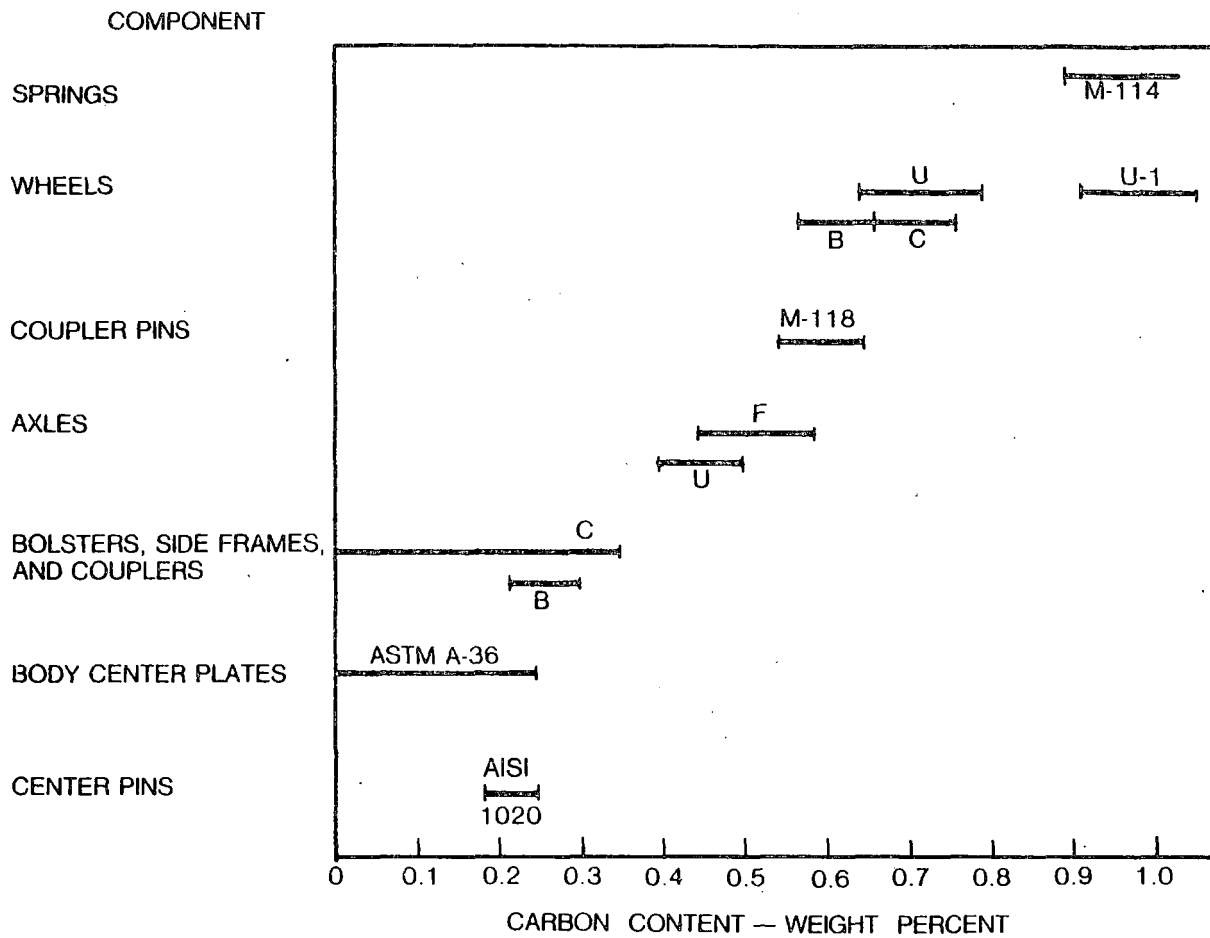


Figure 3-1. Carbon Content of Freight Car Components

and the roller bearing adapter when the car traverses curved track. The side frame also twists horizontally relative to the bolster during negotiation of curved track or truck hunting.

3.2.2 Component Testing - Side Frames

The dynamic tests are performed by fatigue testing four representative side frames from each new design, as summarized in Table 3-2. To pass the test, a side frame must not develop a critical size crack before a minimum number of cycles at a given load. (A more detailed description of these component tests is given by The Aerospace Corporation (1977) in Task 1 Technology Assessment Report.) Manufacturers' inspection and testing practices for side frames are summarized in Table 3-2.

3.2.3 Manufacturing and Processing Quality Control - Side Frames

Once the new design has successfully passed the component tests, the materials are subjected to quality control (QC) tests to ensure product reliability. AAR recommends chemical composition by ladle analysis and tensile tests. In addition, the grade C casting steel must not exceed hardenability as determined in a Jominy test of 40 Rockwell "C" at 10/16 in. The final inspection involves nondestructive testing to ensure that the quality of the frame meets the standards set by the specimens that passed the component tests.

Tests made after inspection to ensure the quality of the manufactured component include coupon testing in order to obtain the material properties after processing and testing of the entire component. The only component inspection that the manufacturer is required to perform on the side frame under AAR standards is visual inspection for "injurious defects." Some manufacturers also make use of magnetic particle and x-ray inspection to determine the quality of new designs or critical regions of the casting.

Table 3-2. Summary of Manufacturers' Inspection and Testing Practices for Side Frames

TEST	GRADE B	GRADE C	TEST FREQUENCY	TEST SPECIMEN
CHEMICAL COMPOSITION			EACH HEAT	LADLE ANALYSIS
TENSION			NOT SPECIFIED	
HARDNESS		HARDENABILITY	NOT SPECIFIED	JOMINY TEST SPECIMEN
FRACTURE TOUGHNESS				
MICROSTRUCTURE EXAMINATION				
VISUAL SURFACE INSPECTION			EACH SIDE FRAME	SIDE FRAME
MAGNETIC PARTICLE INSPECTION			OCCASIONALLY	CERTAIN REGIONS ON SIDE FRAME
ULTRASONIC INSPECTION				
X-RAY INSPECTION			OCCASIONALLY	SIDE FRAME: NEW DESIGN OR DUBIOUS REGION OF CASTING
STATIC (rigidity)			2 SPECIMENS PER NEW DESIGN	SIDE FRAME
DYNAMIC (SLC)			4 SPECIMENS PER NEW DESIGN	SIDE FRAME

3.2.4 Service Performance/Inspection - Side Frames

Inspection and repair standards are described in the Field Manual of the AAR Interchange Rules (AAR, 1977). In order to ensure safe operation of freight cars in service, FRA requires that a typical freight car (i. e., one that is not subjected to high utilization) be inspected 8 years after construction or reconditioning and every 4 years thereafter. Periodic inspection, which consists of examination of the wheels, axles, bearings, adapters, truck components, draft systems, couplers, center sill, body bolsters, and body center plate, is done visually and with gages. An example of an FRA periodic inspection checklist is shown in Figure 3-2.

The Field Manual defines damage and wear limits for components as well as rules for repair. All cracks detected in side frames must be either weld repaired and stress relieved by heat treatment or scrapped. Welding is permitted only in noncritical regions (e. g., side frame columns and journal boxes). Worn areas may be built up, but no post heat treatment is allowed on them. Neither welding nor building is permitted where the original section has been reduced more than 40 percent by cracks or wear.

3.3 TRUCK BOLSTERS

3.3.1 Design/Prototype Testing

Limiting design dimensions for truck bolsters are given in Section D of the AAR Manual of Standards and Recommended Practices (1977). Actual design and prototype testing is left to the manufacturer. A wide variety of static and dynamic service loads is imposed on the truck bolster and must be considered in design. The bolster is subjected to static vertical loads from the weight of the car as it is applied to the center plate.

Car Int. & No. _____ Type of Car _____	Final Inspector _____ Class of Car _____																								
<u>COUPLER "E" TYPE</u>	<u>UNCOUPLING DEVICE</u>																								
1. Shank BT More Than 9/16" _____ 2. Shank Worn More Than 7/16" _____ 3. Contour More Than 5 5/16" _____ 4. Crack or Break _____ 5. Grade B (Remove & Inspect) _____	1. Vertical & Lateral Movement _____ 2. Clearance between Rod Eye & Lock Lift (1/4" Min.) _____																								
<u>COUPLER "F" TYPE</u>	<u>DRAFT SYSTEM</u>																								
1. Shank Worn More Than 7/16" _____ 2. Contour More Than 3 13/16" _____ 3. Interlocking Surface _____ 4. Mfgr. Prior to 3/70 (Remove & Inspect) _____	1. Yoke Bro. _____ 2. Yoke Strap Worn More Than 25% _____ 3. Draft Key Worn More Than 25% _____ 4. Cushioning Device Def. _____																								
<u>COUPLERS "E" OR "F"</u>	<u>CAR BODY</u>																								
1. Lock Lift Inop. _____ 2. No Anticreep _____ 3. Lock Def. _____ 4. Knuckle Down _____ 5. Knuckle Cracked or Broken _____ 6. Knuckle Pin Bro. _____ 7. Thrower Miss. or Inop _____ 8. Excessive Free Slack (1" or More) _____	1. Clearance Above Rail Less Than 2 1/2" _____ 2. Center Plate Engagement Less Than 1" _____ 3. Center Plate Loose or Broken _____ 4. Center Sill Bro., Cracked or Bent _____ 5. Coupler Carrier Bro. or Missing _____ 6. Body Bolster, Cross Bearer or Sidesill Bro. _____																								
<u>TRUCKS & COMPONENTS</u>	<u>WHEELS & WHEEL ASSEMBLY</u>																								
1. Side Frame Bro., Patched, Cracked, Worn, Cast Date or Patt. No. _____ 2. Bolster Bro., Patched, Cracked, Painted, Worn, Cast Date or Patt. No. _____ 3. Any Part Less than 2 1/2" Above Top of Rail _____ 4. Side Brg. Bro. or Miss. _____ 5. Side Bearing Clearance _____ 6. Springs or Snubbers Bro. W.O. or Miss. _____ 7. Spring Planks, Bro., Missing or Worn _____	1. Thin Flange _____ 2. Vertical Flange _____ 3. High Flange _____ 4. Rim Thickness _____ 5. Rim, Flange Plate or Hub Cracked or bro. _____ 6. Shelled Tread _____ 7. Slid Flat _____ 8. Hole in Plate _____ 9. Groove Tread _____ 10. Scrape, Dent, or Gouge in Wheel Plate _____ 11. Loose Wheel _____ 12. Welding on Wheel _____ 13. Wheel Overheated _____ 14. Wheel Painted _____ 15. Wheel Assy. Out of Gage _____																								
<u>AXLES</u>	<u>ROLLER BEARING</u>																								
1. Axle Bent, Bro. or Cracked _____ 2. Scrape, Dent or Gouge Between Wheels 1/8" or More _____ 3. Welding on Axle _____ 4. Axle Painted _____ 5. Journals Worn Beyond Acceptable Limits _____ 6. Journal Collar Bro. _____ 7. Journal Surface Defective _____	1. Derailed _____ 2. Submerged in Water _____ 3. Overheated _____ 4. Cap Screw Lock Bro., Loose or Missing _____ 5. Cap Screw Lock Bro., Loose or Missing _____ 6. Frame Key, Loose or Miss. _____ 7. Seal, Loose or Defective _____ 8. Adapter, Worn, Bro., Cracked, Bent or Missing _____																								
<u>PLAIN JOURNAL BOXES</u>	<u>Stenciling on Car When Released:</u>																								
1. No Free Oil _____ 2. Box Lid Bro., Bent or Missing _____ 3. Contains Foreign Matter _____ 4. Holes or Crack in Box _____ 5. Lube Pad Miss. or Defective _____ 6. Journal Brass Bro., Worn, or Missing _____ 7. Journal Wedge Bro., Bent, Worn or Missing _____ 8. Journal Stops, Bro., or Missing Where Equip. _____	<table style="width: 100%; border-collapse: collapse;"> <tr> <td style="width: 33%; text-align: center;">Blt.</td> <td style="width: 33%; text-align: center;">RCD</td> <td style="width: 33%; text-align: center;">Insp.</td> </tr> <tr> <td>_____</td> <td>_____</td> <td>_____</td> </tr> <tr> <td>_____</td> <td>_____</td> <td>_____</td> </tr> <tr> <td>_____</td> <td>_____</td> <td>_____</td> </tr> <tr> <td style="text-align: center;">COTS</td> <td style="text-align: center;">RPKD</td> <td style="text-align: center;">LUB</td> <td style="text-align: center;">IDT</td> </tr> <tr> <td>_____</td> <td>_____</td> <td>_____</td> <td>_____</td> </tr> <tr> <td>_____</td> <td>_____</td> <td>_____</td> <td>_____</td> </tr> </table>	Blt.	RCD	Insp.	_____	_____	_____	_____	_____	_____	_____	_____	_____	COTS	RPKD	LUB	IDT	_____	_____	_____	_____	_____	_____	_____	_____
Blt.	RCD	Insp.																							
_____	_____	_____																							
_____	_____	_____																							
_____	_____	_____																							
COTS	RPKD	LUB	IDT																						
_____	_____	_____	_____																						
_____	_____	_____	_____																						

Source: Berwind Railway Service Co., Wilmington, California

Figure 3-2. Sample FRA Periodic Inspection Checklist

The bolster is supported by the springs on the side frame. In motion, some of the weight may be shifted from the center plate to the side bearings. Braking and inertial forces, especially from high-speed coupling of empty cars, result in longitudinal loading at the bolster bowl rim from the body center plate and where the side frame columns meet the bolster. Horizontal twisting of the bolster relative to the side frame can also occur when the truck negotiates curved track.

3.3.2 Component Test - Bolster

The only required component test for a bolster is a static test. Manufacturers are required under AAR Standard M-202 to test two representative truck bolsters from each new design under static loading conditions. This test involves one transverse loading and two vertical loading tests. The vertical loads are applied separately, first at the side bearing and then at the center plate. To pass the static tests, the bolster must be able to carry the test load without exceeding deflection and permanent set limits. Inspection and test practices for truck bolsters, as shown in Table 3-3, do not include dynamic component tests on bolsters, but as of this writing, an AAR Recommended Practice is being developed.

3.3.3 Manufacturing and Processing Quality Control - Bolsters

Truck bolsters are large castings of the same material as side frames and therefore are subjected to the same QC tests of chemical composition by ladle analysis, tensile tests, and hardenability. Only visual inspection for injurious defects is required on each bolster. Manufacturers, however, supplement these inspection practices for special cases. Examples of additional inspection procedures are magnetic particle and

Table 3-3. Summary of Manufacturers' Inspection and Testing Practices for Bolsters

TEST	GRADE B	GRADE C	TEST FREQUENCY	TEST SPECIMEN
CHEMICAL COMPOSITION			EACH HEAT	LADLE ANALYSIS
TENSION			NOT SPECIFIED	
HARDNESS		HARDENABILITY	NOT SPECIFIED	JOMINY TEST SPECIMEN
FRACTURE TOUGHNESS				
MICROSTRUCTURE EXAMINATION				
VISUAL SURFACE INSPECTION			EACH BOLSTER	BOLSTER
MAGNETIC PARTICLE INSPECTION			OCCASIONALLY	CERTAIN REGIONS ON BOLSTER
ULTRASONIC INSPECTION				
X-RAY INSPECTION			OCCASIONALLY	BOLSTER: NEW DESIGN OR DUBIOUS REGION OF CASTING
STATIC (rigidity)			2 SPECIMENS PER NEW DESIGN	BOLSTER
DYNAMIC (SLC)				

x-ray inspection of critical regions of bolsters (e.g., those near the center where maximum bending moment occurs) to ensure surface and internal quality.

3.3.4 Service Performance/Inspection - Bolsters

Bolsters are inspected visually and with gages during FRA periodic inspections. AAR wear gages precisely define wear limits of truck bolsters, but the Field Manual does not explicitly define the size, geometry, and location of those cracks which are allowed to remain unrepaired in bolsters. As with side frames, it is stated that broken or cracked bolsters must be either scrapped or weld repaired and that cracking which reduces any section by more than 40 percent cannot be welded. Inspectors at Berwind Railway Service indicated that identification of critical cracks and flaws is largely a matter of the inspector's experience and judgment.

3.4 COUPLERS

3.4.1 Design/Prototype Testing - Couplers

AAR has established design standards for couplers. Freight cars employ only AAR coupler types E, F, and E/F. Manufacturers' design variations on each coupler type are subjected to AAR approval. Each accepted design is classified by a catalog number. Dimensional restrictions for individual designs of a given AAR coupler type are fairly well constrained in order to ensure proper fitting, interchangeability, and correct coupler operation.

Couplers experience relatively low vertical loads in service. They are loaded longitudinally during periods of freight car acceleration and deceleration. Rapid acceleration and deceleration (such as that which occurs in high-speed coupling of cars in the hump yard) results in severe impact loading of couplers.

3.4.2 Component Testing - Couplers

Full-scale static testing of newly manufactured coupler bodies and knuckles is required no less than once per year per design group and frequently more often. The manufacturer must test the component statically to establish its conformance with maximum permanent set and minimum ultimate strength requirements.

3.4.3 Manufacturing and Processing Quality Control - Couplers

The static tension test serves as a periodic check of casting integrity. Materials for the casting are also subjected to the quality control tests shown in Table 3-4. AAR manufacturing standards require chemical composition control by ladle analysis and mechanical properties as determined in tensile tests. Grade C casting steel must not exceed hardenability as determined in a Jominy Test of 40 Rockwell "C" at 10/16 in. Grade E steel must produce the minimum hardness at 7/16 in. in the standard Jominy Test.

Unlike the truck components, coupler steel must possess minimum impact properties determined by testing standard (ASTM-A370) Charpy-V-notch Type "A" Specimens. Impact specimens of grades C and E casting steel must absorb a minimum of 15-ft-lb energy at 0° and -40°F, respectively (AAR Standard M-211).

Couplers, like truck castings, are occasionally subjected to magnetic particle and x-ray inspection. X-radiography helps detect internal casting flaws and magnetic particle inspection augments the universally practiced visual surface inspection. Visual inspection criteria are rather detailed. Defects in critical areas of the coupler are not permitted. Surface discontinuities outside the critical areas are repaired or permitted

Table 3-4. Summary of Manufacturers' Inspection and Testing Practices for Couplers

TEST	GRADE C	GRADE E	TEST FREQUENCY	TEST SPECIMEN
CHEMICAL COMPOSITION			EACH HEAT	LADLE ANALYSIS
TENSION			ONE PER EACH SIDE OF CASTING PER HEAT	TENSION TEST SPECIMEN FROM TEST COUPONS INTEGRALLY OR CAST FROM KEEL BLOCKS
HARDNESS	(HARDENABILITY)		ONCE PER GRADE STEEL EVERY 3 MONTHS	JOMINY TEST SPECIMEN
FRACTURE TOUGHNESS	15 ft-lb REQUIRED CVN AT GIVEN TEMPERATURE		ONCE PER 2 WEEKS PRODUCTION OR 50 HEATS PER GRADE STEEL	CVN TYPE A AS PICTURED IN FIGURE 11, ASTM 370
MICROSTRUCTURE EXAMINATION				
VISUAL SURFACE INSPECTION			EACH COUPLER	COUPLER
MAGNETIC PARTICLE INSPECTION			OCCASIONALLY	CERTAIN AREAS OF COUPLER
ULTRASONIC INSPECTION				
X-RAY INSPECTION			OCCASIONALLY	COUPLER: NEW DESIGN OR PROBLEM AREA
STATIC (rigidity)	TENSILE: PERMANENT SET, ULTIMATE STRENGTH		ONCE PER 5000 E AND 5000 F COUPLERS OR ONCE EVERY 3 TO 6 MON	KNUCKLE AND BODY
DYNAMIC (SLC)				

according to their length and depth. Those greater in depth than 10 percent of the section thickness and those located on gaged surfaces must be weld repaired.

3.4.4 Service Performance/Inspection - Couplers

Current coupler service inspection practices are governed by AAR interchange rules. Wear limits are carefully defined for couplers (as they are for the other freight car components). Any cracks in critical areas condemn the coupler. Weld repair of the coupler body, knuckle, or knuckle lock is permitted under the conditions described in AAR Standard M-212.

3.5 AXLES

3.5.1 Design/Prototype Testing

Dimensional requirements for axle design are given in Section D of the AAR Manual of Standards and Recommended Practices (1977). These requirements are based on limitations in allowable stress values that reflect extensive fatigue tests. The static weight of the car is transferred to the axle journals through the bearings. This load is transferred to the wheels so that the axle is essentially loaded in four-point bending. The resultant bending moment produces tensile stresses along the upper side and compressive stresses on the lower side of axle which occur in cycles as the axle rotates. Lateral loads on the wheels are transferred to the axle as a bending moment. Longitudinal loads occur when the wheel slips on the rail as the wheel traverses curved track, resulting in a torque applied to the axle.

3.5.2 Component Testing - Axles

AAR conducted extensive fatigue testing of axles to establish maximum allowable design stress levels, although current recommended practices specify no dynamic (fatigue) or static full-scale component tests other than a drop test for Grade U axles (Table 3-5). The drop test involves two rotations of the axle and reduces to a destructive test for establishing the defect quality of the axle.

3.5.3 Manufacturing and Processing Quality Control - Axles

Freight car axles are carbon steel forgings and may be either heat treated (Grade F) or nonheat treated (Grade U). AAR standards require ladle analysis to control chemical composition during manufacture. Tensile testing is required only of the heat treated axles, and a drop test is only required of a specified number of untreated axles (i. e., the drop test on the axle is used to replace the small coupon tensile test on the heat treated axle).

Quality control tests and inspection procedures practiced by axle manufacturers are summarized in Table 3-5. AAR Standard M-101 for freight car axles describes two types of inspections for detecting flaws in newly manufactured axles: ultrasonic inspection and visual surface inspection.

The manufacturer is not required to inspect axles ultrasonically, but some (like United States Steel Corporation) do. The AAR recommends that internal flaws that cause instrument indications greater than those caused by the following "test flaws" be cause for rejection of an axle. A test flaw is a flat bottom hole, 1-in. deep, with diameters at distances from the transducer as shown in Table 3-6.

Table 3-5. Summary of Manufacturers' Inspection and Testing Practices for Axles

TEST	GRADE U	GRADE F	TEST FREQUENCY	TEST SPECIMEN
CHEMICAL COMPOSITION			EACH HEAT	LADLE ANALYSIS
TENSION	AXLE (DROP TEST) 1/SIZE CLASS/HEAT		5% OF AXLES PER SIZE CLASS PER HEAT	TENSION TEST SPECIMEN FROM AXLE OR TEST PROLONGATION
HARDNESS				
FRACTURE TOUGHNESS				
MICROSTRUCTURE EXAMINATION			ONE PER SIZE CLASS PER HEAT	UNDISTORTED PORTION OF TENSION TEST SPECIMEN
VISUAL SURFACE INSPECTION			EACH AXLE	AXLE
MAGNETIC PARTICLE INSPECTION				
ULTRASONIC INSPECTION			EACH AXLE	AXLE
X-RAY INSPECTION				
STATIC (rigidity)				
DYNAMIC (SLC)				

Table 3-6. Test Flaw Diameters (in.) for
1-in.-Deep Flat Bottom Holes

Grade	Distance Away From Transducer (in.)		
	Up to 15	15 to 30	30 to midlength
F	1/8 in. dia.	1/4 in. dia.	3/8 in. dia.
U	1/4 in. dia.	3/8 in. dia.	3/4 in. dia.

Visual surface inspection of each axle is required of the manufacturer. The purchaser has the right to reject any axle with injurious defects (Table 3-7). Among those defects which are considered injurious are any "discontinuities" (cracks, hairlines, stringers, or fine seams) with circumferential orientation and any discontinuities in the axle fillets. Longitudinal flaws must not exceed a specified maximum length (e.g., 1/2 in.) or cumulative length in a given region of the axle.

3.5.4 Service Performance/Inspection - Axles

Axles on freight cars in service are inspected for journal wear and general damage of the journal or the axle body. Scratches or scrapes or grooves less than 1/8-in. deep must be ground out to a smooth contour. Scratches between the wheel seats deeper than 1/8-in. may not be ground out; the axle is immediately condemned. These scratches are located by eye during inspection. Most field inspection shops do not utilize ultrasonic inspection or dye penetrants to detect flaws. Axles with any visible cracks must be removed from service, as must axles that have any dents or scratches that indicate that impact has occurred. According to Berwind Railway Services, if flaws detected on the axle journal cannot be removed with a nonabrasive cloth, the axle is defective. Rusted, pitted, broken, or scratched journals or fillets and overheated journals are cause for removal of the axle as are seams and flaws detected during ultrasonic inspection. No weld repair is permitted on axles. Journal wear limits are quantitatively defined in Rule 42 of the Field Manual. AAR and FRA Service Inspection Criteria are summarized in Table 3-8, which is consistent with the periodic inspection checklist shown in Figure 3-2.

Table 3-7. Damage Tolerance Limits on Flaws Found in Newly Manufactured Axles, According to AAR Standard M-101.

INDIVIDUAL FLAWS

Circumferential Seam or Crack -- None

Longitudinal Discontinuities
(Hairline, Stringer, or Fine Seam)

- Fillets -- None
- Axle Body (Between Wheel Seats) -- 1/2 in.
- Journal, Roller Bearing Axle -- 3/4 in.
- Dust Guard, Roller Bearing Axle -- 1/2 in.
- Wheel Seat -- 2 in.

COLLECTIVE TOTAL OF SMALL FLAWS
(1/4 in. < Small < Limit)

Longitudinal Discontinuities

- Axle Body -- 1-1/2 in. in 2 in. of Body Length
- Journal, Plain Bearing -- 1-1/2 in. in Any One End of Axle
- Journal, Roller Bearing -- 2 in. in Any One End of Axle
- Wheel Seat -- 4 in. in One End of Axle

Table 3-8. FRA and AAR Periodic Inspection Criteria for Axles

AXLES ARE DEFECTIVE WHEN	FRA	AAR
<u>All Axles</u>	<u>Subpart D:</u> <u>Section 215.53:</u>	<u>Rule 42 and 43</u> <u>Section A:</u>
Broken or cracked	a	2a
Damage between wheel seats 1/8 in. or deeper scrapes, dent, or gouge	b	2b
Scrapes (1/8 in.) between wheel seats must be ground out to smooth contour		<u>Section C: 2</u>
<u>Welded</u>	c	<u>Section D: 2e</u>
Bent (FRA-producing a runout of more than 3/8 in. at center of axle)	d	1e
Painted (AAR-coated) to conceal defects	f	<u>Section E: 6</u>
<u>Plain Bearing Axles</u>		<u>Rule 42</u>
Worn beyond designated journal wear limits	e	3a
Break in journal collar	<u>Section 215.55:</u> a	3a
Journal overheated	b	1d
Journal (FRA-or fillet) rusted or pitted	b	pg. 208, 3f; pg. 209, 1b&c
Journal or fillet surface	b	
Ridge, Scratch	b	
Depression	b	
Circumferential Score	b	
Corrugation	b	
Journal or fillet seamy (any flaws detected by ultrasonic inspection optional)		b;d
Fillet at back end of journal exceeds wear limits		2e
Seams or flaws detected by ultrasonic device		2e
Wrong size axle (not standard to car)		2f
<u>Roller Bearing Axles</u>		<u>Rule 43</u>
Worn beyond designated journal wear limits		<u>Section A</u> 1
Journal seamy		pg. 218
Journal rusted or pitted due to flood damage		pg. 215, 1.a
Journal overheated		2c, 1b
Fillets at back of journal under limits		pg. 218
Seams or flaws detected by ultrasonic device		pg. 218
Wrong size axle - not standard to car		2d

3.6 WHEELS

3.6.1 Design/Prototype Testing

Wheel designs must conform to dimensional requirements given in Section G of the AAR Manual of Standards and Recommended Practices (1977). The wheel load environment is highly complex and consists of thermal as well as mechanical loading. The main load to the wheel is vertical. The eight car wheels support the weight of the entire car on the rails. This load is applied between the wheel seat and the wheel rim-rail contact point resulting in high stresses. The wheel/rail contact and wheel/plate stress patterns are repeated with each wheel revolution. Lateral loads are due to flange contact with the rail during truck hunting and negotiation of curved track.

Thermal loading of the wheels is the result of friction energy absorption by the wheel tread during braking. This local heating at the tread causes expansion of the rim relative to the plate and tensile stresses and bending moments in regions of the plate. When the heated wheel cools, the rim shrinks causing circumferential tensile stresses in the rim.

3.6.2 Component Testing - Wheels

As summarized in Table 3-9, no full-scale component tests are required on wheels, either static or dynamic.

3.6.3 Manufacturing and Processing Quality Control - Wheels

Railroad wheels are cast or wrought carbon steel whose chemical composition is controlled by ladle analysis and Brinell hardness testing of the wheel rim.

Nondestructive inspection requirements are more stringent for wheels than for truck castings. Ultrasonic inspection, a means of detecting internal flaws, is required by AAR Standards M-107 and M-208 of all

Table 3-9. Summary of Manufacturers' Inspection and Testing Practices for Wheels

TEST	U	B	C	TEST FREQUENCY	TEST SPECIMEN
CHEMICAL COMPOSITION				EACH HEAT	LADLE ANALYSIS
TENSION					
HARDNESS				EACH WHEEL	WHEEL, ON RIM
FRACTURE TOUGHNESS					
MICROSTRUCTURE EXAMINATION					
VISUAL SURFACE INSPECTION				EACH WHEEL	WHEEL
MAGNETIC PARTICLE INSPECTION				EACH WHEEL	WHEEL
ULTRASONIC INSPECTION				EACH WHEEL	WHEEL
X-RAY INSPECTION					
STATIC (rigidity)					
DYNAMIC (SLC)					

wheels. Magnetic particle inspection, to detect surface flaws, is practiced by most manufacturers to augment the already required visual inspection. The required sensitivities of these inspection methods are given in Table 3-10, which summarizes the manufacturers' inspection and testing practices for wheels.

3.6.4 Service Performance/Inspection - Wheels

The inspection of wheels in service involves the extensive application of wear gages as well as visual inspection. Condemning wear limits for wheels are thoroughly defined in Rule 41 of the AAR Field Manual of the AAR Interchange Rules (1977). Cracks may not be repaired by welding. AAR and FRA inspection criteria for wheels are summarized in Table 3-11. The correspondence between this table and the periodic checklist is readily noted in Figure 3-2.

Table 3-10. Nondestructive Inspection Practices for New Wheels

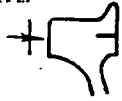
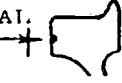
TEST	FREQUENCY	CAUSE FOR REJECTION			COMMENTS	
Ultrasonic Inspection	All wheels After Manuf.	Flaw indication greater than or equal to that from Reference Discontinuity.			Required of Manufacturer By AAR M-107, 208	
		Reference Discontinuities:				
		Flat Bottom Hole Size				
		Test orientation	Diameter	Depth		Hole orientation
		AXIAL. 	1/8"	1-1 1/2"		Perpendicular to rim face at mid thickness of rim.
		RADIAL. 	1/8"	1-1 1/2"		Parallel to rim face, from inside diameter of rim.
or						
Indication from a discontinuity giving a loss of back reflection greater than or equal to that of the reference standard:						
Concave Bottom Hole Size						
Test orientation	Diameter	Depth	Hole orientation			
AXIAL. 	3/8"	1/8"	Perpendicular to back rim face.			
Magnetic Particle Inspection	All wheels after manuf., but not req'd.	The apparatus must be of sufficient sensitivity to detect surface discontinuities exceeding 0.015" in depth and 1/4" long, but interpretation of mag. particle discontinuities based on their location, size, orientation, and shape is unspecified.			Described in M-107, 208 but not required of manufacturer	
Visual Surface Inspection	All Wheels After Manuf.	"Defects liable to develop in or cause removal from service." (Such surface defects (≤ 1/8" depth) may be removed by machining where sufficient stock remains.			Required of manufacturer by AAR M-107, 208	

Table 3-11. FRA and AAR Inspection Criteria for Wheels

FRA		AAR	
<p>Wheels are defective if they have (are):</p> <p>Thin Flange Vertical Flange High Flange Thin Rim Cracked or Broken: Rim</p> <p>Flange Plate Hub</p> <p>Chip in Flange Shelled Tread Slid Flat Spot: 2 1/2" or greater in length 2" or greater in length each two or more adjoining spots</p> <p>Hole in Plate (not by design) Circumferential Groove in Tread > 1/8" Scrape, Dent, or Gouge in Plate > 1/8" Loose Welded Overheated Painted to hide defects Wheel set out of gauge Distance between the inside faces of wheel rims is less than 52 15/16" or more than 53 3/8".</p>	<p>Sub Part C Sec. 215.43</p> <p>a b c d e</p> <p>f g h</p> <p>i j r l m n o 215.45</p>	<p>Wheels are defective if they have (are):</p> <p>Thin Flange Vertical Flange High Flange Thin Rim Cracked or Broken: Rim, or any transverse thermal cracks, tread width 3 3/4" Flange Plate Hub</p> <p>Chip in Flange Shelled Tread Slid Flat Spot: 2 1/2" or greater in length 1 1/2" or greater in length each two or more adjoining spots</p> <p>Hole in Plate (not by design) Circumferential Groove in Tread > 1/8" Scrape, Dent, or Gouge in Plate > 1/8" Loose Welded Overheated Painted Wheel set out of gauge Distance between the inside faces of the wheel rims is less than 53" or more than 53 3/8" "Prohibited" wheels</p>	<p>Rule 41 Sec. A</p> <p>la b c</p> <p>e d p o d j</p> <p>1, pg. 191</p> <p>q l w v</p> <p>Sec. D. Sec. A, 1S E6 Sec. A, lu</p> <p>Sec. A, 1, 2 & 2a&b.</p>

3-24

4. DAMAGE TOLERANCE AND FAILURE MODE ANALYSIS

In this section, the data from the previous two sections are combined with strength and toughness data generated from all available literature sources. Correlations are used wherever possible to obtain fracture-toughness values. Analysis is performed in an attempt to identify testing procedures and materials changes that would advance the state-of-the-art of the railroad industry's structural integrity practices with respect to failure mode and damage tolerance. These procedures must be consistent with inspection and maintenance practices, and they must be cost effective. The parameters necessary to perform such an analysis are the fracture toughness (K_{Ic}) and the yield strength (σ_{ys}) or K_{Id} and σ_{yd} , which are the same properties measured under dynamic loading conditions. The railroad industry is currently performing research in this area as evidenced by the work of Sharkey and Stone (1975), but only a limited amount of the data has been incorporated into an analysis of structural integrity. The prime index of toughness has been the Charpy impact test, the results of which have been included only in the standard for castings used in couplers. In this section, every attempt is made to generate fracture-toughness numbers by using the best available correlation parameter between Charpy V-notch (CVN) impact energy and K_{Id} .

4.1 MATERIALS - GENERAL

As noted in Section 2, the only quality assurance requirement common to all of the components is the control of chemical composition. For mechanical property control, minimum tensile values are specified, but the test frequency is rather arbitrary, especially for castings. Hot rolled Grade F axles require tensile tests from prolongations or actual axles. Only hardness is measured on each wheel in order to ensure successful heat treatment. By contrast, hardenability measured with

the Jominy bar is used for quality control of the side frames, bolsters, and couplers. Couplers are included for comparison because they do have some impact toughness requirements in their specifications, contrary to the absence of similar requirements for the other components.

Tables 4-1 through 4-4 summarize fracture-toughness data for steels from the available literature sources; these data can be used in the analyses of side frames, bolsters, couplers, and wheels. Included are Charpy V-notched impact values that were used to estimate the dynamic fracture toughness (K_{Id}) of steels based on a correlation developed by Rolfe and Barsom (1977) for bridge steels.

$$K_{Id}^2 = (5E) (CVN)$$

or

$$K_{Id} = 12.24 \sqrt{CVN} \times 10^3$$

where

K_{Id} = Dynamic fracture toughness (psi $\sqrt{\text{in.}}$)

E = Elastic modulus = 30×10^6 psi (for steel)

CVN = Charpy V-notch impact energy (ft-lb)

The correlation has been shown to be quite good for bridge steels at temperatures up to the NDT (nil ductility transition temperature per ASTM Standard E208-69). The NDT is measured at a strain rate of 10/sec and is estimated to be the temperature at which $(K_{Id}/\sigma_{yd})^2 \approx 0.4$, where σ_{yd} is the dynamic yield strength, and σ_{ys} is the yield strength at a slow strain rate. At temperatures below the NDT, the fracture toughness becomes independent of strain rate; whereas at temperatures above NDT, the fracture toughness is much higher at slow strain rates 10^{-5} /sec than at the 10/sec rate; i. e., $K_{Ic} \gg K_{Id}$.

Table 4-1. Yield-Strength and Fracture-Toughness Values for Bolsters and Side Frames at Various Temperatures

Material	T (°F)	σ_{yd} (ksi)	CVN ₂ (ft-lb)	K_{Id} (ksi√in.)		Source
				Measured*	Estimated@	
Casting Grade B Bolsters & Side Frames	-70	--	6	29	30	Sharkey and Stone, 1975
	-30	--	11	30	41	
	-20	--	11	33	55	
	32	--	21	--	56	
	70	38	29	--	66	
	100	--	34	--	71	
120	--	37	--	74		
Casting Grade C Bolsters, Side Frames & Couplers	-70	--	20	--	55	
	-30	--	28	51	65	
	-20	--	29	57	66	
	0	--	32	--	69	
	32	--	39	--	76	
	70	60	47	--	84	
	100	--	56	--	92	
	120	--	60	--	95	

*Instrumented impact test with precracked Charpy specimen.

@Estimated using Barsom bridge steel correlation:

$$K_{Id}^2 = 5E(CVN),$$

where

$$E = 30 \times 10^6 \text{ psi, (CVN) = ft-lb, and } (K_{Id}) = \text{psi} \sqrt{\text{in.}}$$

Table 4-2. Yield-Strength and Fracture-Toughness Values for Couplers at Various Temperatures

Material	T (°F)	σ_{ys} (ksi)	CVN (ft-lb)	K_{Id} (ksi $\sqrt{\text{in.}}$)		Source
				Measured*	Estimated@	
Casting Grade C Couplers	-70	--	--	--	--	AAR Coupler Steel Study, 1970
	-30	--	6	--	30	
	0	--	11	--	41	
	30	--	16	--	49	
	70	60	21	--	56	
	120	--	33	--	70	
Grade C Couplers	0	--	15	--	47	AAR Standard M-211
Casting Grade E Couplers	-70	--	17	58	51	Sharkey and Stone, 1975
	-30	--	23	--	59	
	0	--	28	--	65	
	32	--	31	--	68	
	70	100	35	--	72	
	100	--	39	--	76	
	120	--	40	--	77	
Casting Grade E Couplers	-70	--	10	--	39	AAR Coupler Steel Study, 1970
	-30	--	13	--	44	
	0	--	15	--	47	
	30	--	18	--	52	
	70	100- 135	23	--	59	
	120	--	28	--	65	
Grade E Couplers	-40	--	15	--	47	AAR Standard M-211
<p>*Calculated from curves from instrumented impact tests with precracked Charpy specimens. @Estimated using $K_{Id}^2 = 5E(\text{CVN})$.</p>						

Table 4-3. Yield-Strength and Fracture-Toughness Values for Wheels at Various Temperatures

Material	T (°F)	σ_{ys} (ksi)	CVN* (ft-lb)	K_{Id} (ksi $\sqrt{in.}$)		Source
				Measured [@]	Estimated ^{*,#}	
Class U Cast	-40	--	---	--	--	Carter and Caton, 1974
	75	54/52	1-2.5/3	21	12-19/21*	
	150	--	--	--	--	
	300	--	--	59	--	
Class U Wrought	-40	--	--	32	--	
	75	59/59	4/3	32	24/21	
	150	--	--	43	--	
	300	--	--	63	--	
Class C Cast	-40	--	--	--	--	
	75	93/60	4/-	--	24/-	
	150	--	--	--	--	
	300	--	--	--	--	
Class C Wrought	-40	--	--	--	--	
	75	87/52	3/2.5	22	21/19	
	150	--	--	36	--	
	300	--	--	--	--	
Class A Wrought	-40	--	--	--	--	
	75	66/47	6.5/8	37	31/35	
	150	--	--	59	--	
	300	--	--	63	--	

*-/- indicates properties for wheel rims/plates, respectively.
[@]Instrumented impact test with precracked Charpy specimen. These tests have been made without regard to specimen location or orientation.
[#]Estimated using

$$K_{Id}^2 = 5E(CVN).$$

Table 4-4 Yield-Strength and Fracture-Toughness Values for Wheel Rims at Various Temperatures

Material	T (°F)	σ_{ys} (ksi)	CVN (ft-lb)	K_{Id} (ksi√in.)		Source
				Measured*	Estimated [@]	
Class BR Cast	-70	--	3.5	--	23	AAR Report No. 123, 1973
	-30	--	4	--	24	
	0	--	4	--	24	
	30	--	4.5	28.5	26	
	70	87	4.5	29	29	
	100	--	6	29.5	30	
	150	--	8	31	35	
	200	--	11	37.5	41	
Class U-1 Cast	-70	--	2	--	17	
	-30	--	2	--	17	
	0	--	2.5	18	19	
	30	--	2.5	18	19	
	70	80	3.5	18.5	23	
	100	--	4	19	24	
	150	--	6.5	20	31	
	200	--	7.5	--	34	
300	--	14.5	--	47		

*Instrumented impact test with precracked Charpy specimen.
[@]Estimated using $K_{Id}^2 = 5E(CVN)$
[#]Estimate based on carbon content (1% by weight).

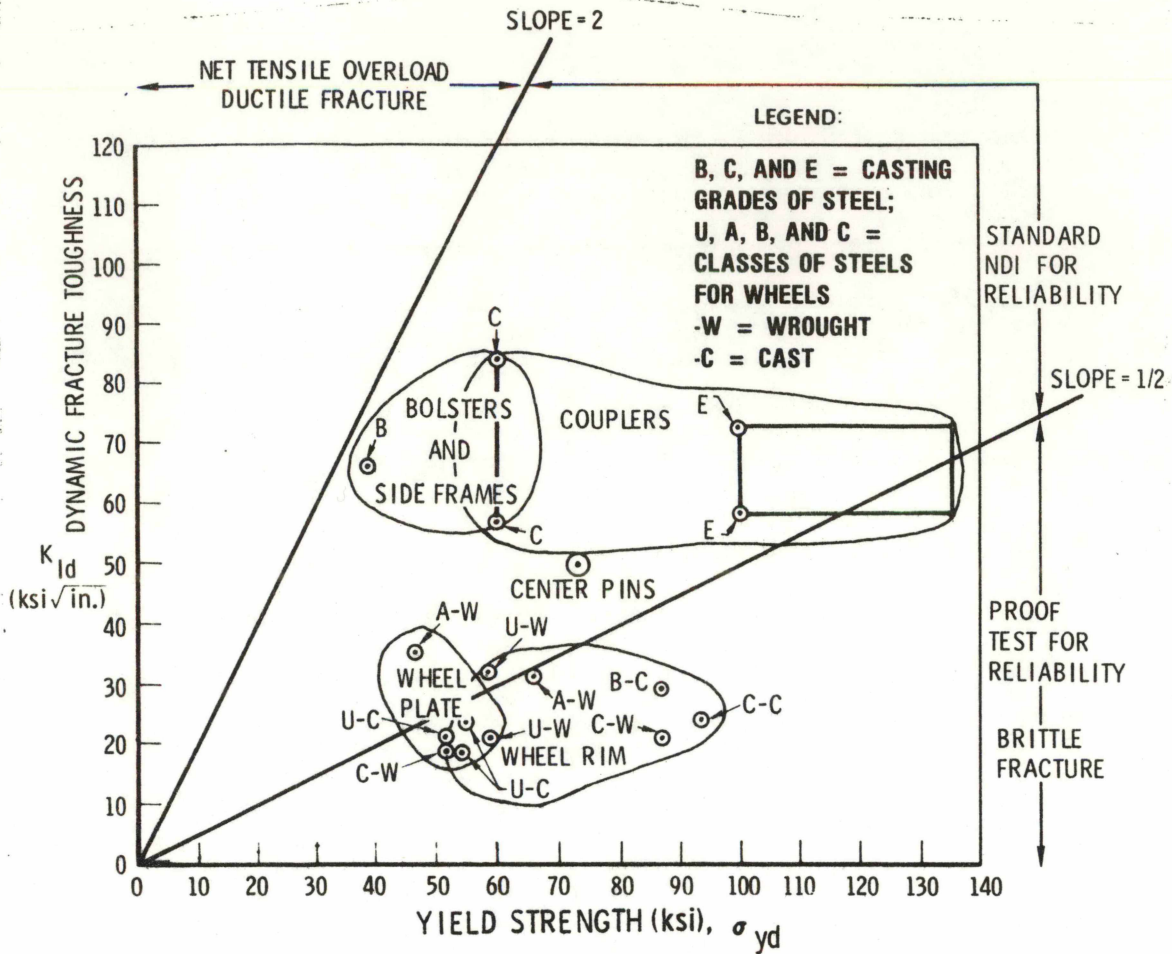
Damage tolerance is the amount of damage in the form of cracks that a stressed component can sustain without failing. The magnitude or size of the crack depends not only on the fracture toughness K_{Id} but also on the ratio K_{Id}/σ_{yd} measured at the appropriate loading rate. Tables 4-1 through 4-4 contain comparisons of measured and calculated dynamic, K_{Id} , ($10s^{-1}$) fracture-toughness values, the results of which suggest a reasonable correlation using the Barsom-Rolfe relationship.

4.1.1 Ratio Analysis Diagram

In order to establish the inherent damage tolerance of steels used in a freight car truck, a ratio analysis diagram (Pellini, 1971) was generated from the data in Tables 4-1 through 4-4 and is shown in Figure 4-1. The zones are delineated by radial lines from the origin that represent constant values of the ratio K_{Id}/σ_{yd} . Because the critical defect or crack size is also proportional to this ratio, the radial lines can also be interpreted to represent different levels of damage tolerance, increasing as the ratio increases.

Regions delineated are $K_{Id}/\sigma_{yd} = 1/2\sqrt{\text{in.}}$ and $K_{Id}/\sigma_{yd} = 2\sqrt{\text{in.}}$ Below $1/2$, the conventional NDI (nondestructive inspection) is considered to be inadequate in establishing the structural integrity of a component simply because the limit of damage tolerance is smaller than the reliable detection limits of existing ultrasonic, radiographic, and magnetic particle techniques. Springs and wheels fall into this category. In principle, their safe life can only be established by proof testing which is done for springs but not for wheels.

Ratios of K_{Id}/σ_{yd} above $1/2$ but less than 2 represent a region where conventional NDI is adequate in establishing the safe life of components. By far, the Grade B and C bolster castings have the best damage



Not shown is the point corresponding to springs at $\sigma_{yd} = 248$ and $K_{Id} = 25$

Figure 4-1. Relative Location of Various Rail Vehicle Components on the Ratio Analysis Diagram (Room Temperature)

tolerance, but the higher strength Grade E coupler castings are verging into regions where the damage tolerance is only for extremely small defects before brittle fracture becomes a potential failure mode.

Note in Figure 4-1 that fracture toughness K_{I_d} must be increased as the yield strength increases in order to maintain a constant level of damage tolerance. In order to comply, the coupler specification* calls for a 15-ft-lb requirement for Grade C couplers at 0° F but for the higher strength Grade E couplers, the 15-ft-lb requirement is at -40° F.

4.1.2 Thickness Effects

A conservative factor in the analysis of damage tolerance is based on the assumption of plane-strain fracture toughness, but in actuality, the thickness is small enough to deform under plane-stress conditions where the toughness is much higher. The plane-strain conditions can be estimated from ASTM Standard E399-74 by

$$B \geq 2.5(K_I / \sigma_y)^2,$$

measured at the appropriate strain rate and temperatures. For thickness (B) values less than those given by the above relationship, the failure mode is usually ductile, but for B values greater than given by the above relationship, a potential brittle failure mode exists. Figure 3-1 is repeated in Figure 4-2 with estimates of strength and dynamic fracture toughness (K_{I_d}) plotted in order to display the inverse relationships of strength and toughness as a function of carbon content. The significance of this

*AAR Standard M-211, Section A.

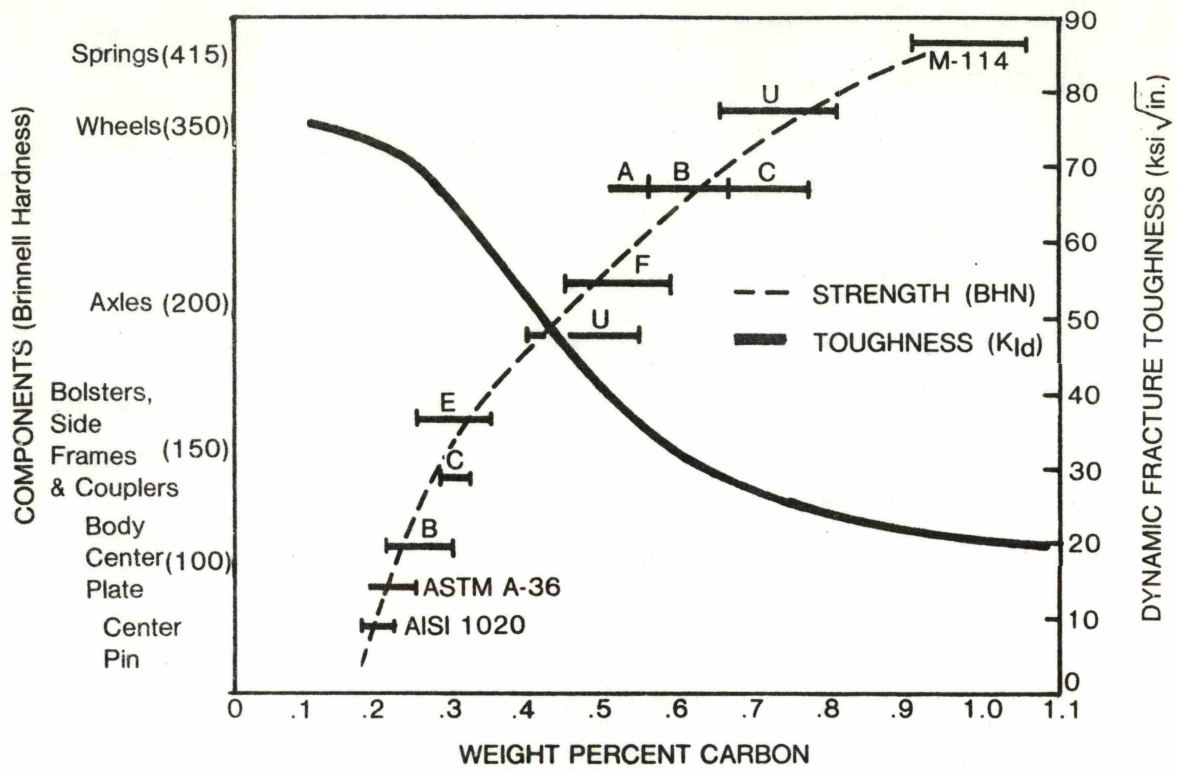


Figure 4-2. Effect of Carbon Content on Strength and Toughness of Railroad Steel Components

estimate is displayed in the upper part of Figure 4-3, where both the damage tolerance and the thickness required for potential brittle failures is seen to decrease with increasing carbon content. If the nominal thickness of the various truck components are superimposed on Figure 4-3, it is readily noted that the body center plate (BCP), center pin (CP), bolsters, and side frames have adequate damage tolerance such that their eventual failure mode will be ductile fracture, but the couplers are of large enough dimensions to be susceptible to brittle fracture. As the section size of a component increases, the potential for brittle fracture also increases. Graphically, this effect is shown in Figure 4-3; the potential for brittle fracture increases as the thickness of the component increases. As noted, the potential for brittle fracture increases from couplers, to axles, to wheels, and to springs.

To ensure structural integrity as the potential for brittle fracture increases, more stringent NDI or redundancy must be incorporated into the design. This is the case with springs, which are designed to the fail-safe criterion, because of the extremely high potential for brittle fracture and inherently small tolerance to damage. Therefore, the above analysis supports what has already been learned by trial and error with springs, which are essentially proof tested for structural integrity and designed to redundant, fail-safe concepts. Wheels obtain their structural integrity from rather rigorous NDI (Table 3-10). The current railroad steels are of a relatively lower grade when compared to the materials technology limits for high toughness steels. Because cost is the governing factor, the structural integrity of railroad freight car truck components is rigorously constrained to a balance between types and intervals of inspection and service loads. Figure 4-4 relates the toughness of railroad steels to other steels.

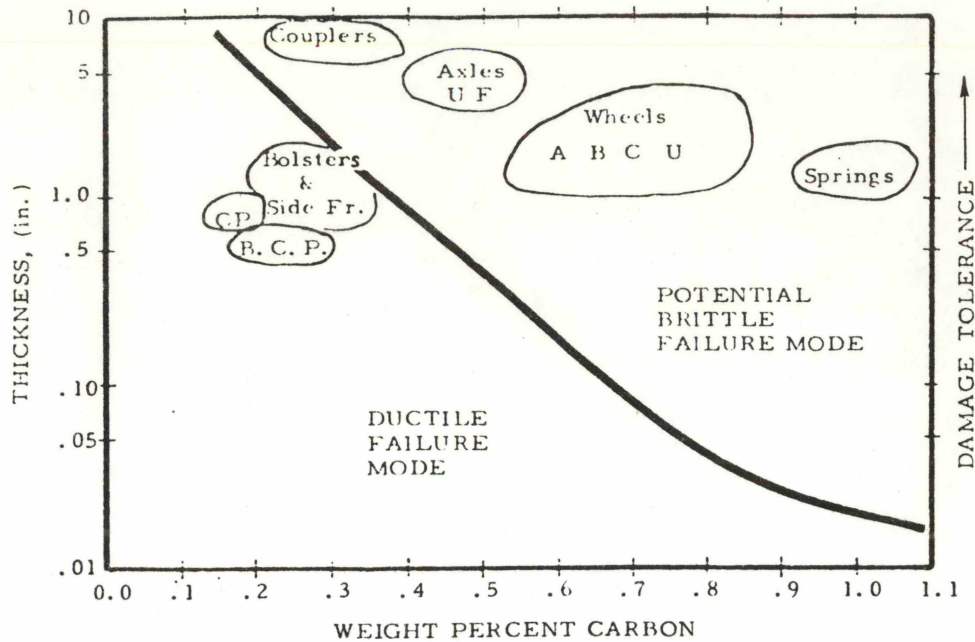
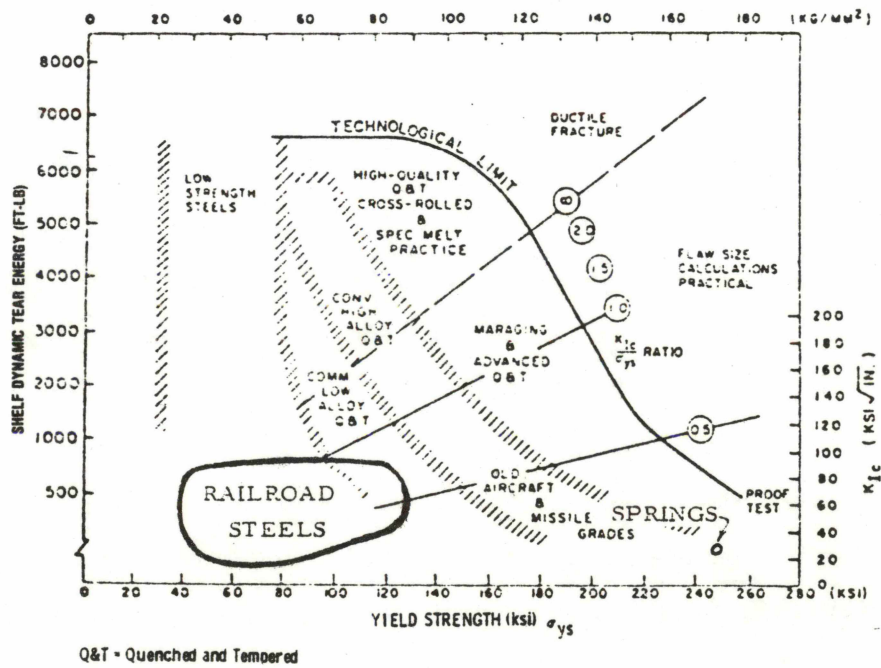


Figure 4-3. Potential Failure Modes of Freight Car Components at Room Temperature



Source: Pellini, 1971.

Figure 4-4. Location of Railroad Steels Relative to the Fracture Toughness Technology Limit

4.1.3 Temperature Effects

The analysis of the steels to this point has been based on room temperature data. As the temperature decreases, the steels become more brittle. Most design approaches center on a relative temperature based on the NDT (nil ductility transition temperature as described in Section 4.1). Nuclear reactors and the Alaskan pipeline are designed such that the lowest anticipated service temperature (LAST) is 120°F above NDT. The U. S. Department of the Navy, the American Bureau of Shipping, and the Offshore Platform Industry apply design constraints such that the LAST is 30°F above the NDT. The NDT temperature can be estimated by the temperature where $K_{Id}/\sigma_{yd} = \sqrt{0.4} = 0.63$. From Figure 4-1, which is room temperature (RT) data, it can be concluded that bolsters and side frames operate above NDT at RT, whereas wheels and springs operate below NDT at RT. Grade E couplers are borderline, and a lower temperature would definitely aggravate the potential of brittle fracture.

In a structural integrity analysis, the main influence of the fracture-toughness, yield-strength ratio is on the potential failure mode and the damage a component can withstand at the maximum operating stress. In the following sections, specific components will be addressed with regard to failure mode potential and damage tolerance.

4.2 SIDE FRAMES/BOLSTERS/COUPLERS

4.2.1 Design/Prototype Testing

The structural integrity of side frames and bolsters made from Grade B and Grade C castings is adequate for railroad service loads based on damage tolerance considerations. The ratio analysis diagram (RAD), Figure 4-5, identifies the range of critical defect sizes since the square of the ratio is directly proportional to crack size. The crack that corresponds to a ratio above $\frac{1}{2}$ can be readily detected with standard NDI, although

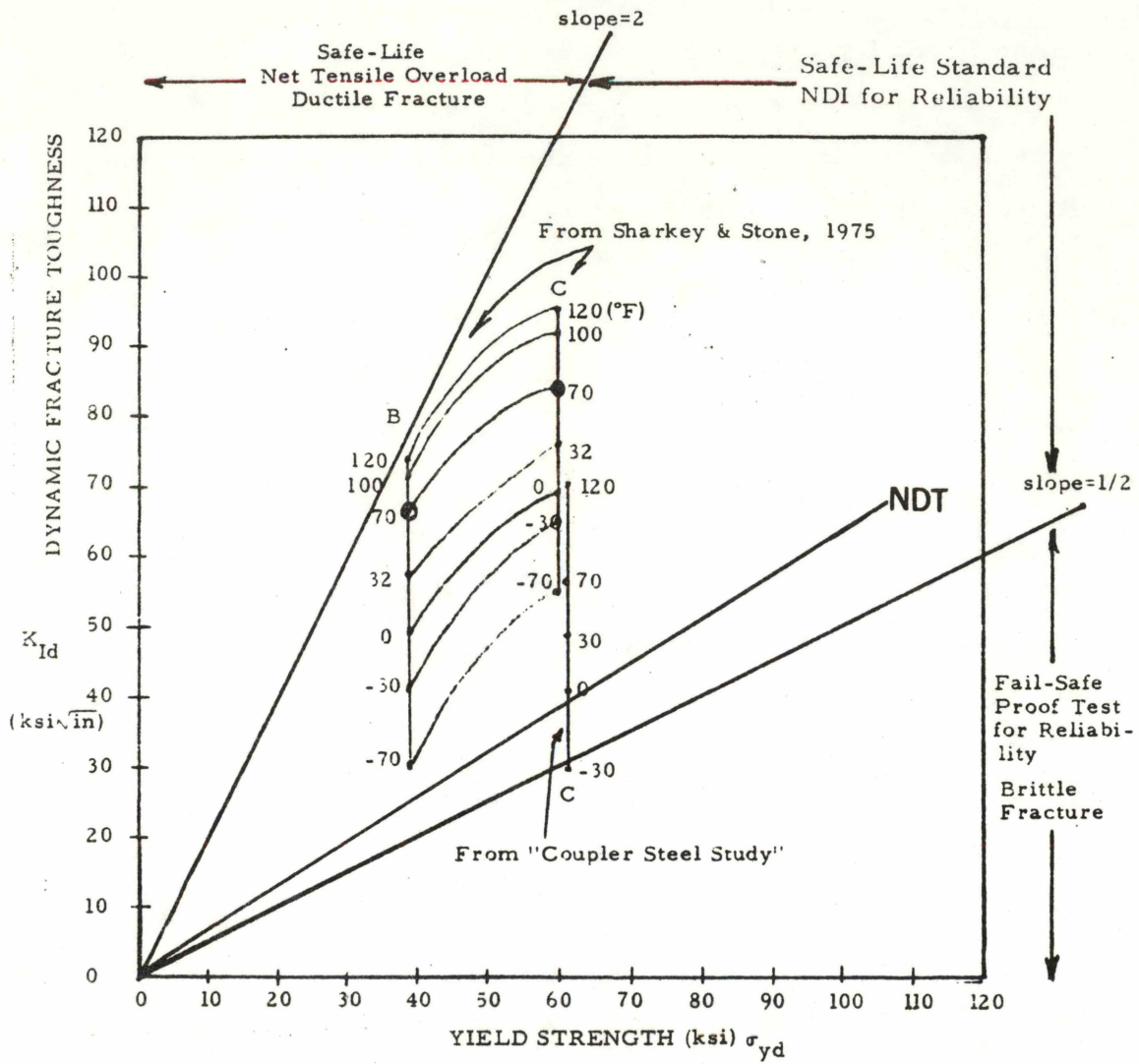
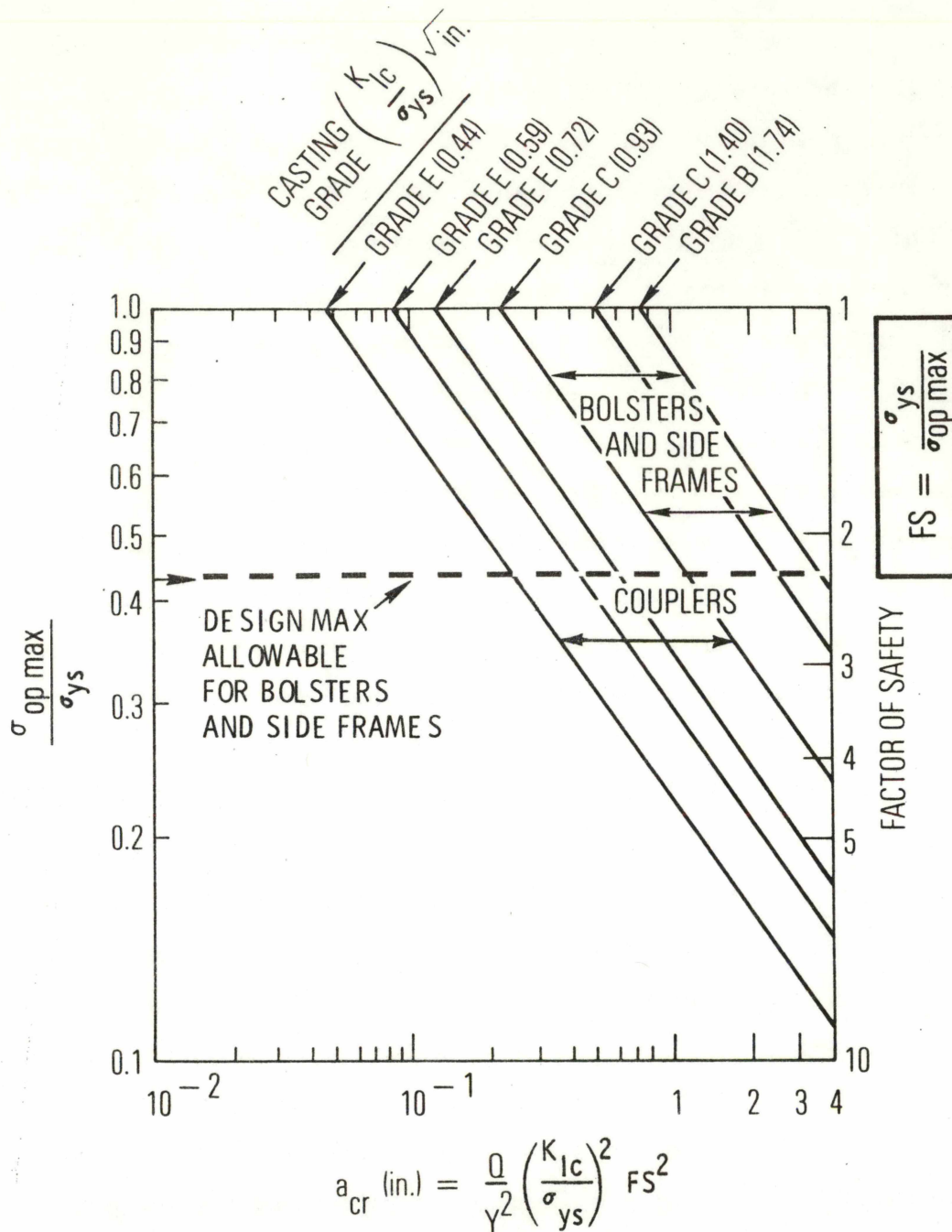


Figure 4-5. Relative Location of Grades B and C Castings (Bolsters and Side Frames) on the Ratio Analysis Diagram at Various Temperatures

accessibility becomes a problem during a service inspection. From Figure 4-3, it is observed that the failure mode of bolsters and side frames is one of plane stress (ductile shear). From Figure 4-5, it is noted that even at the LAST of -70°F , they are generally operating above the NDT temperature. The only exception appears to be some data reported on Grade C casting material which were used in couplers. With the existing quality control practices, the limiting failure mode would be one of tensile overload. The life of the side frame and bolster are regulated by high cycle fatigue and appear to be critical only from crack nucleation considerations. Therefore, prototype testing is directed toward evaluating design detail that accelerates the nucleation of a crack. One such detail would be design detail that produced regions of high stress concentration. Apparently, current design practices are adequate as noted by the precipitous drop in accidents due to side frame failure (Figure 2-4) over the last 10 years.

The design of side frames/bolsters is based on a maximum allowable stress of about 0.42 of the yield stress. By taking the reciprocal of this value, a factor of safety of about 2.4 is established. The margin of safety, which is found by subtracting 1 from the factor of safety, would be 1.4. Figure 4-6 shows the damage tolerance of different casting grades. The Grade E couplers, if they were designed to the same factor of safety as side frames and bolsters, would have the least damage tolerance, and a crack as small as 0.25-in. deep at maximum allowable stress would cause failure. Grade C couplers, in comparison, can tolerate up to 1 in. of cracking before they become critical. Increasing the factor of safety in design would be an alternative method for increasing the damage tolerance. For example, Grade E couplers with a factor of safety of 5 would increase their damage tolerance to 2 in.



Y = Dimensionless Crack Geometry Parameter
 Q = Dimensionless Shape Factor

Scale drawn for Q = 1 and Y = 2, values appropriate for a long shallow surface flaw.

Figure 4-6. Damage Tolerance of Casting Steel Grades at Room Temperature

4.2.2 Component Testing - Truck Castings

Static component tests can be interpreted to be proof tests that establish the nonexistence of a defect of some maximum size. In Figure 4-6, the crack size can be estimated by the intercepts at $\sigma_{\text{proof}} = \sigma_{\text{ys}}$ or FS = 1 for the various casting grades of steel. For Grade C bolsters and side frames, the absence of a defect size above 0.25 in. would be established. The guaranteed service life would then be the number of cycles it would take for the 0.25-in. crack to grow to about 1 in. By comparison, static loading Grade B bolsters/side frames would establish a maximum initial crack size of about 0.8 in. In this case, reliable nondestructive inspection techniques would be of more economic value in ensuring the safety life cycle. However, from theoretical considerations, proof testing couplers would be of significant value in establishing their lifetimes; the limitations are primarily from a practical point of view. At the maximum operating stress of the best Grade E coupler castings measured to date, a 1-in. crack would cause brittle failure unless the factor of safety was increased to 5. This estimate was made for room temperature; at lower temperatures, the damage tolerance is even less.

The concern for inadequate toughness in couplers is emphasized in Figure 4-7 where the coupler steel study data are compared to other data on Grade C and Grade E castings. Note that even room temperature is below NDT for some of the casting Grade E coupler steels.

In Figure 4-7, the K_{Id} value of 47 corresponds to the 15-ft-lb AAR requirement for couplers. For Grade C steels, under the 0°F requirement, the separately cast coupons of Sharkey and Stone were found to be acceptable, but most of the steels tested in the Coupler Steel Study would have been rejected. The same conclusion can be drawn for a -40°F requirement on the Grade E castings. A problem that becomes evident is

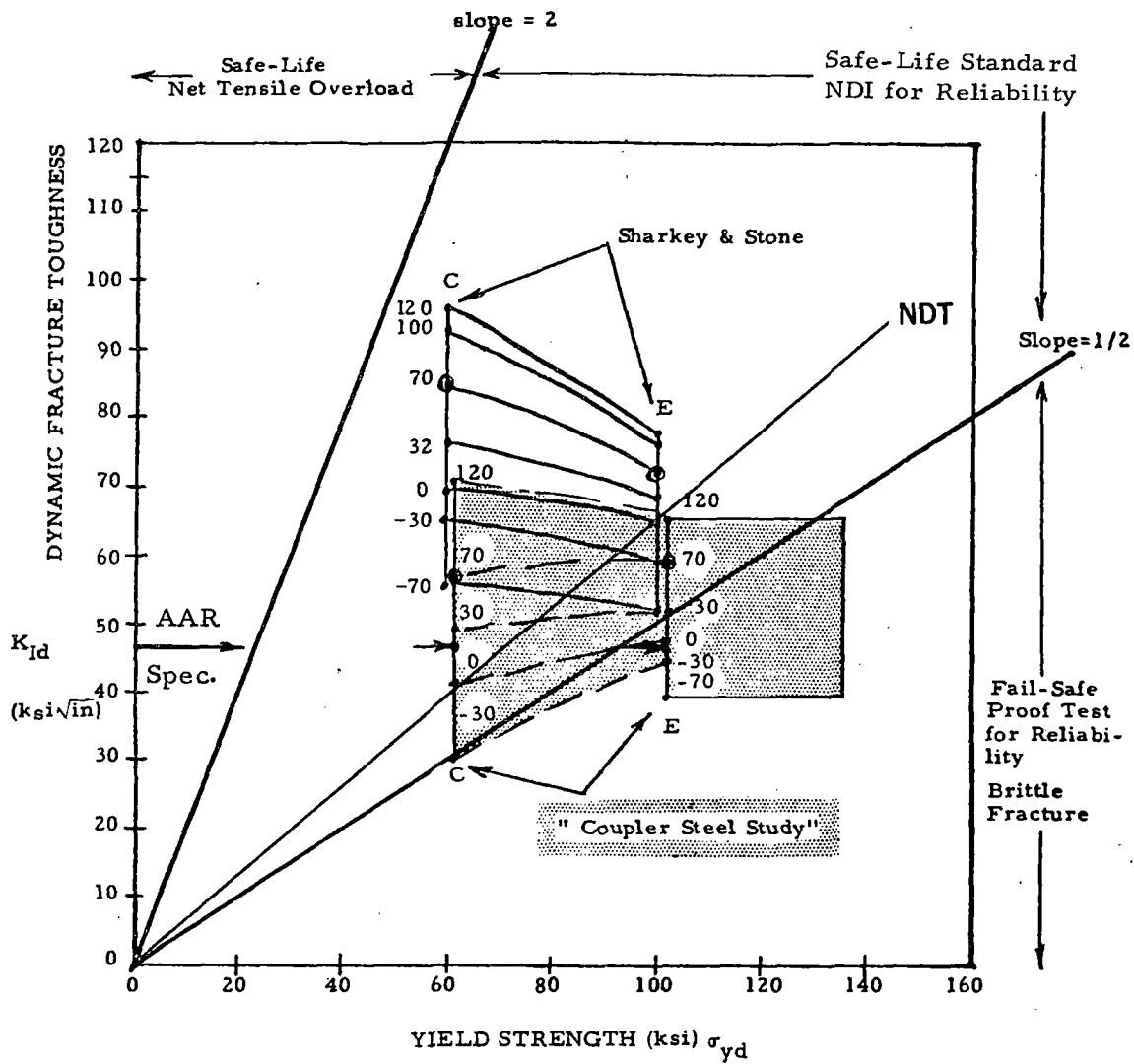


Figure 4-7. Relative Location of Grades C and E Castings (Couplers) on the Ratio Analysis Diagram at Various Temperatures

the use of separately cast test coupons having inherently higher toughness than test coupons machined from large castings. The location of a small test coupon in a large casting could also be critical.

4.2.3 Manufacturing and Processing/Quality Control

Coupler castings have Charpy V-notch requirements; however, they seem to be minimal. In addition, the location of the test samples or the use of separately cast test bars is not identified. The trend is in the proper direction, but more attention should be given to the significance of the test and the specified test temperature. A correlation with fracture toughness of railroad steels should be established similarly to the work done in bridge steels.

A major problem with bolsters and side frames occurs with overloads introduced in hump yards. In this case, enough ductility or fracture toughness should be designed into the component such that the failure mode not only be of plane stress but such that the remaining net section will bend and not break in the presence of a crack, i. e., failure by net section yielding instead of plane stress fracture. Rough calculations on bolster and side frames suggest that the toughness-to-yield strength ratio (K_{Ic}/σ_{yd}) is about 2, which is consistent with the ratio analysis diagram. For couplers, the requirement would certainly be more severe. Testing of cracked components to failure in the laboratory would be a method of verifying the analysis. In general, the AAR standards and recommended practices do not allow defects in critical areas. Essentially, they advocate the concept of "zero defects" which has long been known to be impractical. Some lower limit of flaw detection in each of the components must be established in order to reliably perform a safety life-cycle (SLC) analysis.

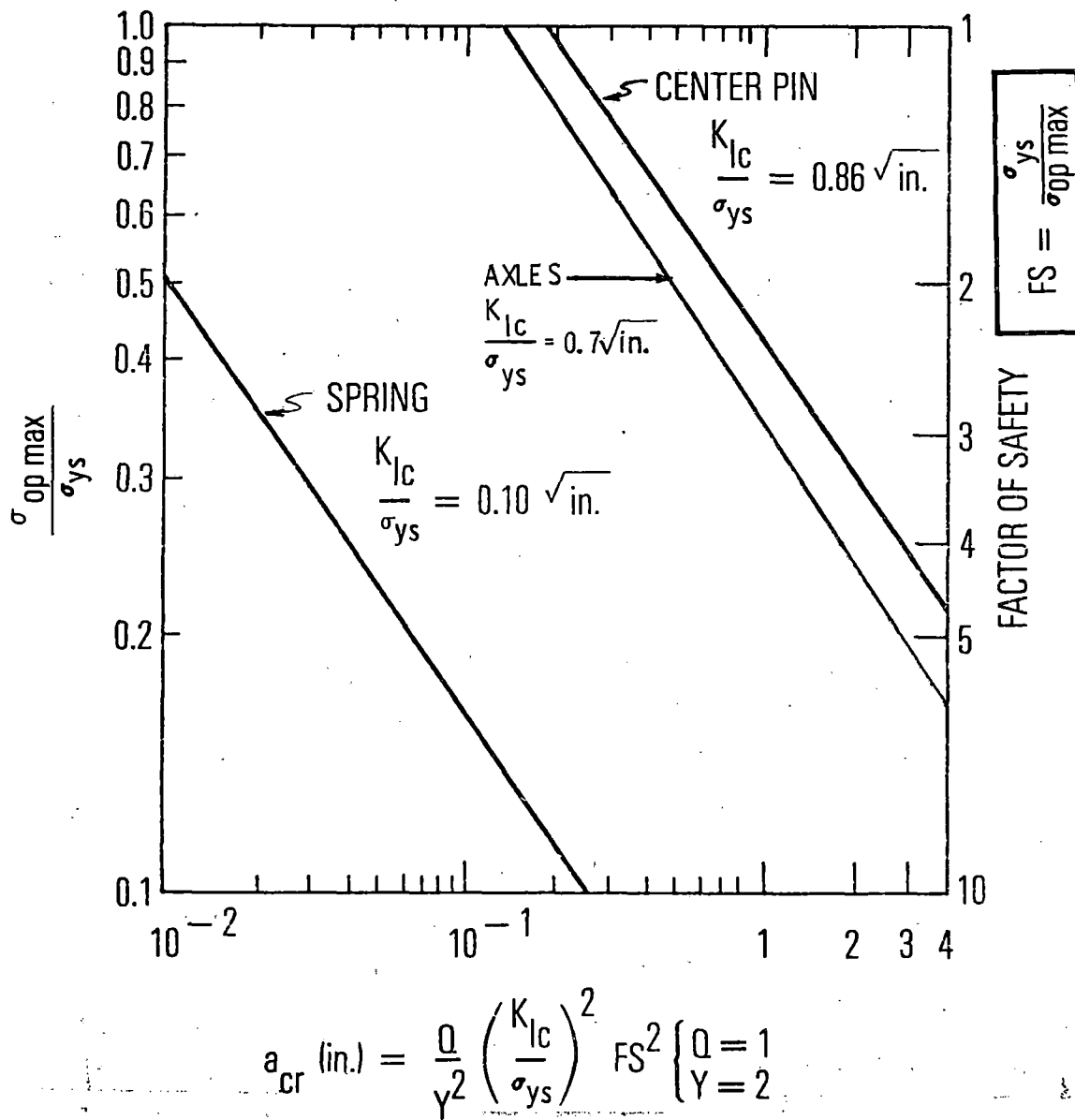
4.3 AXLES/SPRINGS/CENTER PINS

4.3.1 Design/Prototype Testing

No Charpy V-notch or fracture-toughness data were available for axles. Failures in axles have dropped precipitously, with failures in the section between the wheels almost nonexistent. Only the journals have been a major source of failure. Surface finish effects on fatigue have been evaluated and operating stresses are below the endurance limit.

4.3.2 Component Testing

Grade U axles are subjected to a drop test in combination with flaw detection limits that are capable of detecting a 3/4-in., penny-shaped flaw at mid-length of the axle. If the drop test causes permanent deflection, yield point loading is assumed. The damage tolerance in terms of toughness-to-yield strength ratio (K_{Id}/σ_{yd}) can be estimated as being greater than or equal to $1.13\sqrt{0.75/2}$ or $0.70\sqrt{\text{in.}}$, for both Grade U and Grade F axles. This is near the value of $0.86\sqrt{\text{in.}}$ found in tests conducted at Aerospace Material Sciences Laboratory on a used center pin. For comparison, similar data were generated on a spring, the results of which were used to plot Figure 4-8. The springs are extremely brittle ($K_{Ic}/\sigma_{ys} = 0.10\sqrt{\text{in.}}$) in comparison to the axles which essentially operate above the NDT temperature because their damage tolerance ratio exceeds $0.63\sqrt{\text{in.}}$. If the fracture toughness of axles were known, then a drop test would be an effective proof test that could be used to establish life cycles. If the toughness were strain-rate sensitive, drop tests at lower temperatures could be used to ensure an even greater lifetime and an extended inspection period.



Y = Dimensionless Crack Geometry Parameter
 Q = Dimensionless Shape Factor

Figure 4-8. Damage Tolerance of Axles, Center Pins, and Springs at Room Temperature

4.3.3 Quality Control - Axles

Based on toughness estimates, tolerance for 1-in. long, shallow surface cracks would require a factor of safety on stress of about 3. Therefore, quality control must be such to detect flaws of this size during inspection, especially during service inspections. Springs, because of their brittle nature, are subject to a proof test and good metallurgical analysis utilizing microstructural control to ensure proper heat treatment, cleanliness, and the absence of surface defects, including decarburization.

4.4 WHEELS

4.4.1 Design/Prototype Testing

Wheel design has been extensively analyzed. However, it continues to be a problem in the industry because of extremely complex stress states, especially during braking and dynamic interaction loads with the rail. Rims are designed to withstand wear and therefore are of high hardness, resulting in a relatively brittle material.

Figure 4-9 provides detailed information for Class U, A, B, and C wheel rim steels. The general trend from Class A to B to C wheels is higher strength with decreasing toughness resulting in less damage tolerance with increased strength. As noted, the NDT for these steels is far above room temperature. Specifically, the NDT is about 200^oF for cast Class U wheels, about 100^oF for Class A, and over 300^oF for Class B and C wheel rims. Therefore, minute thermally included cracks in these components can cause brittle failure.

4.4.2 Component Testing - Wheels

No testing is performed on the wheels. The damage tolerance of the rims is extremely small as noted in Figure 4-10. At room temperature

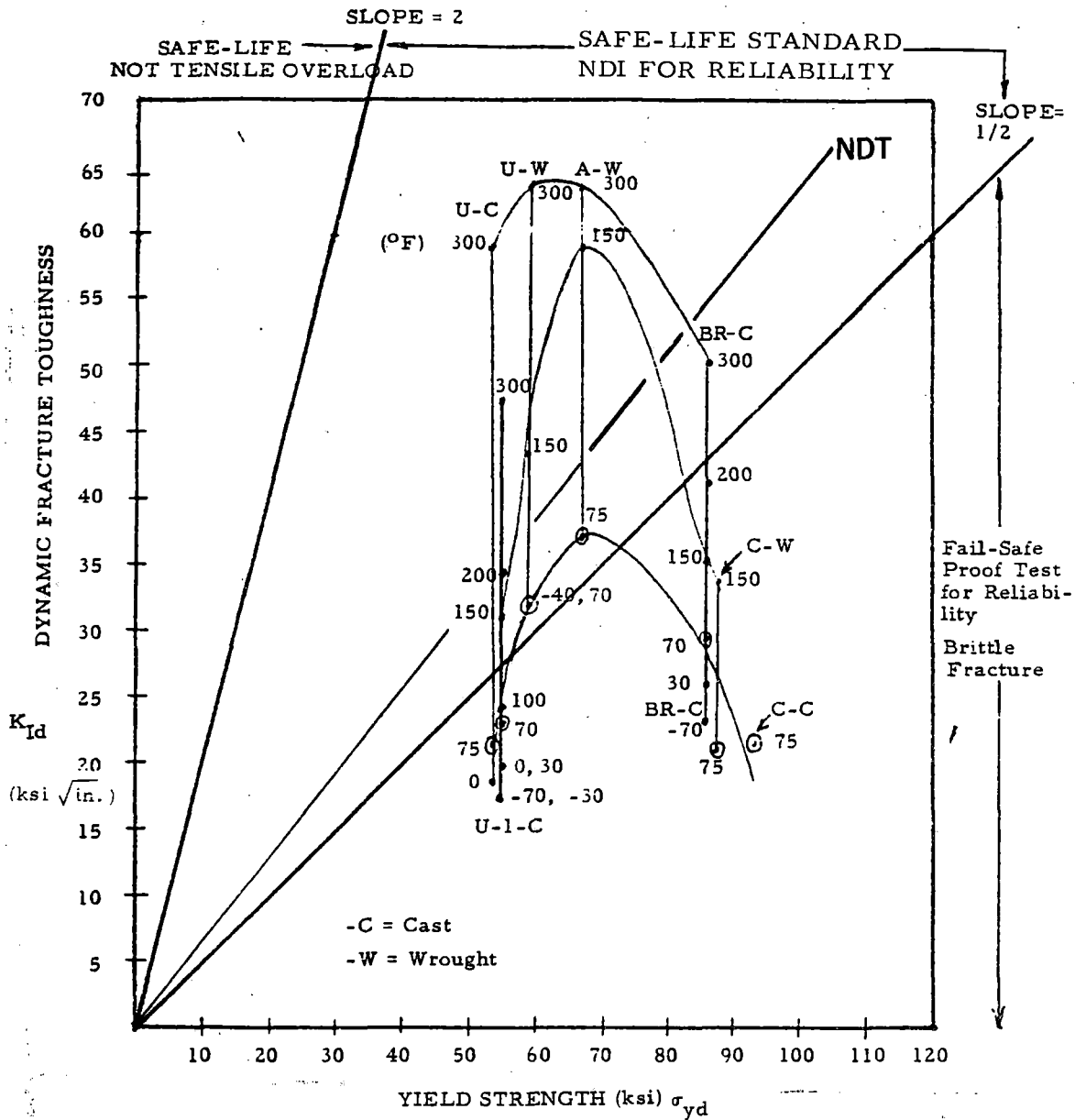
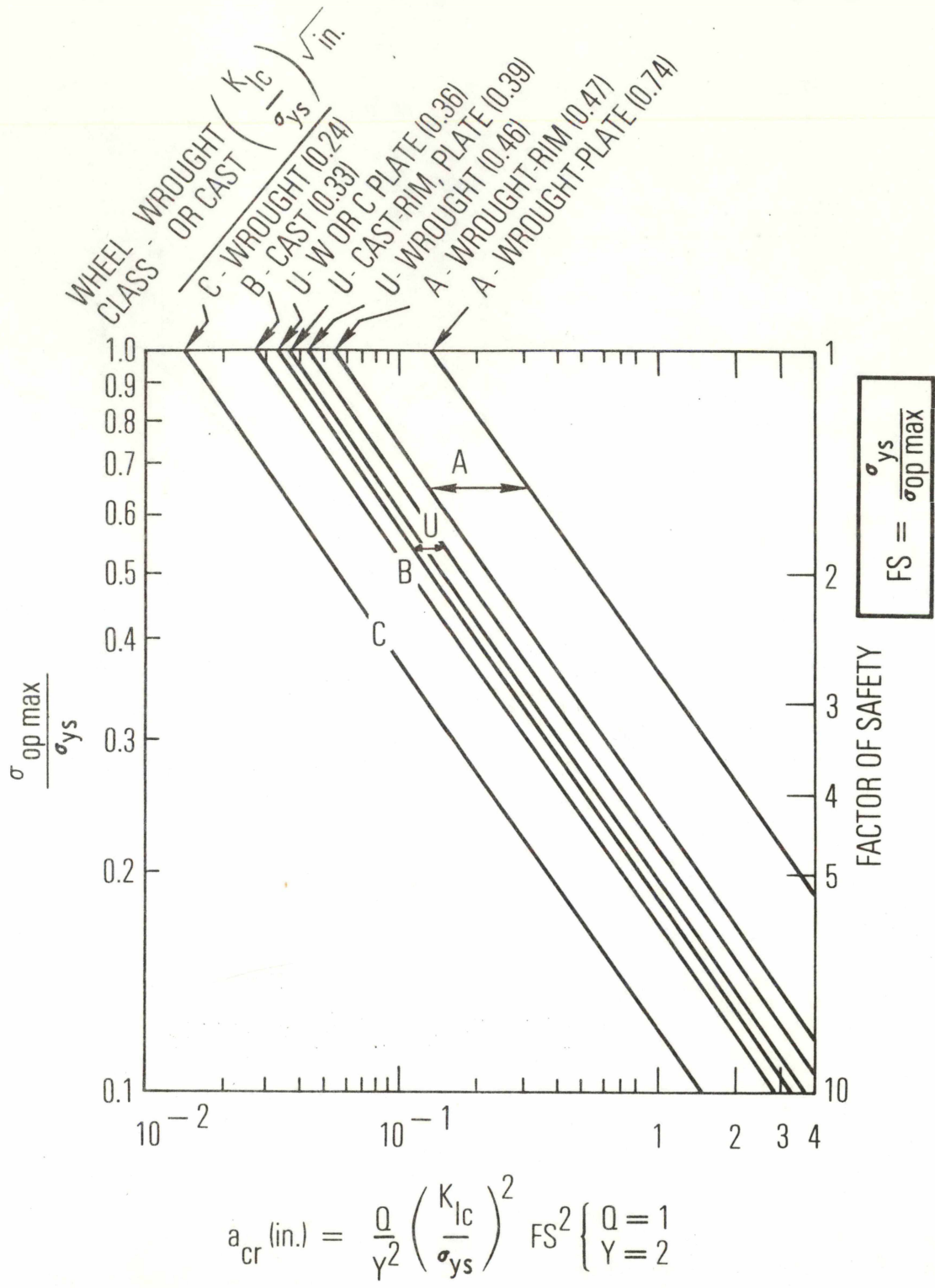


Figure 4-9 Relative Location of Classes U, A, B, and C Wheel Rims on the Ratio Analysis Diagram at Various Temperatures



Q = Dimensionless Shape Factor
 Y = Dimensionless Crack Geometry Parameter

Figure 4-10. Damage Tolerance of Wheel Rims at Room Temperature

and with an estimated factor of safety of 2.5, critical-size cracks are about 0.1-in. deep for Class C and about 1.0-in. deep for the rim steel with the most damage tolerance--Class A, wrought. Ideally, the wheel rims should be proof-tested, but instead, high-resolution, nondestructive inspection techniques are used for reliability. As noted in Table 3-9, ultrasonics are used to detect 1/8-in. defects in the radial and axial direction. As noted from Figure 4-10, this sensitivity is only adequate if a factor of safety of at least 3 is used on the yield stress. When actual operating stresses exceed this value, brittle failure is probable.

4.4.3 Quality Control - Wheels

The quality control of wheels appears minimal when the criticality of the component is considered. The inherently low damage tolerance is of a nature that the required crack detection limits are below the detection limits of existing NDI practices. Only low operating stresses, i. e., high factors of safety at 3 to 10, can produce some reasonably sized critical defects (about 1 in.) that would cause fracture. But in actuality, any local thermal stress, or impact stress due to rail interaction with a foreign object, could conceivably cause fracture of a wheel. It appears that the wheel steels could use some of the existing material technology to advance their quality with regard to increased damage tolerance.

5. SAFETY LIFE-CYCLE PREDICTION TECHNIQUES

The fatigue response of materials subjected to static loading with superimposed random vibrations, shock, or load cycling is an important technological area. Its applications encompass conventional structures such as railroad car components, aircraft, bridges, ships, and offshore structures. Air Force and other military applications extend to long-term life of movable missiles (e. g., the MX intercontinental missile), communications spacecraft, and life assessment of the space shuttle transportation system.

In addition to reviewing the conventional approach to fatigue life prediction and life-prediction analysis based on crack growth under constant amplitude cyclic stresses, the random loading aspects of crack propagation are discussed in this section. They are used to generate an estimate of the safety life cycle. The basic technical approach selected is to extract, from the statistical cycle loading spectrum, a characteristic loading. This characteristic cyclic loading may then be used to forecast the future propagation of the crack, including a transition to unstable or catastrophic growth (i. e., outright or abrupt fracture). This general approach is oriented toward providing convenient design charts for rapid identification of design or maintenance difficulties and benefits gained by nondestructive inspection (NDI). Fracture mechanics methodology is used extensively.

The specific component discussed is the freight truck side frame. Specific topics include setting manufacturing limits for flaw sizes (i. e., quality control through NDI), periodic field inspection, and accelerated acceptance testing (i. e., the Association of American Railroads fatigue acceptance test).

5.1 CONVENTIONAL FATIGUE ANALYSIS

In the past, many designers conservatively designed all parts for infinite life (i. e., greater than 10^6 cycles) by restricting the maximum operating stress to a value of about 1/3 UTS (ultimate tensile strength). In spite of this conservatism, fatigue still remains the most common cause of structural failure. Finite life concepts have been introduced based on a rotating beam, small-specimen, alternating stress test that defines the number of cycles to failure as a function of the maximum stress (S-N curves). The reverse bending test implies a stress ratio or minimum-to-maximum stress ratio of -1. For other mean and alternating stresses or stress ratios, the modified-Goodman diagram* is used to determine an equivalent fully alternating stress, that can be related to the S-N curve determined from a reverse bending test.

The endurance limit of an actual structural component is often found to be considerably lower than the endurance limit of the rotating beam specimen; therefore, a variety of modifying factors must be employed. These include: surface factor, size factor, reliability factor, temperature factor, stress concentration factor, and the miscellaneous-effects factor. Once these factors have been properly accounted for, the Palmgren-Miner cycle-ratio summation theory (Miner's rule)* is then applied to account for cumulative damage under conditions of stress cycles of different magnitude. Manson's approach is a modification of Miner's rule that attempts to take into account the order in which the stresses are applied and the damage to the static UTS that occurs as a function of a small number of cycles. The approach is still considered to be very crude but remains the best analytical approach to date. Random stress

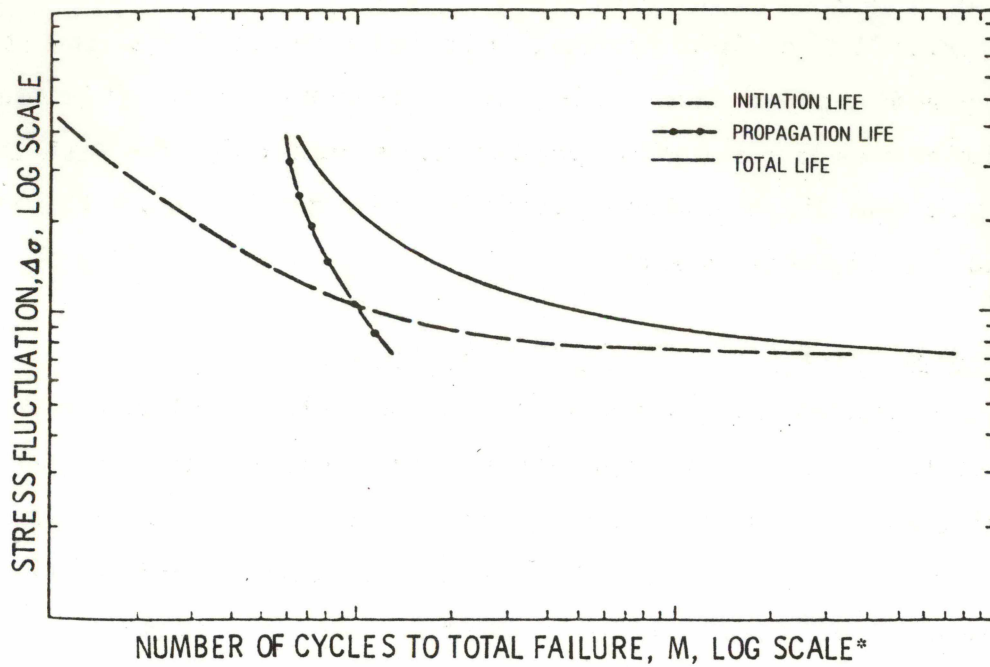
*For detailed discussion, see Shigley, 1977.

history profiles present still a higher level of difficulty, but recently much effort has been put into cycle counting methods that most accurately predict the actual life cycling; namely, (1) range mean analysis, and (2) rain flow or pagoda-roof method (Anderson & Stephens, 1974). It is because of the complexities in making life prediction estimates that the AAR Design for Fatigue Specification shows relatively little detail (Association of American Railroads, 1976, Section 4.6).

5.2 CONSTANT AMPLITUDE SLC ANALYSIS

Conventional fatigue analysis on reverse bending test coupons consist of applying a constant amplitude alternating stress on a test sample and measuring the number of cycles until it breaks. The results produce a conventional S-N curve. The total life can then be divided into the number of cycles to initiate a crack and the number of cycles to propagate a crack until the part breaks. This division of the total fatigue life is illustrated in Figure 5-1. The propagation life is the only part that can be analytically predicted based on fracture mechanics and is the basis for SLC predictions of crack growth. The portion of life that can be predicted depends on the ability to define an initial crack size as indicated by Figure 2-3. In most cases, the initial crack size is related to the limits of NDI. To calculate the remaining cycles of life due to crack growth, fracture mechanics principles must be applied. The procedure to analyze the SLC by fracture mechanics is to:

- Estimate the maximum initial size flaw in a structure based on the quality of the inspection or on the proof test loading procedures;
- Determine the fracture toughness for the appropriate section thickness, and
- Obtain an expression for the fatigue crack growth rate of the steel being analyzed.



*For initiation and propagation life, the curves show the proportions of cycles that add up to total cycles to failure.

Source: Rolfe and Barsom, 1977

Figure 5-1. Typical Fatigue Life S-N Curve Separated into Crack Initiation and Crack Propagation

Examples for room temperature and an air environment of the Paris (1963) law expression for two types of steels under constant amplitude load fluctuation are:

$$\text{martensitic steels: } \frac{da}{dN} = 0.66 \times 10^{-8} (\Delta K_I)^{2.25}$$

$$\text{ferrite-pearlite steels: } \frac{da}{dN} = 3.6 \times 10^{-10} (\Delta K_I)^3$$

where da/dN = fatigue-crack growth per cycle of loading, in./cycle,
 ΔK_I = stress-intensity-factor range, ksi $\sqrt{\text{in.}}$

- Integrate the expression to determine the number of life cycles that can be related to the crack propagation portion of the fatigue life.

As an example, using Paris' law, the minimum number of cycles for a side frame with a 1/4-in. crack to grow to 1/2 in. under a uniform loading distribution from zero to the maximum allowable stress (16 ksi for B grade, 25 ksi for C grade) would be approximately 10^5 cycles for B grade castings and approximately 2.5×10^4 cycles for C grade castings. Thus, the necessary requirements to make SLC predictions are:

- Minimum initial crack size detected with 100-percent reliability,
- Fracture toughness,
- Crack growth rate data, and
- Stress amplitude.

For random stress history profiles, SLC requires modeling or counting methods for accurate life-cycle predictions. More detail regarding appropriate analytical methods for this problem is given in the next section.

To demonstrate the difference in results between constant amplitude and random load calculations, a conservative estimate based on the Paris law is compared to a more refined analysis based on actual random stress history profile calculations as given in Section 5.3, viz:

$$\text{Grade B} = \frac{\text{life-random loading}}{\text{life-uniform loading}} = \frac{3 \times 10^6 \text{ cycles}}{1 \times 10^5 \text{ cycles}} = 30X \quad (1)$$

Correspondingly,

$$\text{Grade C} = \frac{\text{life-random load}}{\text{life-uniform load}} = \frac{4 \times 10^5 \text{ cycles}}{2.5 \times 10^4 \text{ cycles}} = 16X$$

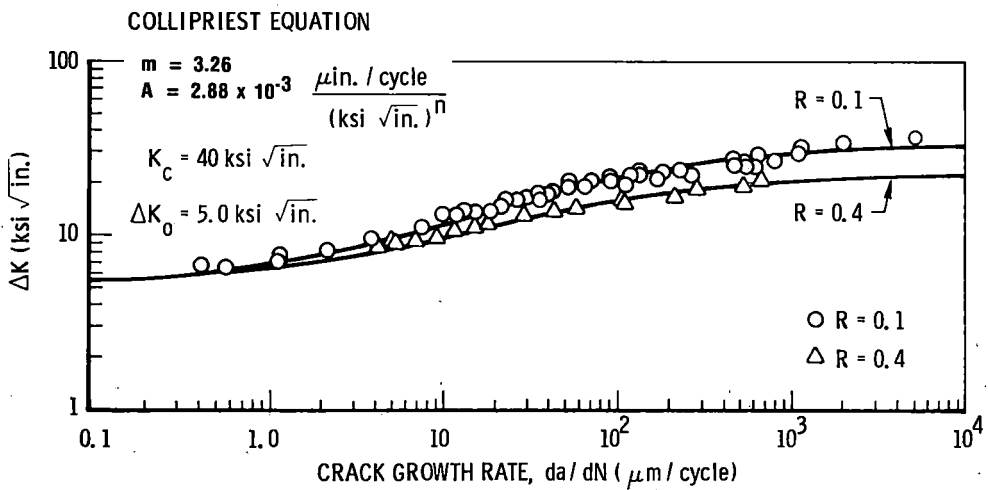
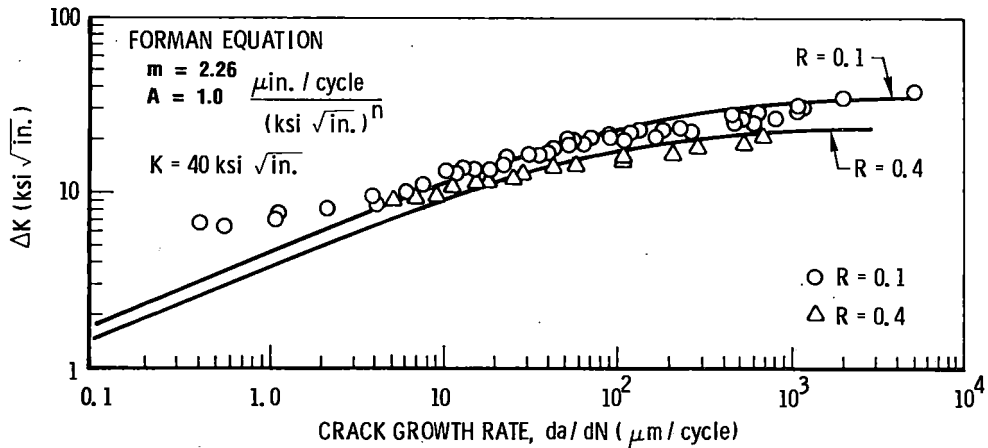
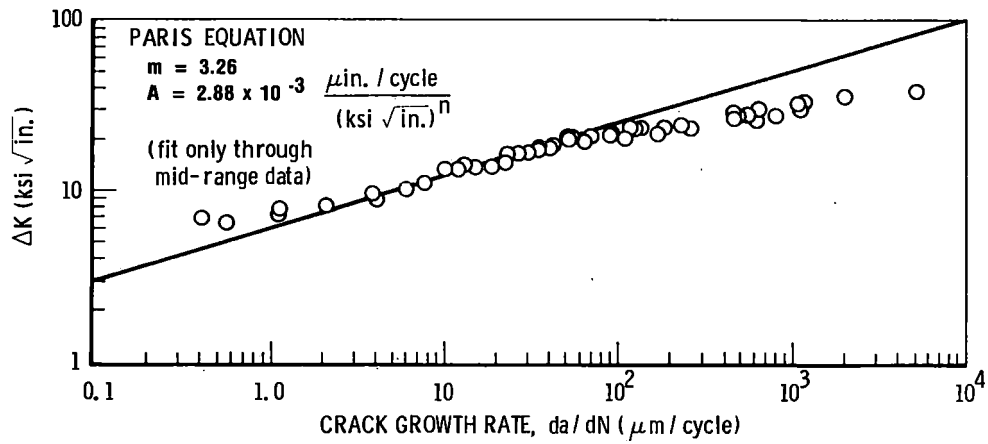
Hence, a simplified analysis based on constant amplitude or uniform loading distribution is overly conservative and would add to the cost by requiring more inspection periods because the predicted life cycles would be much less.

5.3 RANDOM LOAD EFFECTS

The details of a technically refined safety life-cycle crack growth prediction technique for randomly loaded structures will now be discussed. Essentially, this technique provides the analytical basis for guidelines. As discussed in the following sections, too many assumptions had to be made to consider the analysis exact, primarily because of the nonavailability of data. Side frames and bolsters are first-priority components for this study. The basis for this priority is the emerging availability of load spectra data for both components, and the clear evidence that a period of stable crack growth can be observed in the materials of construction. Therefore, the side frame of a freight car track was selected for this analysis as an illustrative example of the SLC prediction methods.

5.3.1 Crack Growth Laws

The available empirical fatigue crack growth laws are obtained primarily from plots of the logarithm of crack growth rate versus the logarithm of cycle stress intensity (Figure 5-2). The experimental conditions are generally constant amplitude sine wave stress cycles. Paris



R is defined as the ratio of minimum-to-maximum stress.

Source: Forman, et al., 1967

Figure 5-2. Fatigue Crack Growth Data and Interpretations

and Erdogan (1963), Forman et al. (1967), and Collipriest and Ehret (1972) have presented the crack growth equations that have received the most acceptance. The following additional selection criteria eliminate two of the crack growth equations from consideration.

- Stress ratio effects (R) must be included.
- Catastrophic crack growth (i. e., critical crack sizes, a_c) must be included.
- Threshold conditions for crack growth are desirable.
- Mathematical tractability of the form of the crack growth law is desirable.

The simplified Paris (1963) relation was rejected for the detailed random load analysis because it fails to include catastrophic growth and/or stress ratio effects. The Paris law is:

$$\frac{da}{dN} = A (\Delta K)^m = A [Y(\Delta\sigma)\sqrt{\pi a}]^m \quad (2)$$

Where:

- N = number of fatigue cycles,
- ΔK = cyclic stress intensity factor = $Y(\Delta\sigma)\sqrt{\pi a}$,
- Y = crack and specimen geometric factor (on the order of unity),
- $\Delta\sigma$ = cyclic stress,
- a = crack half-length* or characteristic dimension,
- A = an empirical material parameter, and
- m = an empirical crack growth exponent.

The Collipriest (1972) empirical equation contains the desired features of catastrophic propagation, stress ratio, and lower threshold stress intensity, but seriously compromises mathematical tractability.

The Collipriest equation is:

$$\frac{da}{dN} = A(K_c \Delta K_o)^{m/2} \exp \left[\ln(K_c / \Delta K_o)^{m/2} \tanh^{-1} \left\{ \frac{\ln[(\Delta K)^2 / \{[1-R]K_c (\Delta K_o)\}]}{\ln[(1-R) K_c / \Delta K_o]} \right\} \right] \quad (3)$$

*This somewhat inconvenient terminology, which is historical in fracture mechanics literature, is based on theoretical convenience and is retained in this report.

where:

K_C = fracture toughness, or stress intensity
 ΔK_0 = threshold stress intensity,
 R = stress ratio: $(\sigma_{\min} / \sigma_{\max})$, and
 ΔK = cyclic stress intensity.

The Forman (1967) empirical equation retains the desired features of catastrophic growth, stress ratio, and mathematical tractability, but does not incorporate the lower threshold cyclic stress intensity for growth. The Forman equation is:

$$\frac{da}{dN} = \frac{A(\Delta K)^m}{(1-R)K_C - (\Delta K)} \quad (4)$$

The Forman relation was adopted for the random load analysis because it is conservative in ignoring the growth threshold, somewhat overestimating the rate of early crack growth, and, therefore, underestimating the total fatigue life due to crack growth.

5.3.2 Significant Indices of Random Loading Parameters

The theoretical analysis of the response of linear systems to random input is well developed. Linear systems that have been analyzed for response to random input include optical lens systems, active and passive electrical and electronic circuits, and linear (elastic) structural dynamic response resulting from mechanical and/or aerodynamic stimulation. Such systems are usefully characterized by linear differential equations. For linear systems, the power spectrum concept is a powerful analytical tool. The energy indices of such systems are the squares of the velocities (kinetic energy) or the squares of the displacements (stored elastic energy). Thus, central concepts generally relate to mean values and mean square values for governing parameters.

The crack growth rate equations are nonlinear first-order differential equations. This nonlinearity suggests that the mean and/or mean square of the driving parameters (cyclic loading factors) may be inappropriate descriptors of response under random loadings. Examining the Paris (1963) empirical crack growth equation suggests that the instantaneous crack growth rate depends on the cyclic stress intensity raised to an arbitrary (material-dependent) power. The appropriate statistical index of random loading for crack propagation is the stress intensity to the same material-dependent power. Because the cyclic stress intensity is linearly related to cyclic stress, the appropriate cyclic statistical index is the mean of the cyclic stress intensity taken to the power m . For relatively rigid structural members (nonfluttering) loaded in the elastic range, the stress is proportional to load; hence, the appropriate load statistic is the mean of the cyclic load taken to the power m .

The Forman (1967) empirical relation has certain similarities to the Paris relation for small cyclic stress intensities, particularly for cyclic stresses significantly less than those giving rise to immediate catastrophic failure (i. e., for $(\Delta K) \ll K$). An attractive, mathematically simple generalization is that the appropriate loading statistic for the Forman relation is the (material-dependent) mean of the cyclic stress intensity taken to the power m . Thus, if the instantaneous crack growth rate is given by

$$\frac{da}{dN} = A \frac{(\Delta K)^m}{(1-R) K_c - (\Delta K)} \quad (5)$$

the average growth rate of an ensemble of cracked specimens under random loading is approximated by

$$\frac{\overline{da}}{\overline{dN}} = \frac{\overline{A(\Delta K)^m}}{(1-R) K_c - [\overline{(\Delta K)^m}]^{1/m}} \quad (6)$$

where:

$\overline{(\Delta K)}^m$ = average of the cyclic stress intensity taken to the power m
(the overbar means average)

$\frac{d\bar{a}}{dN}$ = average crack growth per load cycle

For a linearly loaded structure, the relationship between stress at a specific location, say \vec{x} , and applied load, say P, is estimated by $\sigma = \phi(\vec{x}) P$ where $\phi(\vec{x})$ is an influence coefficient, or $\sigma = \phi P$. The cyclic stress is similarly linearly related to the cyclic load $(\Delta\sigma) = \phi(\Delta P)$.

For a given location within a component, the proportionality between load and stress may be obtained by theoretical analysis (by various exact or approximate elasticity solutions including finite element analysis) or by experiment (e.g., photoelasticity, strain gages). The heuristic derivation given above leads to crack growth relations such as:

$$\frac{d\bar{a}}{dN} = \frac{A \overline{(Y\sigma)}^m (\pi\bar{a})^{m/2}}{(1-R)K_c - (\pi\bar{a})^{1/2} \left\{ \overline{(Y\sigma)}^m \right\}^{1/m}}$$

or:

$$\frac{d\bar{a}}{dN} = \frac{A(\overline{Y\tilde{\sigma}})^m (\pi\bar{a})^{m/2}}{(1-R)K_c - (\pi\bar{a})^{1/2} (\overline{Y\tilde{\sigma}})} \quad (7)$$

where:

$$\tilde{\sigma} = \left(\frac{\overline{(\sigma)^m}}{(\sigma)} \right)^{1/m}$$

The working hypothesis is that the appropriate index of load or stress spectrum for crack growth computations is the mth root of the mean mth power of the statistical variable. The appropriate exponent (m) for statistical loading is to be deduced from the appropriate exponent (m) for simple loading. This working hypothesis should be verified by experiment. The scope of the present investigation does not include verification testing.

5.3.3. Common Loading Spectra

A variety of mathematical expressions are available to describe actual random service loading. Fatigue life-cycle predictions are sensitive to detailed characteristics of the random load spectrum. This sensitivity is central to the planning of data collection programs and extrapolation of life predictions from one type of car or one track condition to another.

The standard mathematical probability distributions that might be used to mathematically model random load spectra include the uniform, Gaussian, Rayleigh, gamma, and beta distributions. The different probability functions are described in detail in the appendix. The applicability of these functions with regard to SLC will now be discussed with the use of the crack growth life prediction models.

5.3.4 Crack Growth Predictions from Crack Growth Equations

The Forman (1967) crack growth relation:

$$\frac{da}{dN} = \frac{A[Y(\Delta\tilde{\sigma})\sqrt{\pi a}]^m}{(1-R)K_c - Y(\Delta\tilde{\sigma})\sqrt{\pi a}} \quad (8)$$

where the material parameters are:

- A = crack growth coefficient
- m = crack growth exponent
- K_c = fracture toughness

and the loading and component design-dependent parameters:

- R = minimum/maximum stress ratio
- $\Delta\tilde{\sigma}$ = effective cyclic stress range
- Y = crack geometry term

can be integrated to provide the following relationship between initial crack size a_o , final crack size a_N , and number of fatigue cycles N.

$$N = \frac{2(1-R)K_c}{\pi A [Y(\Delta\tilde{\sigma})]^m} \cdot \frac{1}{(m-2)} \left\{ \frac{1}{(\pi a_o)^{m-2/2}} - \frac{1}{(\pi a_N)^{m-2/2}} \right\} \\ + \frac{2 Y \Delta\tilde{\sigma}}{\pi A [Y(\Delta\tilde{\sigma})]^m} \cdot \frac{1}{(m-3)} \left\{ \frac{1}{(\pi a_N)^{m-3/2}} - \frac{1}{(\pi a_o)^{m-3/2}} \right\} \quad (9)$$

The special cases (i. e., where $m = 2$ or 3) require separate treatment because of singularities in the above relationship. For $m = 2$, the integration results are:

$$N = \frac{(1-R)K_c}{A [Y(\Delta\tilde{\sigma})]^2 \pi} \left[\ln (a_N/a_o) \right] - \frac{2\sqrt{a_o}}{\sqrt{\pi} A [Y(\Delta\tilde{\sigma})]} \left[(a_N/a_o) - 1 \right] \quad (10)$$

and for $m = 3$ the results are:

$$N = \frac{(1-R)K_c}{2A(Y\Delta\tilde{\sigma}\sqrt{\pi})^3 \sqrt{a_o}} \left[1 - \sqrt{a_o/a_N} \right] - \frac{\ln(a_N/a_o)}{\pi A (Y\Delta\tilde{\sigma})^2} \quad (11)$$

Engineering interest is centered on determining the approximate number of cycles required to cause significant crack growth under the intended service conditions and not the dependence of crack size on the number of fatigue cycles. A convenient definition of significant crack growth is infinite crack growth; $a_N = \infty$. The number of fatigue cycles for infinite growth of a crack of initial size a_o may thus be written:

$$N_{a_o} = \frac{2}{\pi A (Y\Delta\tilde{\sigma})^m} \left\{ \frac{(1-R)K_c}{[(m-2)(\pi a_o)]^{(m-2)/2}} - \frac{Y(\Delta\tilde{\sigma})}{[(m-3)(\pi a_o)]^{(m-3)/2}} \right\} \quad (12)$$

From this relationship, the number of cycles for growth from size a_0 to a_1 may be obtained by:

$$N_{(a_0 \rightarrow a_1)} = N_{a_0} - N_{a_1}$$

Certain design structures, such as railroad cars, are conveniently described in terms of a static mean load or stress with a superimposed fluctuating (equivalent) load or (equivalent) stress. In this case, it is desirable to change variables using the following relationships:

$$\begin{aligned} \Delta\sigma &= \sigma_{\max} - \sigma_{\min} \\ R &= \sigma_{\min} / \sigma_{\max} \\ \sigma_{\text{mean}} &= (\sigma_{\max} + \sigma_{\min}) / 2 \\ \sigma_{\min} &= \sigma_{\text{mean}} - (\Delta\sigma) / 2 \\ \sigma_{\max} &= \sigma_{\text{mean}} + (\Delta\sigma) / 2 \\ R &= [2\sigma_{\text{mean}} - (\Delta\sigma)] / [2\sigma_{\text{mean}} + (\Delta\sigma)] \end{aligned}$$

The previous relationship thus becomes:

$$N_{a_0} = \frac{2}{\pi A [Y(\Delta\tilde{\sigma}) \sqrt{\pi a_0}]^m} \left\{ \frac{Y(\Delta\tilde{\sigma}) K_c}{[2\sigma_{\text{mean}} + (\Delta\sigma)] [m-2]} - \frac{Y(\Delta\tilde{\sigma}) \sqrt{\pi a_0}}{(m-3)} \right\} \quad (13)$$

This equation describes the fatigue life of a structure containing a small initial defect of size a_0 when it is subjected to a fluctuating load or stress ($\Delta\tilde{\sigma}$) superimposed on a mean or static loading (σ_{mean}).

The special cases for $m = 2$ and 3 can be treated as follows: The cyclic crack growth rate approaches infinity as the crack size approaches the critical crack size (a_c).

$$\frac{da}{dN} \rightarrow \infty \quad \text{as} \quad a_N \rightarrow [(1-R)K_c / \Delta\tilde{\sigma}]^2 / \pi = a_c \quad (14)$$

Substitution of this value for a_N into the integrated forms of the growth relationships provides:

$$N_{\infty} = \frac{(1-R)K_c}{\pi A [Y(\Delta\tilde{\sigma})]^2} \ln \left\{ \left[\frac{(1-R)K_c}{Y(\Delta\tilde{\sigma})} \right]^2 \frac{1}{\pi a_o} \right\} - \frac{2\sqrt{a_o}/\pi}{A(Y\Delta\tilde{\sigma})} \left[\frac{(1-R)K_c}{Y(\Delta\tilde{\sigma})\sqrt{\pi a_o}} \right]^{-1} \quad (15)$$

for $m = 2$ and

$$N_{\infty} = \frac{(1-R)K_c}{2 [Y(\Delta\tilde{\sigma})\sqrt{\pi}] \sqrt{a_o}} \left[1 - \frac{Y(\Delta\tilde{\sigma})\sqrt{\pi a_o}}{(1-R)K_c} \right] - \frac{2}{A(Y\Delta\tilde{\sigma})^2} \ln \left\{ \frac{(1-R)K_c}{Y(\Delta\tilde{\sigma})\sqrt{\pi a_o}} \right\} \quad (16)$$

for $m = 3$.

For the more general case ($m \neq 2$ or 3), one may write:

$$N_{\infty} = \frac{2(1-R)K_c}{\pi A [Y(\Delta\tilde{\sigma})]^m} \frac{1}{(m-2)} \left\{ \frac{1}{(\pi a_o)^{(m-3)/2}} - \frac{1}{(\pi a_c)^{(m-2)/2}} \right\} - \frac{2Y\Delta\tilde{\sigma}}{\pi A [Y(\Delta\tilde{\sigma})]^m} \frac{1}{(m-3)} \left\{ \frac{1}{(\pi a_c)^{(m-3)/2}} - \frac{1}{(\pi a_o)^{(m-3)/2}} \right\} \quad (17)$$

If desired, in all the above equations, the change of variables results in the simple substitution:

$$(1-R) = (\Delta\tilde{\sigma}) / [\sigma_{\text{mean}} + (\Delta\tilde{\sigma})/2]$$

Equations 14 through 17 form the basis for the life estimation charts in Section 5.3.6.

Another model for treating spectrum loads was proposed by Barsom (1976). As discussed in Appendix B, the results are shown to be consistent with the proposed model, which appears to be a general form of the Barsom model. Sufficient data do not exist to discriminate at this time.

5.3.5 Distribution Function for Load Spectra of Railroad Cars

Data have been recently reported from instrumented freight cars running on a field track (Johnson, 1974 and 1976, and AAR M203, Section A). The reduced data for vertical track loading are given (Figure 5-3) for a loaded hopper car and a loaded tank car (100-ton capacity, 263-kip rail load). The character of the car type is evident in two ways. First, the tank car load distribution function at higher speeds appears more curved (sigmoidal). Second, the load spectrum appears greater for the tank car, even though equal mass is involved. Sloshing of the liquid may account for both effects.

For the loaded hopper car, the data (Figure 5-3) suggest a logarithmic linear approximation for the number of exceedances per mile (N_M) and the maximum or minimum loadings (P_{max} and P_{min}) as:

$$P_{max} = P_{mean} - Q \ln(N_M/N_o)$$

$$P_{min} = P_{mean} + Q \ln(N_M/N_o)$$

or

$$\Delta P = 2Q \ln(N_M/N_o)$$

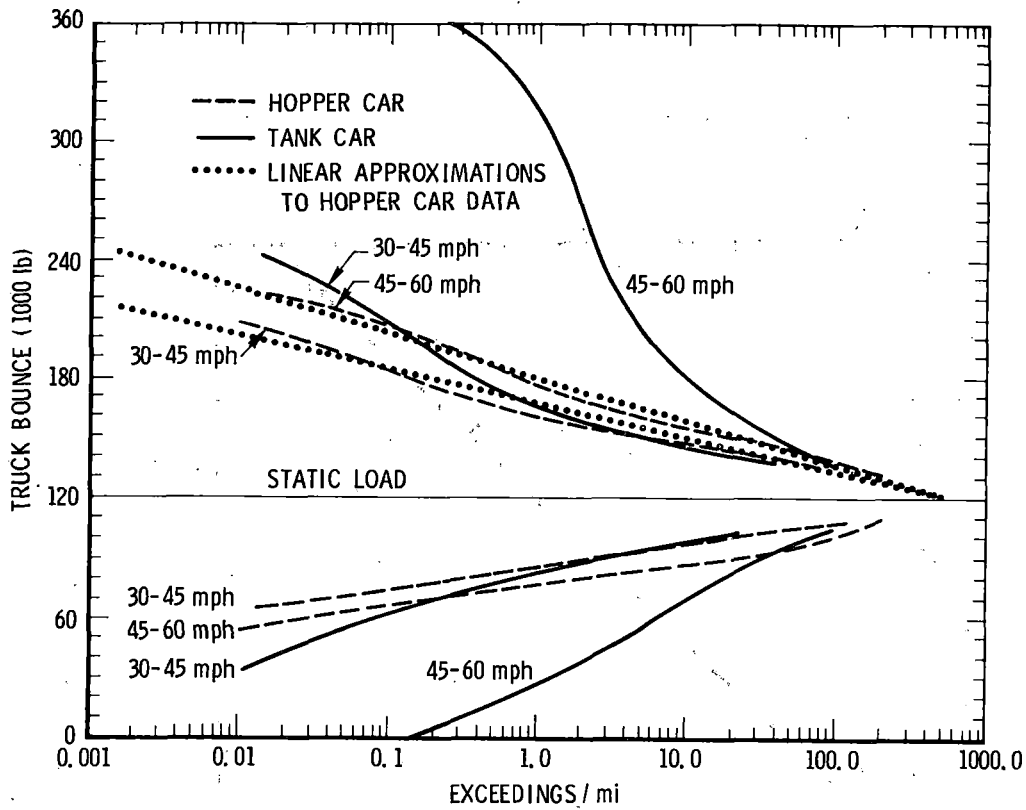
or

$$N_M = N_o \exp - (\Delta P/2Q)$$

Graphical curve fitting provides the data in Table 5-1.

The speed dependence of the load spectrum is then controlled by the parameter Q ; the linear dependence of Q on velocity is approximated as shown in Figure 5-4. The available data thus indicate that a good approximation is:

$$Q = BV$$



Source: Johnson, 1976

Figure 5-3. Truck Bounce Load Spectra

Table 5-1. Hopper Car Load Distribution Parameters

Speed Range (mph)	Median Speed (mph)	P_{mean} (kip)	N_o (cycles/mile)	Q (kip)
45-60	52.5	120	600	9.77
30-45	37.5	120	600	7.37

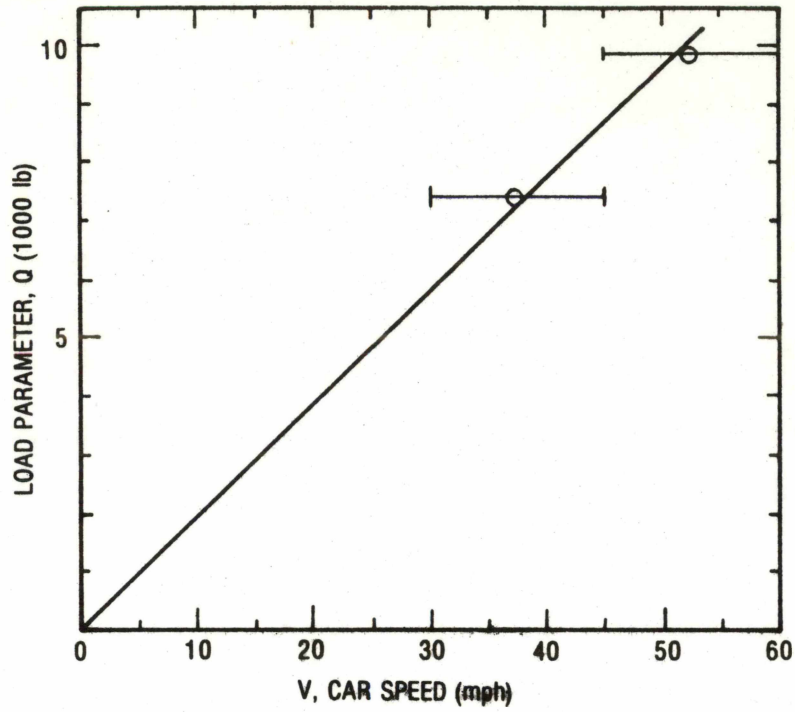


Figure 5-4. Apparent Dependence of Load Parameter on Car Velocity for Loaded Hopper Car

where:

$$B = 0.190 \text{ (kip/mph).}$$

Since $N_M = N_0 \exp \left[-\left(\frac{\Delta P}{2Q}\right) \right]$, it follows that the mean cyclic load is given by

$$\overline{(\Delta P)} = (2Q)$$

By comparing the load spectra of Figure 5-3 with the mathematical descriptions discussed (in Appendix A), it is seen that the loaded hopper car truck bounce approximates a particular gamma loading distribution (i. e., with $\alpha = 0$).

The gamma distribution shown in Appendix A can be used to estimate the appropriate equivalent cyclic load for crack growth. For example, for a material with crack growth exponent $m = 3.3$ (a low alloy steel), the effective cyclic load for growth is essentially twice the mean cyclic load. The reason for this magnification is the nonlinear nature of crack growth and the greater physical consequences of large load cycles relative to small load cycles.

5.3.6 Life Prediction Diagrams

Reduced to the simplest elements, the variables relevant to crack propagation lifetimes are still sufficiently numerous to require a series of figures for proper presentation. These variables are given in Table 5-2.

In the elementary sense, nine significant parameters are introduced. Three are related to material properties (i. e., fracture toughness and two cyclic growth parameters); four are related to the stress environment (e. g., load-stress relationship, mean static stress, and statistical characteristics of the cyclic random stressing); and two are related to the defect state of a given component (i. e., the defect size and shape).

Table 5-2. Crack Propagation Variables for Life Estimation

Material Parameters	Defect Parameters	Loading Parameters
Fracture toughness, K_{Ic} Crack growth exponent, m Growth coefficient, A	Crack size, a_0 Crack shape, Y	Load/stress proportion, ψ Mean stress, σ_{mean} Cyclic stress distribution function Equivalent cyclic stress, $\Delta\sigma$

Before graphically presenting life prediction diagrams, several factors must be considered. The load/stress relationship is beyond the scope of this investigation and should be separately treated for each component. Preliminary member sizing is often performed on the basis of static stress. This is explicitly true for railroad truck components specified by load ratings. The AAR design specifications (M203, Section A) specifically identify allowable static stresses for various grades of materials and applications (e. g., class B steels in bolsters or side frames). In this regard, it is sensible to use mean stress as a major parameter (of nearly equal significance to other material properties) in life-time prediction diagrams.

The cyclic stress distribution function (which may be car-dependent, as in the comparison between loaded hopper car versus loaded tank car) and equivalent cyclic stress were discussed previously. Thus the experimental procedures for determining these variables are already available.

The major remaining considerations are the crack size and shape. In all of the previous derivations, crack shape could be treated by adjusting the cyclic stress $\Delta\sigma$ by a multiplying factor Y. Initial crack size depends on manufacturing and field inspection technology and is a dominating variable in the life-cycle methodology.

With these comments in mind, relevant variables (Table 5-3) and systematic variation of life prediction factors (Table 5-4) are treated systematically in life prediction charts (Figures 5-5 through 5-10) for each case. In keeping with the empirical observation that very slow cyclic crack growth rates tend to be equal for most structural steels, it was assumed that $da/dN = 3 \times 10^{-7}$ in./cycle for a cyclic stress intensity ΔK of 10 ksi $\sqrt{\text{in.}}$.

Table 5-3. Structure of Variables in Life Prediction Charts

Axes	Constant Factors	Parametric Variable	Indirect Variables*
Load cycles to failure, N	Mean stress, σ_{mean} (Static stress)	Equivalent cyclic stress, $\Delta\tilde{\sigma}$	Cyclic stress distribution function
Initial crack size, a_0	Fracture toughness, K_c		Crack shape, Y
	Crack growth exponent, m		Load/stress transformation, ψ
	Growth coefficient, A		

*Indirect variables are processed by other charts and equations to produce the variables included in the charts.

Table 5-4. Systematic Variation of Life Prediction Factors

Case	Fracture Toughness, K_c	Growth Exponent, m	Growth Coefficient, A	Mean Stress, σ_{mean}
I	66.0	4.0	1.68×10^{-9}	5
II	66.0	4.0	1.68×10^{-9}	10
III	33.0	4.0	6.90×10^{-10}	5
IV	33.0	4.0	6.90×10^{-10}	10
V	66.0	6.0	5.32×10^{-8}	10
VI	66.0	2.5	1.68×10^{-11}	10

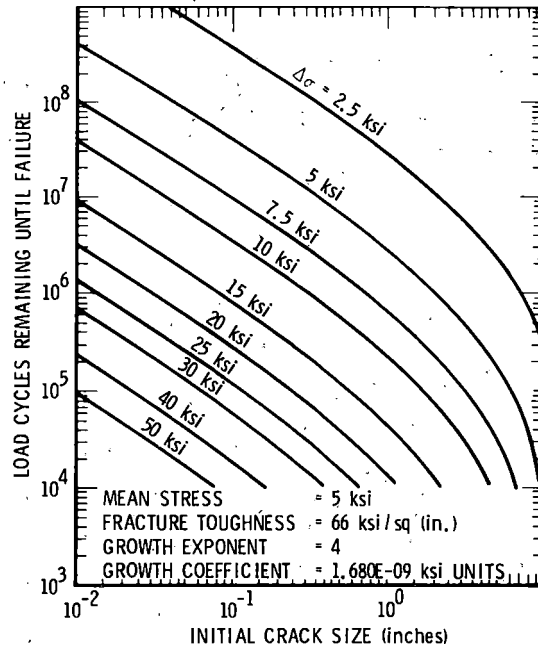


Figure 5-5. Life Prediction Chart - Case I

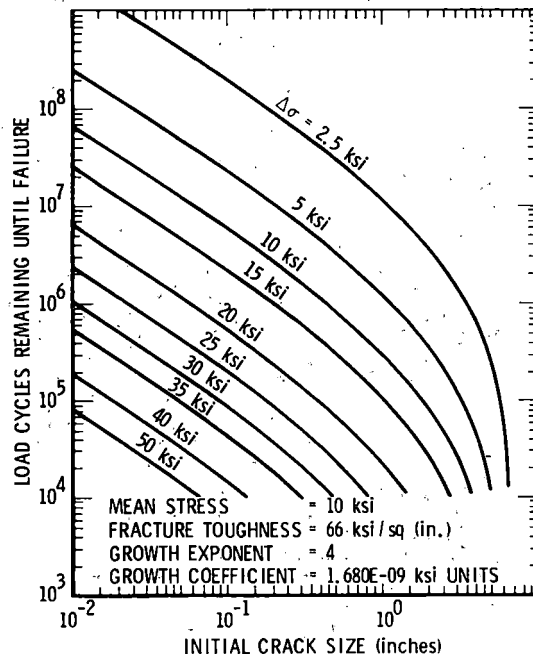


Figure 5-6. Life Prediction Chart - Case II

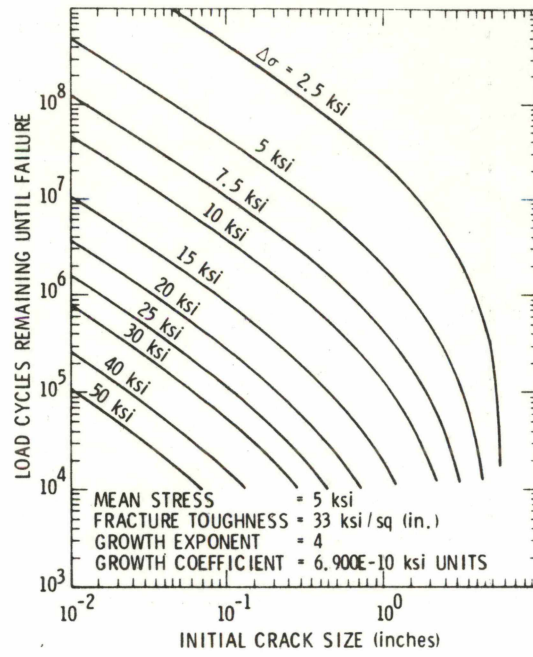


Figure 5-7. Life Prediction Chart - Case III

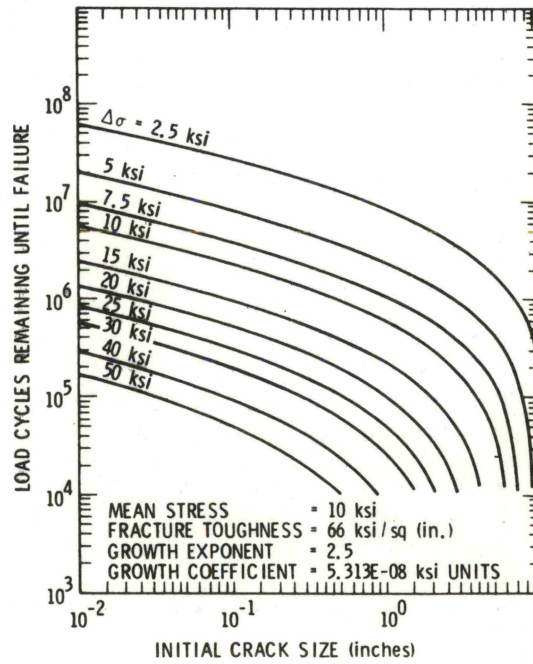


Figure 5-8. Life Prediction Chart - Case IV

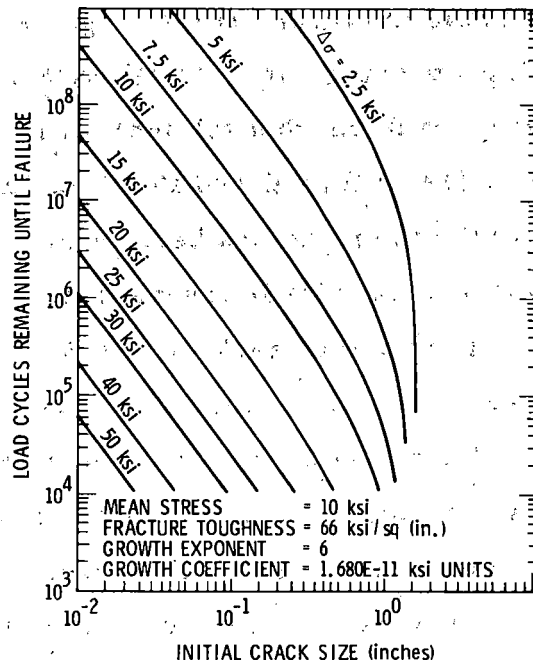


Figure 5-9. Life Prediction Chart - Case V

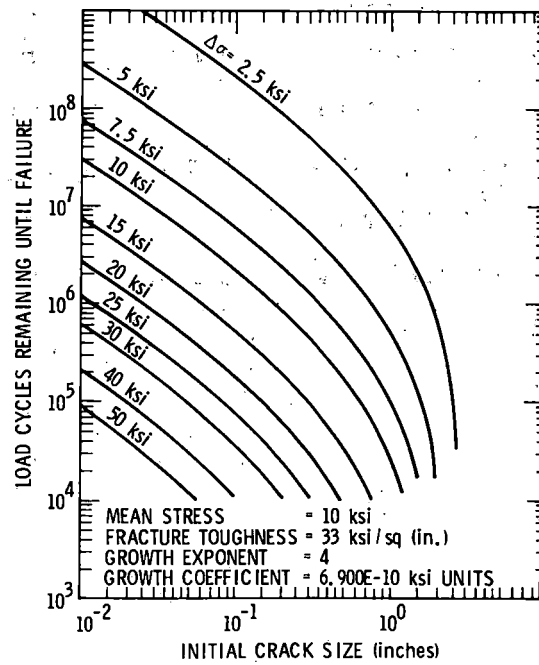


Figure 5-10. Life Prediction Chart - Case VI

Cases I and II (as well as III and IV) illustrate the influence of mean stress. Increasing the mean stress (e. g., static car loading) decreases the crack propagation life. In all cases, increasing the cyclic load (e. g., increasing track roughness) decreases life.

Cases I and III (as well as II and IV) illustrate the effects of fracture toughness (with other parameters held constant). For very small cracks, the crack propagation life is insensitive to fracture toughness. For relatively large cracks, the crack propagation life is significantly increased (or decreased) by increasing or decreasing fracture toughness. Steel composition and/or metallurgical variables are an important controlling factor of fracture toughness, as is service temperature (i. e., decreasing service temperature generally decreases fracture toughness).

Cases V and VI illustrate the effect of the crack growth exponent. For very small cracks under low cyclic loading, increasing the crack growth exponent results in increased crack propagation lifetimes (reduced lifetimes result from large cracks). The crack growth exponent is related to metallurgical variables as well as, to some extent, temperature. As a rough approximation, nearly equivalent propagation lifetimes are attained when the initial cyclic stress intensities approach $10 \text{ ksi} \sqrt{\text{in.}}$. In a mathematical sense, the crack growth exponent is inversely related to the range of applied cyclic stress intensity separating slow from catastrophic growth.

6. APPLICATION OF RANDOM LOAD ANALYSIS TO A SIDE FRAME

In this section, the general safety life-cycle (SLC) random load analysis for crack propagation is applied to a side frame under vertical loading. It is recognized that vertical loading presents only one of the potential failure modes. However, this example is an illustration of the evaluation approach rather than a final analysis.

6.1 SPECTRUM OF CYCLIC STRESSES IN A SIDE FRAME

The data available are expressed in external loadings applied to the side frame; they are not the stresses developed within the side frame structural element. It will be assumed that the stresses are proportional to the loads, but the proportionality constant is not defined. Various analytical methods (e.g., finite element) should be applied, or appropriate experiments could be performed (e.g., photoelastic models, coatings, strain-gaged loadings) to determine the actual stresses developed.

In the absence of definitive stress information, estimation, and sensitivity studies are adopted; the source of the estimate is a paper by Johnson (1974). He estimates that current railroad truck design practice, as allowed by the AAR 203 standard and as implemented in existing components, results in static stress of approximately 8000 psi for the static load.

The proportionality constant would therefore be:

$$\psi \cong \frac{8000 \text{ psi}}{120 \text{ kip}} = 67 \text{ psi/kip}$$

Thus, for loaded hopper cars run in the 45- to 60-mph range, using the values from Table 5-1, the mean cyclic stress, $\overline{\Delta\sigma}$, would be:

$$\overline{\Delta\sigma} = \psi \overline{\Delta P} = \psi 2Q = 1309 \text{ psi}$$

6.2 SIGNIFICANT LOADING PARAMETER FOR STEEL CASTINGS USED FOR SIDE FRAME MATERIAL

The significant statistic of this loading distribution depends on the fatigue crack propagation characteristics of the side frame materials. Relatively little is known about the fatigue crack propagation properties of railroad side frame steel components. The limited data available from Johnson (1974) are reproduced in Figure 6-1 with a fit to the Forman relation and a comparison with another low alloy structural steel. It is evident that the fit must be considered tentative as must any conclusions arising from the use of this fit.

The crack growth exponent is approximately 4.0, and the fracture toughness is taken to be $66 \text{ ksi}\sqrt{\text{in.}}$. The value of these parameters should be reviewed when and if direct data become available.

For the particular gamma loading distribution associated with hopper car side frames in railroad service and for the particular crack propagation exponent of side frame material, Appendix A (Figure A-4(b)) explains for $\alpha = 0$ and $m = 4$, that the significant loading statistic is 2.1 times the average cyclic load. Thus, the effective cyclic loading on a side frame for a car running at a median speed of 52.5 mph is 41.0 kip (i. e., 4.2 Q). The mean (static) loading is 120 kip; therefore, the effective cyclic component is 34.2 percent of the static load. The data given in Figures 5-4 and 5-5 imply that the effective cyclic component scales linearly with average car velocity; thus, the effect of higher and lower speed car operation can be estimated. It should be emphasized that all load spectra available ignore such special events as car switching, humping, and coupling loads.

In the absence of detailed stress analysis, the effective dynamic-to-static loading proportion defined above can be used to bound the crack

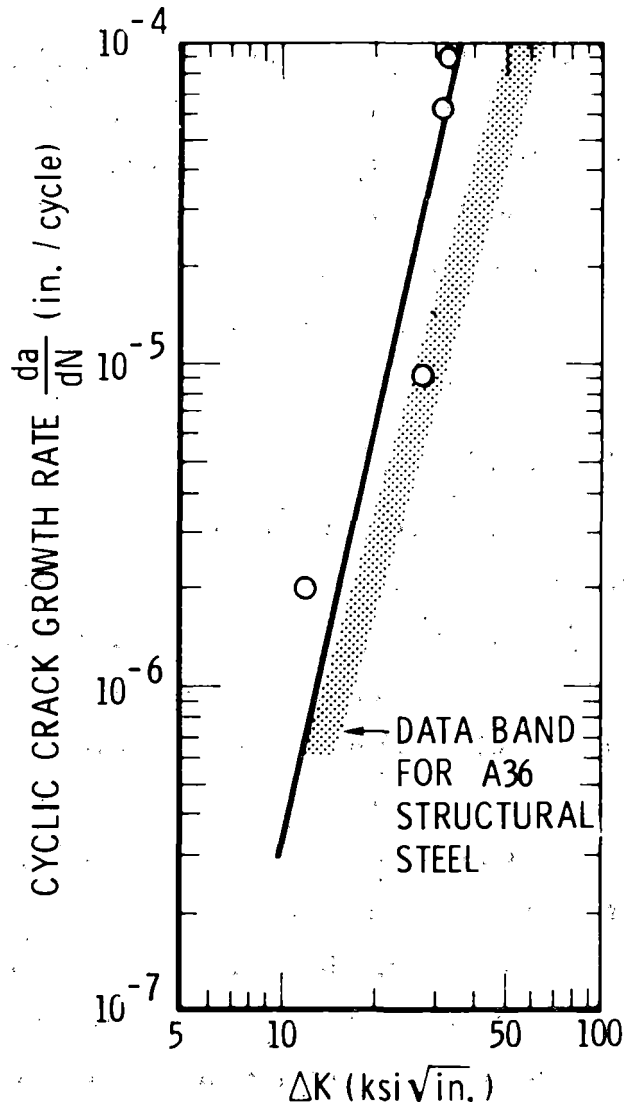


Figure 6-1. Johnson's (1974) Side Frame Crack Growth Data versus Low Alloy Structural Steel Data

propagation response of the side frame. Other bounds can be attained from the maxima allowed by the AAR standards (with and without allowances for stress concentrations from fillets and cutouts) or experienced estimates, such as those of Johnson. It is clear that under the present circumstances (e. g., life prediction of a component in the absence of stress analysis), bounding estimates are appropriate, as is the consideration of large safety factors.

6.3 SIDE FRAME LIFE ESTIMATES

The information available is meager; it consists of the ratio of static and dynamic loads and crude estimates of static stresses (Table 6-1).

For sensitivity analysis, one can consider three nominal mean stresses (10, 15, and 25 ksi). The relevant life estimation curves are given in Figure 6-2 for ambient temperature operation (i. e., $K_c = 66 \text{ ksi} \sqrt{\text{in.}}$). An equivalent chart simulating low temperature operations (i. e., $K_c = 33 \text{ ksi} \sqrt{\text{in.}}$) is given in Figure 6-3 for comparison.

The crack propagation life estimates are insensitive to fracture toughness for small initial cracks (i. e., less than 0.05 in.) and greatly sensitive to initial crack size for large cracks (i. e., greater than 0.5 in.). The greatest sensitivity is noted for the least mean stress cases (e. g., Johnson's estimate - case D - and the AAR nominal allowable - case A).

6.4 ALLOWABLE FLAW SIZE REQUIREMENTS AND SAFE-LIFE ESTIMATES

There are two kinds of opportunities to control, measure, or otherwise limit flaw size. The first is through quality control and inspection of new components during car construction. The second is through periodic service inspection.

Table 6-1. Estimates of Side Frame Loading

Case	Mean (static) Stress (ksi)	Effective Cyclic Stress* (ksi)	Comments
A	16.0	5.5	AAR nominal allowable
B	25.0	8.6	Case A with lightening holes
C	8.0	2.7	Johnson estimate
D	10.0	3.4	Similar to Johnson estimate
E	25.0	5.0	Case B at 31 mph
F	25.0	10.0	Case B at 61 mph

*Effective cyclic stresses for 52.5 mph operation unless otherwise noted.

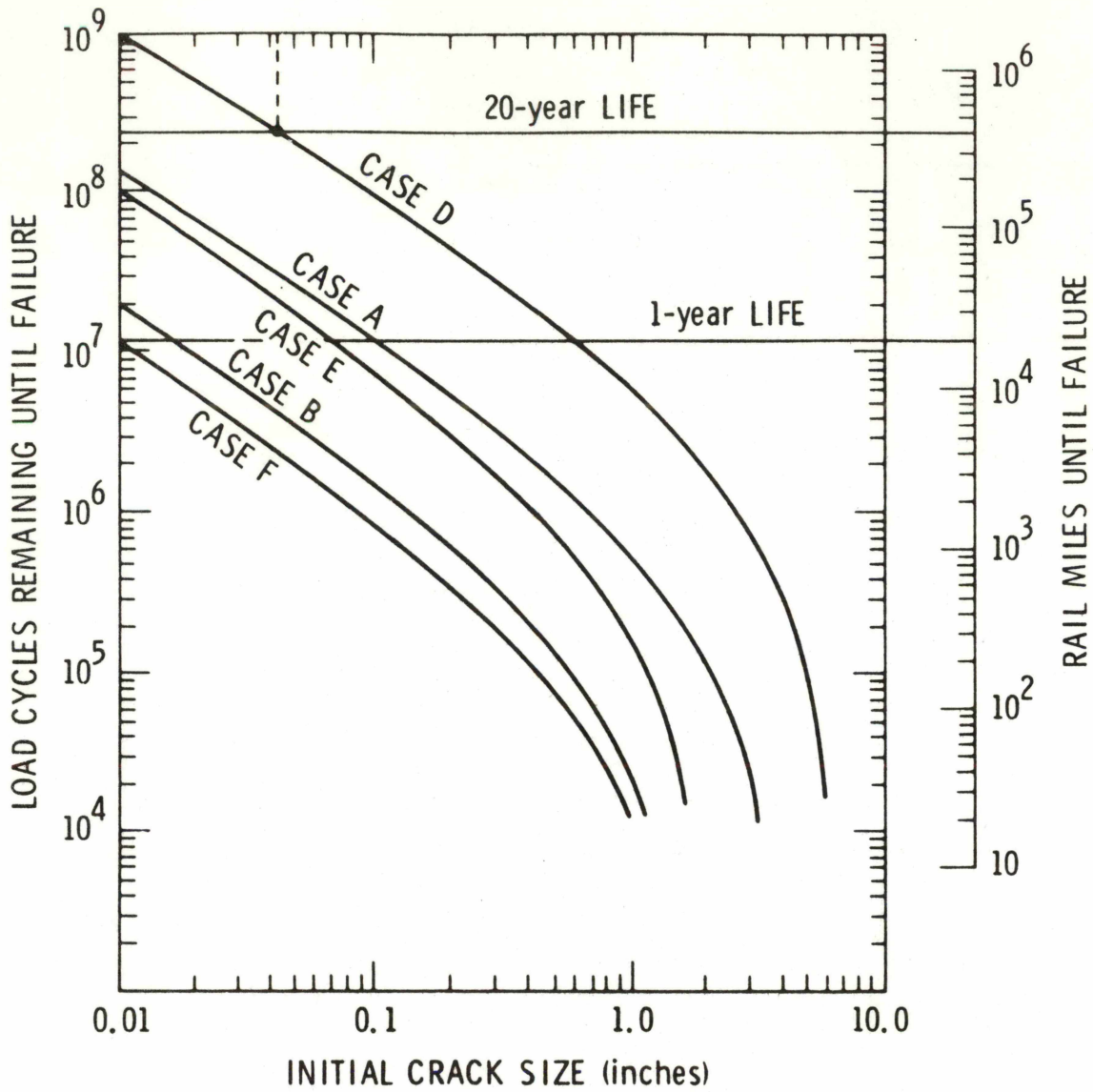


Figure 6-2. Relationships Between Initial Crack Size, Load Cycles, and Rail Miles for Nominal Toughness Conditions ($K_c = 66 \text{ ksi } \sqrt{\text{in.}}$)

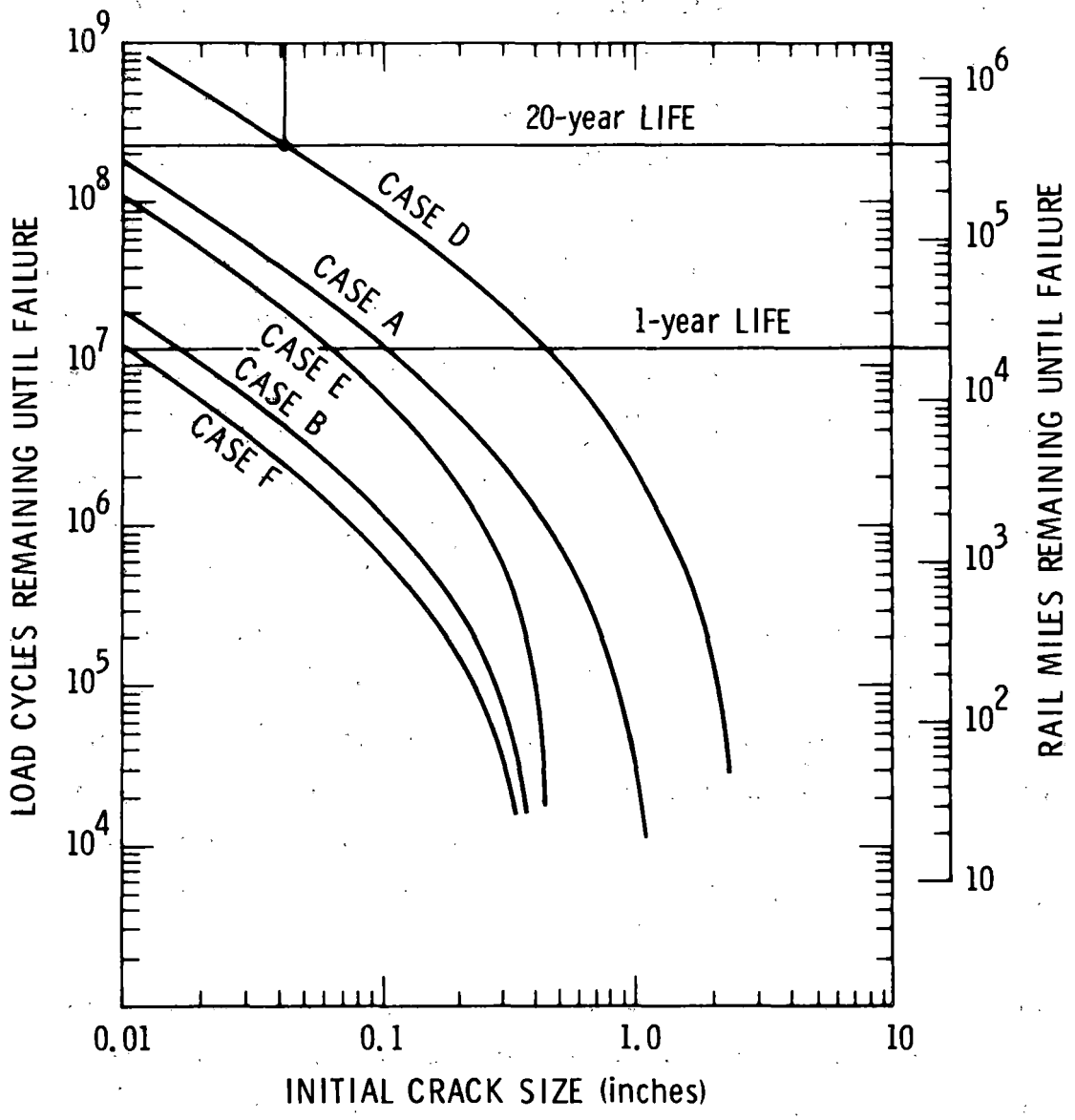


Figure 6-3. Relationship Between Initial Crack Size, Load Cycles, and Rail Miles for Reduced Toughness Conditions ($K_c = 33 \text{ ksi } \sqrt{\text{in.}}$)

6.4.1 Inspection of New Components

The side frame life estimates can be used to define the flaw detection requirements sufficient to ensure a nominal 20-year life for railroad truck side frames. The existing charts assume 100-percent fully loaded utilization at 52.5 mph. The total mileage is estimated at 400,000, based on 20,000 miles per year.

Figures 6-2 and 6-3 indicate that initial flaws of less than 0.040 in. would not be injurious to service life if the modified Johnson side frame stress estimate is correct (Case D). Full utilization of the AAR allowables would provide components with tolerance for noninjurious flaws somewhat less than 0.01 in. The more severe loading (increased static and dynamic stresses) is responsible for this decreased tolerance for initial defects.

Comparison of Cases E, B, and F (in that order) illustrates the life expectancy trend associated with increased service speed. These same cases illustrate (for 1 year of life) decreased initial flaw tolerance trends for increased operational speeds. In Case D, dropping the operational speed from 52.5 to 38 mph would raise the 20-year initial defect tolerance from 0.040 to 0.080 in. (i.e., approximately a two-fold increase).

Initial flaw detection by NDI techniques may be used during component acceptance to provide assurance that injurious flaws are absent. There are a variety of techniques available, each with different characteristics of operation, cost, and minimum detectable flaw size limits. The detection limits and suitability depend upon component geometry, surface finish, the basic metal, and operator skill.

Packman, et al. (1974) is a readily accessible reference for the reliability of flaw detection by ultrasonic (and other) techniques. The

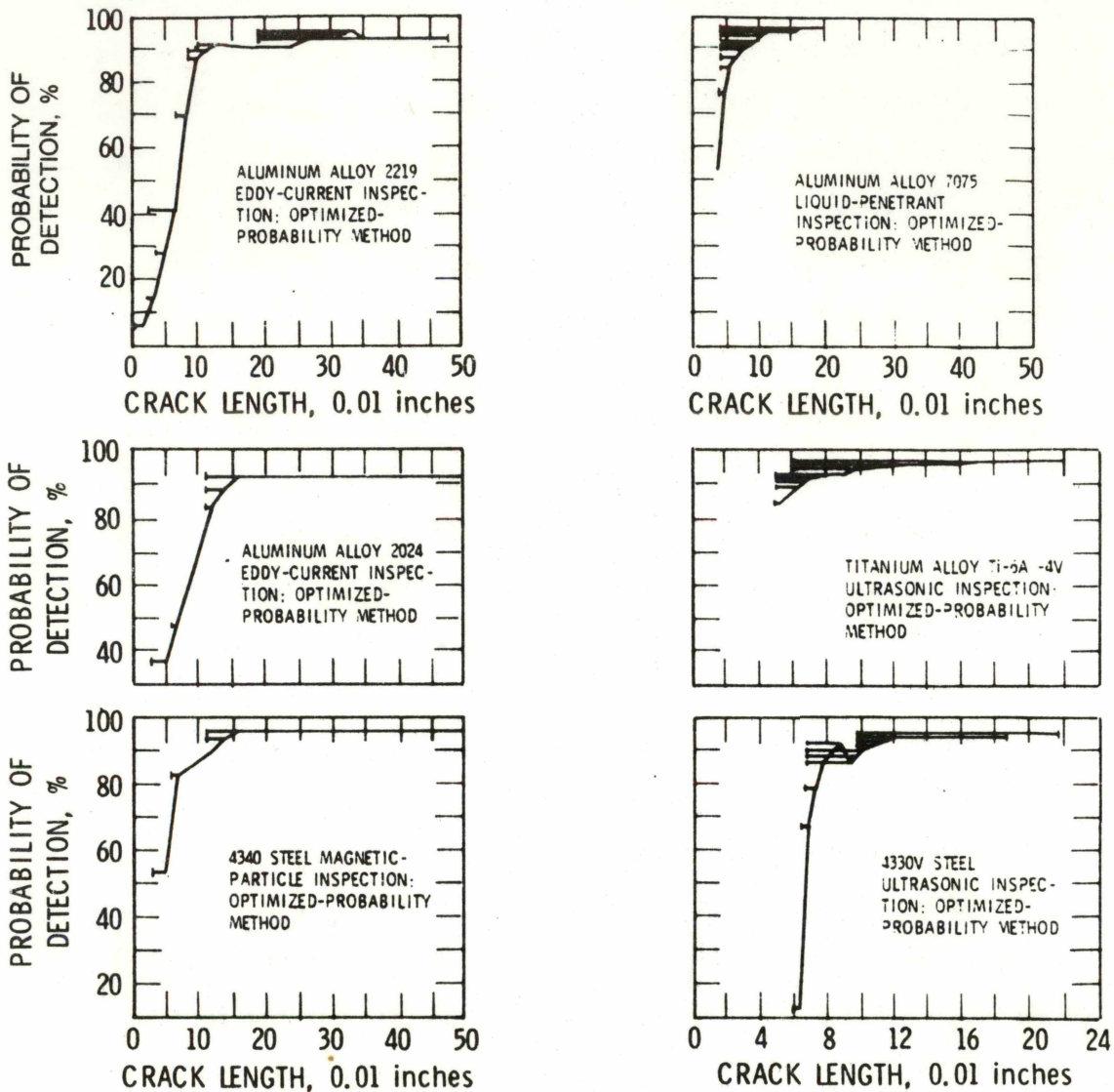
most relevant statement is that limits for a given circumstance and technique should be demonstrated rather than assumed. In effect, generalizations must be treated with caution, but they are unavoidable for preliminary evaluation. The approximate reliability of some NDI techniques is indicated in Figure 6-4 (from Packman). Flaws on the order of 0.10 in. can be considered routinely detectable. Flaws of 0.01 in. are probably outside technological limits, while flaws of 0.05 in. or so represent a lower limit of detection requiring proper technique and trained operators.

By using Johnson's assessment of current side frame design practices, current NDI limits and the 20-year service needs are approximately equal. Use of good NDI practice would then contribute strongly to the reduction of defect-induced side frame failures. Elimination of side frame defect-induced failures might be a logical result of slight reductions in working stress through redesign and improvements in NDI technology. Significant gains in side frame safety would certainly be expected in the future. The reduction in the side frame failure rate noted over the last decade may reflect these same steps.

6.4.2 Periodic Field Inspection

Periodic field inspection may be performed in great detail (as in car rework) or in lesser detail (as in visual inspection in the field). The potential for NDI during car rework is essentially the same as for new components; thus, the previous discussion covers the basic points for inspection during rework.

For this discussion, "careful visual field inspection" will be assumed to reveal flaws on the order of 0.15 to 0.25 in. Figures 6-5 and 6-6 show the associated safe-life intervals for nominal and reduced fracture toughness materials (e.g., ambient and reduced temperature).



^aCAUTION: These charts were derived from inspection data for specific inspection procedures used on a specific specimen design. The charts are not recommended for use as a basis for designing other structures nor for certifying other inspection procedures.

Source: Packman, et al., 1974

Figure 6-4. Lower-Bound Probability of Detection of Failure Cracks as a Function of Crack Size

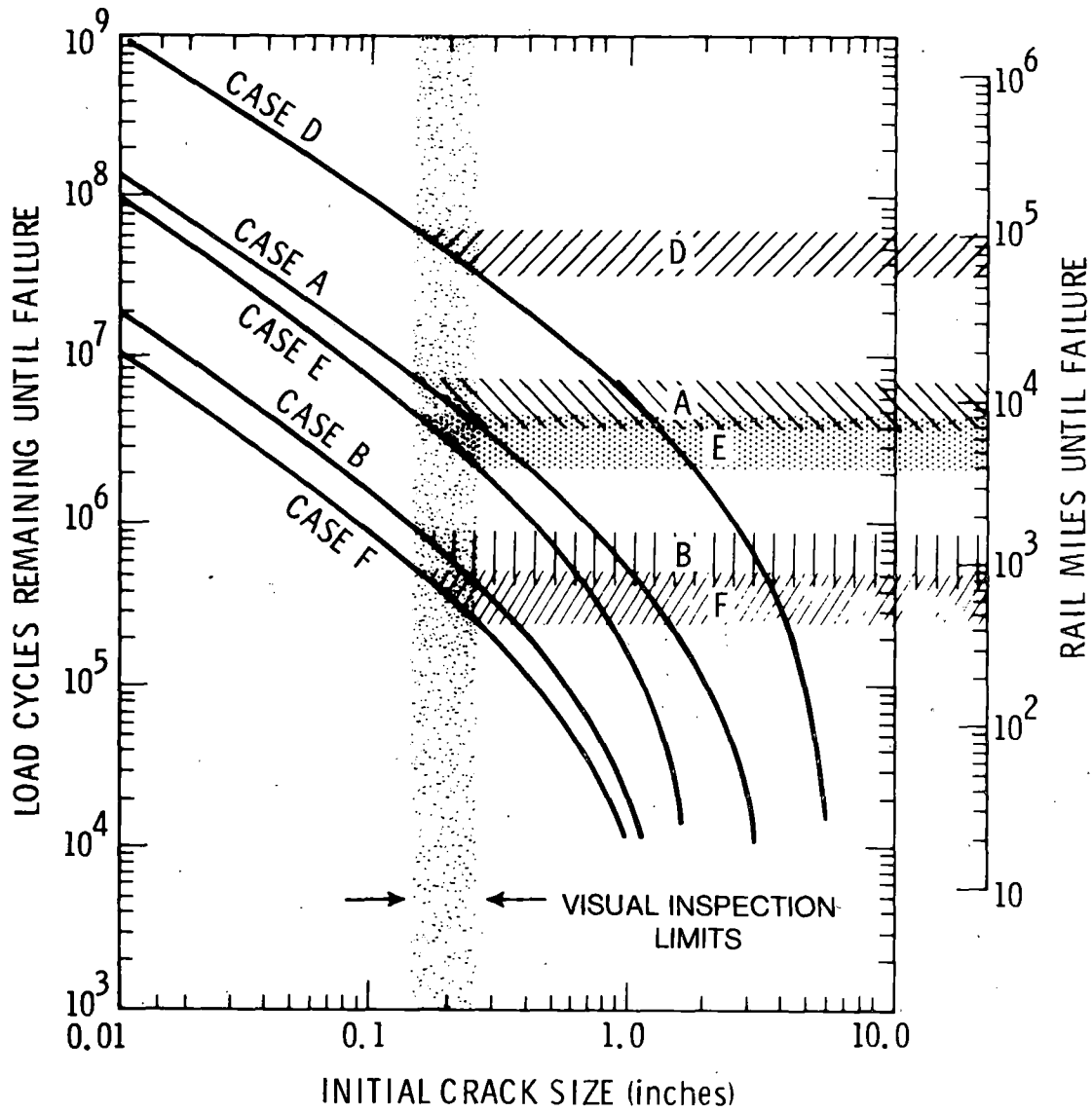


Figure 6-5. Visual Examination Limits for Crack Detection and Associated Safe Life under Nominal Toughness Conditions ($K_c = 66 \text{ ksi} \sqrt{\text{in.}}$)

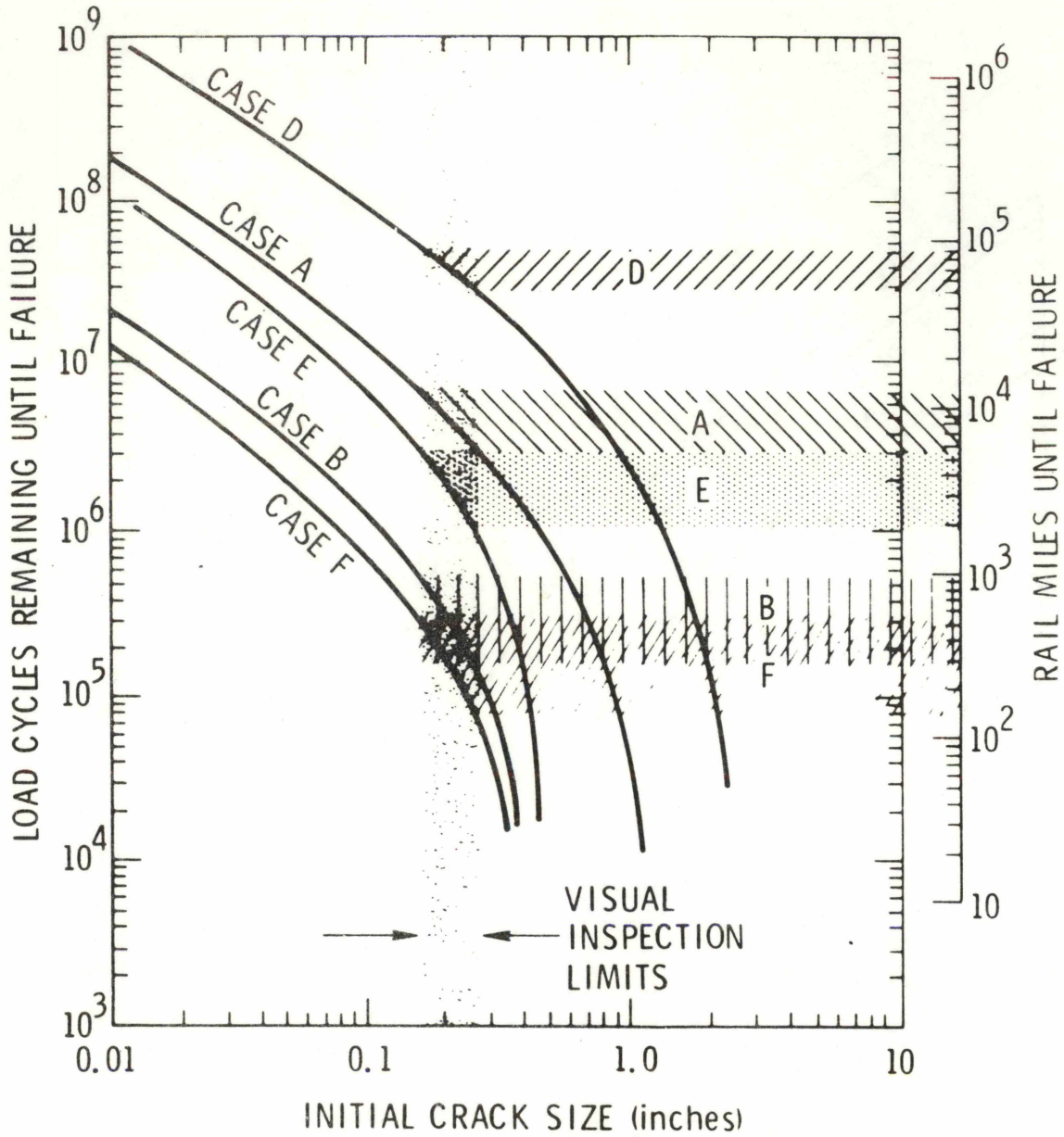


Figure 6-6. Visual Examination Limits for Crack Detection and Associated Safe Life Under Reduced Toughness Conditions ($K_c = 33 \text{ ksi } \sqrt{\text{in.}}$)

For case A, side frames designed to nominal AAR allowables, careful visual inspection would ensure several thousand miles of safe operation. This is true even in the case of reduced fracture toughness; but in this case there is decreased safe life.

From Johnson's assessment (Case D), careful visual inspection would ensure tens of thousands of miles of safe operation. This prediction should not, however, be used to promote laxity in visual inspection or reduce the intervals. One reason is that the present prediction is new and not independently corroborated. The second is that the reliability of a visual inspection process is increased by redundancy (i. e., independent repetition). Frequent visual inspection of side frames is a technically sound mechanism for continual assurance of safe life. Augmenting this with inexpensive, low technology, hand-held aids may be an important consideration, as only moderate-size cracks need be detected.

6.5 SIDE FRAMES IN TEST MACHINES

New side frame designs are required to pass static and dynamic (fatigue) loadings in test machines. The AAR specification M203 states that dynamic testing shall be performed in either of two machines (i. e., the one at American Steel Foundry (ASF) or the one at Dresser). These machines apply a complex pattern of vertical, lateral, twist, and impact loads. The requirements call for testing a group of four sample castings.

To pass, side frames must experience an average of 100,000 load cycles without the development or growth of transverse cracks to 0.5 in. For a 100-ton capacity truck side frame, the maximum vertical cyclic load is taken as 150,000 lb. The ASF machine cycles between zero load and the maximum ($\Delta L = 150,000$ lb), while the Dresser machine cycles between 50,000 lb and the maximum ($\Delta L = 100,000$ lb).

The interpretation of these fatigue test results with regard to SLC is difficult to understand. The dynamic test is not a classical fatigue experiment because of the allowance for some progression of fatigue cracking. It is not a crack propagation test because cracks need not be initially present or nucleated during the experimental loadings. It is not a closely defined simulation of rail service loads, nor is it a closely defined and well understood accelerated life test. Because the current side frame failure rates indicate that only a few per thousand of the side frames in service experience failure, there is doubt as to the statistical significance of a small sample size (four side frames) for design acceptance tests. Therefore, the side frame fatigue test is considered as an index, but its interpretation is unclear.

One possible interpretation of the dynamic test is that it senses some aspects of preexisting flaw size and subsequent growth. The logical questions are: Even if one ignores the statistical sampling aspects, could the marginal passing of the test signify satisfactory field performance? If so, under what conditions?

Truck side frames can be usefully categorized by how closely they are designed to the AAR allowable maximum stresses. Three categories are defined for the following discussion. In the "1X AAR" allowable group are side frames of the 100-ton rating in which $60,000 \text{ lb}_f$ results in 16,000-psi maximum tensile stress in the side frame (i. e., the AAR maximum allowable for grade B castings). The other categories are "3/4 X" and "1/2 X," in which the same force results in stresses of 12,000 and 8000 psi, respectively. The 3/4 X and 1/2 X classifications are progressively more conservative.

For those classifications, the side frame stresses may be calculated for the various test machines. The results for the ASF machine are given in Table 6-2.

Table 6-2. Side Frame Classifications

Classification	ASF Test		
	Design Static Stress (ksi)	Mean Stress (ksi)	Cyclic Stress (ksi)
1 X AAR	16	20	40
3/4 X AAR	12	15	30
1/2 X AAR	8	10	20

For these classifications and cyclic loading conditions, the number of load cycles necessary to grow a crack from an arbitrary initial size to a final size of 0.5 in. may be computed from the results of Section 5.3.4. These results are given in Figure 6-7, along with the 100,000-cycle test demarcation. The material was assumed to be characterized by $K_c = 66 \text{ ksi} \sqrt{\text{in.}}$, $m = 4$, and $A = 1.68 \times 10^{-9}$ as required to fit Johnson's crack growth data. From this figure, it is possible to determine the initial crack size that will grow to the AAR-allowed limit. In effect, then, one can determine the initial crack size detectability limit for the side frame to pass the ASF fatigue test requirement.

The next logical question is the service life that can be associated with each of these side frame classifications and the implied crack detection limit resulting from passing the test. For these cases, the maximum allowable initial crack sizes were computed for 20 years of operation (4×10^5 miles) at 52.5 mph (Table 6-3).

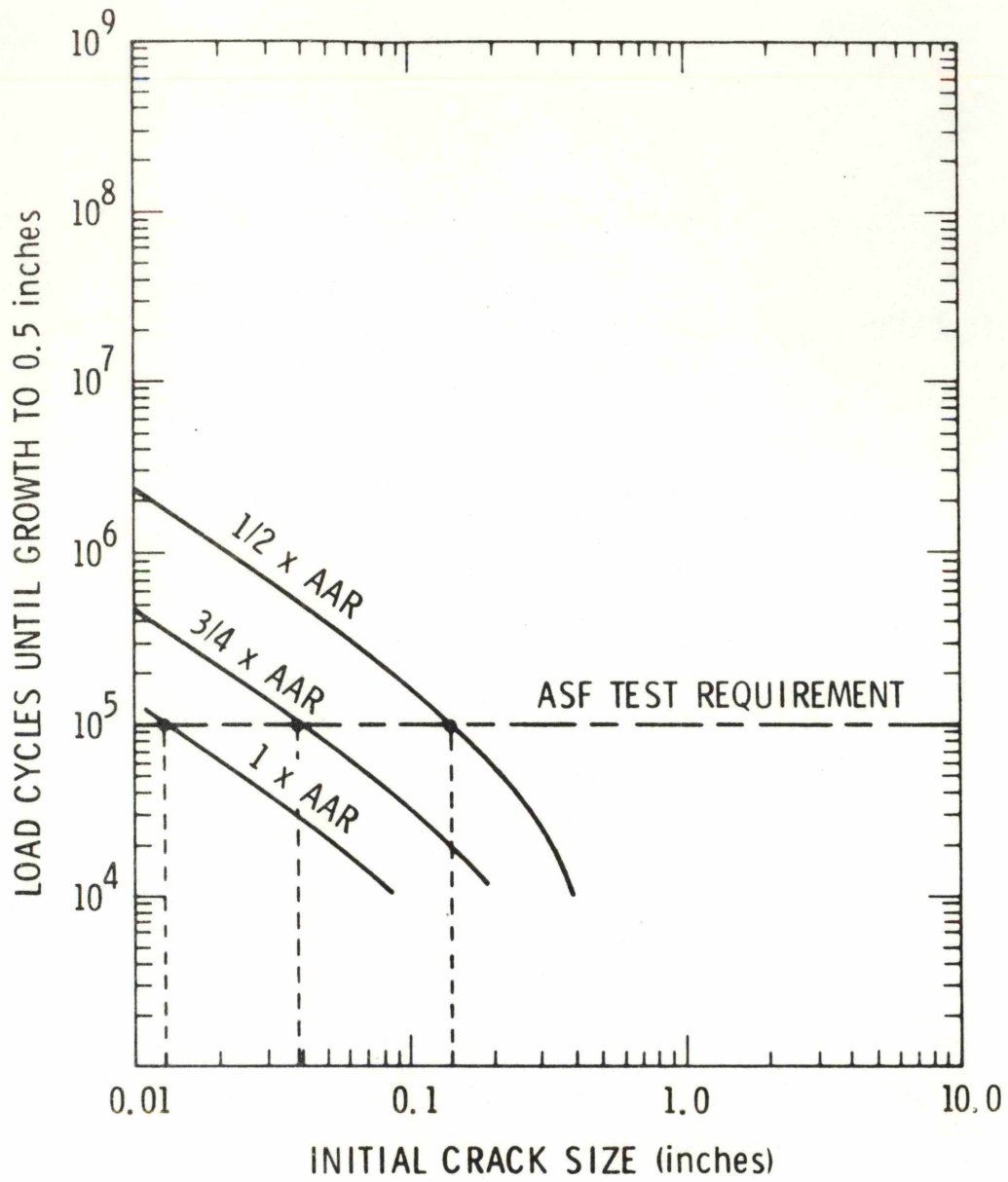


Figure 6-7. Crack Growth Response (growth to 0.5 in.) in ASF Fatigue Test for Varying Degrees of Design Conservatism

Table 6-3. ASF Fatigue Test Compatibility Limits Compared to 20-Year Service Requirements

Classification	Maximum Crack Size Compatible With AAR, ASF Test (in.)	Maximum Allowable Initial Crack (in.) for 20 Year Life
1 X AAR	0.012	0.008
3/4 X AAR	0.038	0.042
1/2 X AAR	0.130	0.085

It is seen that the fatigue test detection limits and 20-year service requirements are approximately equal for the 1 X AAR classification, the least conservative group. For such side frames, ignoring the statistical sampling questions, there is a fairly good match between fatigue test demonstration and service requirement.

For more conservative designs, there is not quite as good a match, but the order ranking is correct. According to the crack propagation methodology, the existing AAR vertical loading fatigue specification is very close to adequate. In the absence of further data, the adequacy of the AAR statement cannot be evaluated. A four-fold increase in test cycles or relatively minor increases in cyclic load would be required to create consistency between the presently predicted 20-year life cycle and the cyclic requirements of the fatigue test.

Another possibility for requirements modification is to decrease the extent of allowable cracking in the fatigue acceptance tests. Figure 6-8 illustrates the number of load cycles required to grow cracks from arbitrary initial sizes to a final size of 0.1 to 0.5 in. For very conservative designs

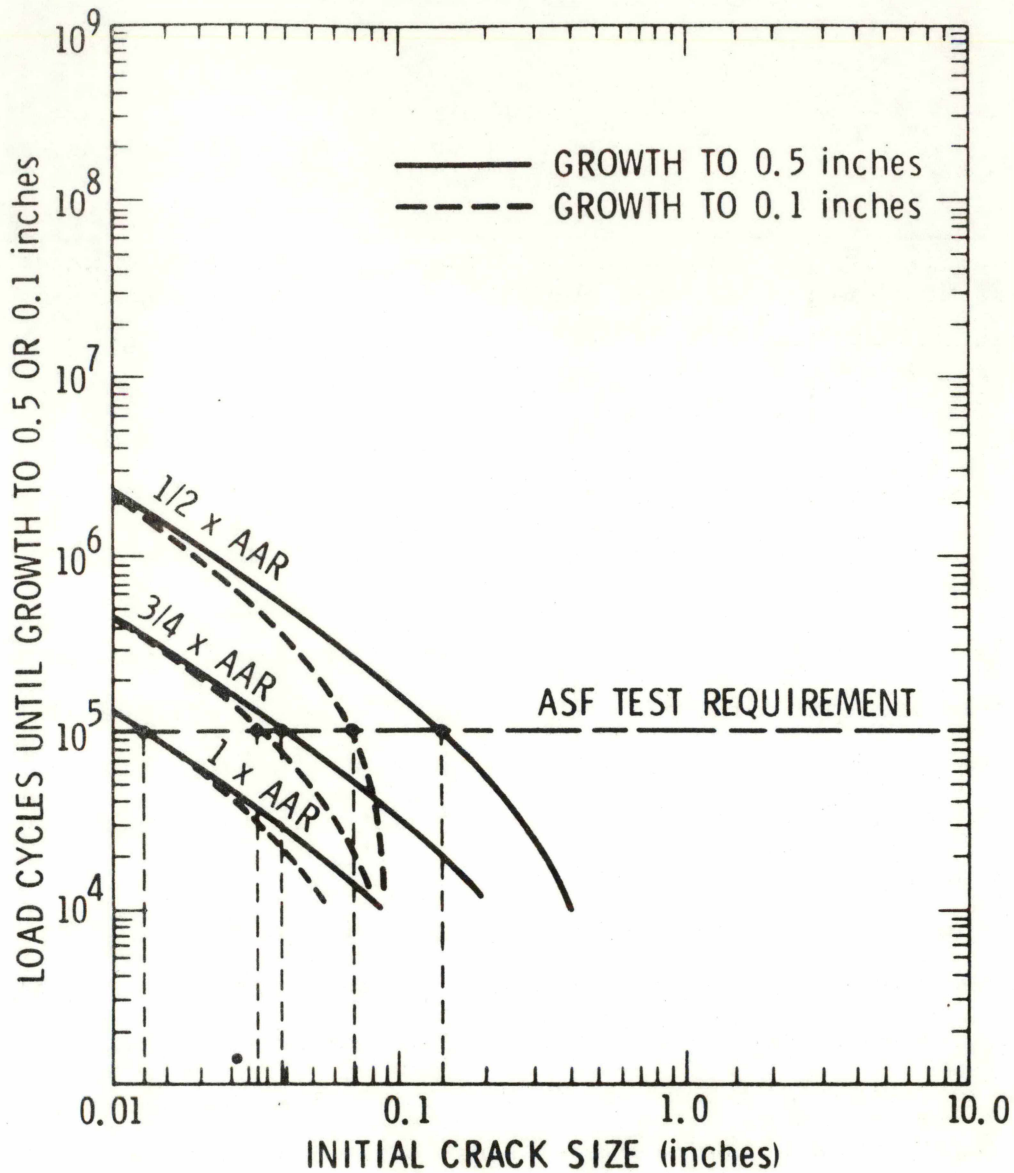


Figure 6-8. Crack Growth Response in ASF Fatigue Test for Varying Degrees of Design Conservatism

(i. e., $1/2 \times \text{AAR}$), the modified acceptance requirement (0.1-in. maximum crack) screens side frames more critically. The maximum tolerable crack for 20 years of service (fully loaded 100-ton hopper can run at 52.5 mph) is greater than the minimum crack detectable in the modified fatigue requirement. An excellent match between the fatigue requirement and the desired design performance would then result if the sampling statistical considerations were ignored.

Before embarking on such a requirements modification, several other factors should be addressed. The first is some form of verification of the present life-cycle methodology. The second is to consider the statistical significance of the sampling procedures. The third is to consider the statistical significance of limited fatigue testing if an effective NDI program is used during truck side frame production. The ordinary statistical significance of small samples should be increased as a result of the NDI information.

The important conclusion is that verification/calibration of the present life-cycle methodology, (perhaps) minor modifications of the AAR fatigue test, and documentation or introduction of effective NDI programs would provide assurance of side frame safe-life performance. The present analysis (considering the uncertainties) reinforces the hypothesis that the fatigue standard is largely responsible for the apparent decline in truck side frame failure rate.

6.6 SAFETY FACTORS AND SENSITIVITY ANALYSIS

Any fatigue methodology should be considered an analytical guideline rather than an absolute prediction. Safety factors should be applied to the results because of the variability of materials response, rare or extreme value statistics of the loading functions, and uncertainties in the data and/or loads.

The major load sensitivity of the present method is in the cyclic rather than the static load (i. e., the stress ratio effect). This can be seen from the derivation and the plotted results.

A major uncertainty in critical input is the crack propagation behavior. The data are limited, and judgment was employed to provide the basis for most of the calculations. Sensitivities have been indicated, and judgment is considered to err in a conservative manner. The inspection requirements may be more severe than necessary, and relaxation of these requirements would be anticipated as a result of a methodology verification program.

There are uncertainties in the stresses assumed to exist within side frame components. There is a significant effect on the absolute size of tolerable defects for NDI purposes; however, compensating factors occur for the correlation between laboratory fatigue test results and actual service life. The appropriateness of existing fatigue standards is not significantly affected.

As a general principle, a factor of safety should be applied to the resulting safe-life prediction. At the present time, a safe-life factor of safety of 4 or 5 would not be unwarranted. A proper demonstration program could be applied to reduce the factor further and provide statistical significance.

7. DISCUSSION

It must be clearly understood that the present crack propagation life estimation methodology for pseudorandom loadings is not a classical fatigue methodology. The present life estimate is strictly and explicitly based on crack propagation considerations and is defined as the consequence of preexisting crack-like imperfections. In contrast, classical fatigue methodology attempts to treat the physical processes of crack initiation and propagation in a lumped parameter empirical fashion.

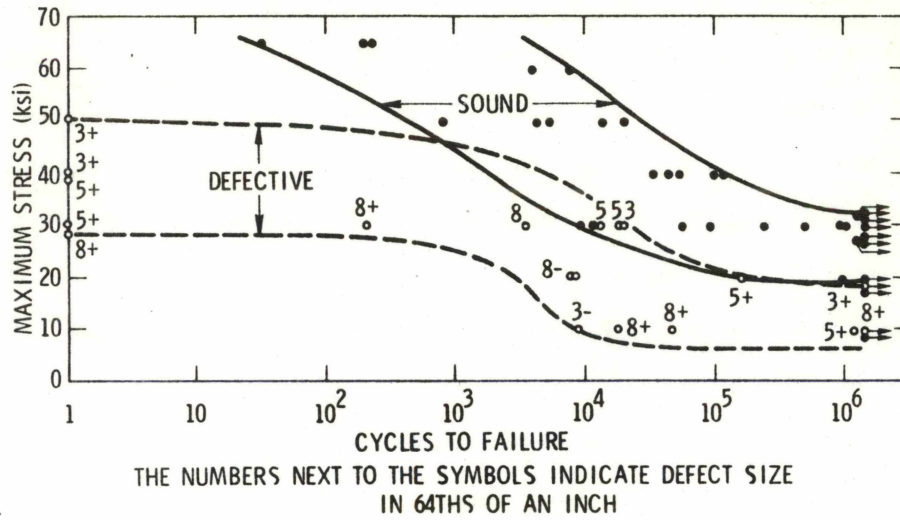
The present SLC crack prediction model serves several purposes. First, it defines a portion of the fatigue life for which structural integrity may be assumed even in the presence of a defect. An example of the difference is shown in Figure 7-1. Second, the SLC crack prediction model defines the defect detection sensitivity required to ensure that fabricated components will not fail prematurely from otherwise undetected defects. Third, it allows for trade-offs between a material's properties, loads, load spectra, and defect sizes in a design or component verification activity.

7.1 RECOMMENDED ACTIVITIES

The present results suggest that substantial gains in rail safety related to truck component failure may be anticipated through the activities described in the following paragraphs.

7.1.1 Laboratory-Scale SLC Crack Prediction Model Verification

The essential hypotheses of the present methodology are the validity of the Forman (Forman et al., 1967) empirical equation for the materials of interest and the validity of the hypothesis for the significant statistical loading parameters. Both of these hypotheses can be demonstrated/calibrated and



Source: Yen, 1969.

Figure 7-1. Effect of Internal Defects on Fatigue Life of an Aluminum Alloy Forged Plate

modified by a near-term laboratory activity. Railroad steels fabricated into special test specimens with controlled statistical loadings would be the primary data source.

A truck component that is sufficiently small to provide actual laboratory component demonstration is the bolster coil spring. Defect size, load spectra, and life interrelationships could be characterized and compared with the prediction. Intentional defects would be an experimental parameter, which could be used to form the basis of a constrained fail safe life-cycle field demonstration for bolster springs in a facility such as the Facility for Accelerated Service Testing (FAST). The fail-safe nature is a result of the redundancy of parallel coil springs in current truck designs.

7.1.2 Full-Scale Test Machines

The full-scale load cycling capabilities of the ASF and Dresser facilities should be utilized in programs to collect data on crack initiation and growth; to critically determine the preexisting crack detection limits implied by the existing fatigue specifications and correlate these data with various NDI techniques; and to define the full-size cyclic and mean stress scaling laws for crack initiation, growth, and detection. Such a program could establish the validity (and any required modifications) of the presently proposed (or any alternative) life-cycle methodology.

For such a program to provide conclusive data, test planning must clearly distinguish between crack propagation-limited safety life-cycle concepts and classical fatigue (i. e., some unspecified combination of initiation, possibly from defects, and subsequent propagation). The experimental objective can be restated as determining the scaling laws of combinations of cyclic and mean stress and initial defect type and size.

The purpose is to correlate these experimental data with a prediction methodology and perform any necessary modifications to the analysis.

7.1.3 Full-Scale Service Tests

Consideration should be given to methodology verification using a facility such as FAST. The objectives should be to demonstrate the predictability of growth of a crack under controlled or measured service loadings for several components on different cars (e. g. , tank car versus hopper car) under controlled operational and track conditions. Components should be instrumented with load transducers at load transfer points, strain gages at selected structural locations, accelerometers, and calibrated crack detection sensors. A combination of these sensors, coupled with scheduled visual and/or instrumented inspection, would be used to minimize the occurrence of component failure.

The primary purpose is to demonstrate the ability to predict the onset and progression of structural degradation resulting from crack growth, not to predict and observe the point of failure. Degraded (cracked) components could then be removed from FAST service and carried to failure in cyclic loading test machines. These failure data could then be compared with the prediction.

7.1.4 Analytical Refinement

The present analysis is a simple first-order approach. The simplifications involved may be reduced by further analytical development and correlation with experimental data. Extensions of the methodology with high payoff potential are identified below:

- Examination of the tank car load spectrum and comparison of this spectrum and the tank car side frame failure and service removal rate with those for hopper cars.

- Incorporation of the Collipriest (or other) crack growth relation in the design charts for a more accurate calculation of crack growth.
- Development of statistical sampling considerations for fatigue acceptance specifications to evaluate the reliability of NDI.
- Extension of the SLC crack prediction model from mean (average) crack growth rates to include probability and reliability bounds on crack propagation under spectrum loading. This would encompass interactions between variable materials properties and the spectrum load. The output would be the extreme value probabilities of failure (failure rates) for operation under various rail service conditions.
- Studies of cost/benefit/risk based on the above analytical activity to define tradeoffs between inspection technology and long-term system benefit.

7.1.5 Extension to Other Components

Extension to other components is implied in the previous discussions. However, since a deficiency noted in the present study was the definition of stress states within the side frame, strong efforts should be directed toward developing an analytical or numerical description of local and global stress distributions.

If numerical methods are applied (e.g., finite element or finite difference codes), it should be required that the data output be stored on magnetic tapes and that the data tape be available as input for the present (or any future) safety life-cycle methodology. The rationale is that the individuals or organizations performing safety life-cycle methodology studies need not be the same specialists who perform the structural analysis.

7.2 LIMITATIONS OF PROPOSED SLC CRACK PREDICTION MODEL

The present safe-life estimation method requires data that are not always readily available. The basic inputs were defined in Table 5-3. during the presentation of safety life-cycle estimation charts. The crack propagation parameters and fracture toughness are not classical design parameters in the railroad industry, and their relative scarcity is therefore understandable. Their immediate unavailability is necessarily a limitation.

The remainder of the inputs (e. g., load spectra, stress distributions) would be inputs to any analytical method. Thus, all life estimation techniques suffer from these limitations. In particular, the conclusions on safe operational limits presented in this report are restricted to loaded 100-ton hopper cars and do not directly extend to tank cars.

Certain other limitations occur because of the crack propagation basis of the method. No a priori information on crack nucleation can be predicted from this method.

The appropriate method of load cycle counting for data reduction purposes has not been defined for this SLC crack prediction method. This limitation is not unique to the present model; rather it is common to all models and serves as one of the justifications for application of safety factors to life-cycle predictions until better methods are found for load-cycle counting of random loads.

As presented, the method purports to predict only mean (average) crack propagation rates under spectrum loading. It does not address the range of crack propagation rates that could occur in actual component production and service. It likewise does not address the associated ranges of conditions under which failure could occur during service.

More specifically, it does not address the joint frequency of faster than normal growth coupled to more frequent than expected extreme values of the load spectrum; therefore, a conservative safety factor must be applied to these predictions. Consideration of the probabilities of faster than normal growth and more severe than expected loadings would provide additional analytical guidelines for an appropriate safety factor. Until demonstrated analytically and experimentally, large factors of safety of 4 or 5 should be applied to the predicted safety life-cycle.

8. SUMMARY

8.1 CURRENT RAILROAD PRACTICES

The testing and inspection practices of the railroad industry as they apply to each phase (i. e., design, manufacture, and service performance) of a freight car structural integrity program are summarized below.

The manufacturer designs a component within certain dimensional constraints specified by the Association of American Railroads. For some components (e.g., bolsters, side frames, couplers) full-scale component tests are used to verify the mechanical load-carrying capacity of the design. Static and fatigue loading tests are currently required of new side frame designs. The Facility for Accelerated Service Testing (FAST) (located in Pueblo, Colorado) is currently used for the accelerated testing of freight car components and systems. These test data provide information on the durability, damage tolerance, and safety life-cycle of components in simulated service environments.

Tests are performed during and after fabrication to ensure consistent product quality. Raw material chemistry is controlled by ladle analysis as required by AAR material standards. The manufacturing process is controlled by testing the mechanical properties of the final product material. In most cases, minimum tensile properties must be met. Specimens are generally taken from test prolongations or test coupons. Drop tests replace tensile tests for grade U axles. Hardness tests, rather than tensile tests are used on wheels. Coupler steel mechanical properties are controlled by Jominy tests for hardenability and Charpy V-notch impact tests as well as tensile tests.

The manufacturer controls the size and extent of fabrication defects by nondestructive inspection of the finished component. All components are inspected visually for surface defects. Magnetic particle inspection and ultrasonic inspection are examples of more sophisticated means of finding flaws nondestructively. Magnetic particle inspection is used to

increase the sensitivity of visual inspection of wheels. Ultrasonic inspection for internal discontinuities is required of wheels and commonly applied to axles.

Field inspection of freight cars is generally limited to visual examination during interchange and visual component inspection (truck intact) every 4 to 8 years. AAR standards and Federal law regulate permissible degree of wear, extent of damage, and weld repair limits.

A review of materials' properties, manufacturing methods, and section size (thickness) revealed that side frames, bolsters, and couplers are made of medium carbon steels which are relatively tough compared to the higher carbon steel wheel castings. Because of their thinner section size, side frames and bolsters have enough toughness to exhibit a potentially ductile failure mode (i. e., exhibiting some degree of shear). The thicker section size of the couplers increases the potential for a brittle fracture mode. The tendency increases as higher strength, Grade E, coupler steels are employed. A correlation of fracture toughness with Charpy impact values was used to analyze the damage tolerance of railroad steels and establish maximum operating stress levels (factors of safety) consistent with visual inspections.

8.2 DAMAGE TOLERANCE AND FAILURE MODES

Side frames and bolsters have fracture toughness that is consistent with inspection limits and the definition of a detectable flaw size of 0.25 in. Component testing of side frames loaded near the yield strength would require a 0.25-in. crack to exist which could cause failure. In effect, the test is a proof test on a limited sample size, and the remaining components rely on nondestructive inspection to ensure that no cracks in the structure exceed 0.25 in. Side frames are fatigue limited with their safety life-cycle dependent on crack initiation due to service exposure which might include aggressive

chemical environments or impact overloads in hump yards. Testing requirements for side frames and bolsters should include: (1) stress intensity calibration of actual components, (2) establishment of failure mode as correlated to fracture toughness and section size using a more exact analysis than presented in this report, and (3) better utilization of failure analysis of broken components to obtain information on transition temperature Charpy data and a more exact description of failure stresses/modes.

Coupler studies have resulted in the inclusion of Charpy data into the AAR Recommended Practices. The large section size and the higher strength steel are the reasons for more rigorous quality control of couplers. The data suggest that the 15 ft-lb at 0° F for Grade C and 15 ft-lb at -40° F for Grade E couplers would have been cause for rejection for most of the couplers examined in the Coupler Steel Study program. Only separately cast (smaller size) castings appear to meet the requirements. To make this requirement more useful, the location of Charpy samples should be specified or a correlation parameter established with separately cast test coupons which are generally higher because of section size effect. A Charpy-fracture toughness correlation for railroad steels similar to that found for bridge steels should also be established.

Wheels are definitely a problem from brittle failure mode considerations. As the class of wheel changes from A to B to C, the higher strengths are accompanied by lower and lower values of damage tolerance. But, the wheels' major design function is against wear, and, therefore, the requirement for greater hardness (resulting in less tough steels) is a necessity. Most of the failures are in the location of the rim due to thermal stresses produced during braking. In theory, proof testing of wheels could be utilized to ensure safe life; but in practice, the approach does not appear to be a reasonable one.

No circumferential cracks are allowed in axles. In addition, there are restrictions on longitudinal discontinuities. The question becomes one of defining a defect size that exceeds the limits of detection of existing nondestructive testing equipment. No data could be found to calculate the damage tolerance limits of axles, but estimates suggest relatively high values approaching a toughness-to-yield ratio of unity. Drop tests in U-Grade axles can be further redefined in terms of interpreting the results on a proof test delineating defect sizes and establishing failure modes.

In general, fracture toughness is an important ingredient in failure mode prediction and in defining maximum operating stresses or safety factors consistent with visual detection of critical defects about 0.1 in. long. For side frames and bolsters, a factor of safety of 2.4 ensures tolerance of a 1-in. crack, which is consistent with current AAR practices. For Grade E couplers, a factor of safety of 5 should be employed. For Class C wheels, a factor of safety of 10 should be used. Axles have enough damage tolerance to be designed to a factor of safety of 3.

From the toughness consideration, railroad steels represent the lower end of the state-of-technology and large improvements in material selection are possible from technical considerations. The major limiting factor is the cost impact, especially with the freight car trucks.

8.3 SAFETY LIFE-CYCLE PREDICTION

Safety life-cycle prediction is more strongly dependent on the parameters that affect crack growth than on fracture toughness. Environmental factors of temperature and chemistry should be considered from the viewpoint of effects on crack nucleation and crack growth. Load simulation and the prediction of the dynamic response of each component are essential for accurate safety life-cycle predictions. Models that are consistent

with test data for predicting crack growth due to random type loads on railroad steels are essential. Verification tests of crack growth in components under actual service loads are also necessary.

The random-loading aspects of crack propagation were used to generate a SLC crack growth prediction technique. The basic technical approach was to extract from the statistical loading spectrum, a characteristic loading which was then used to forecast the future propagation of the crack.

The scope of this effort was restricted to a macroscopic description of fatigue crack growth from preexisting or service-induced flaws. Crack initiation from microscopic considerations is beyond the scope of existing technology. The load conditions consist of a static mean load with superimposed random (statistical) loading.

In order to demonstrate an analytical approach to general safety life-cycle guidelines, fracture mechanics concepts used with crack growth laws based on the oscillatory crack-tip stress-intensity factor and the Forman empirical crack growth relation were selected for implementation. The selection criteria included stress ratio effects, logical transition to catastrophic growth, reasonably analytical tractability, and inherent conservatism relative to available data.

The significant index of statistical loading parameters was sought through the mathematical character of the empirical crack growth differential equation. It was hypothesized that the order of the relevant statistical moment of the loading distribution would be identical to the order of the nonlinearity of the differential equation of crack growth.

The characteristics of the most common probability distribution functions were examined for significant statistical indices (moments) consistent with this hypothesis. These distributions were candidates for a

description of random loadings applicable to various railroad components. The crack growth rate equations were integrated in forms suitable for use with the basic hypothesis.

On the basis of available data, the distribution function for truck side frame vertical loadings was shown to be approximated by a particular gamma distribution. This distribution is linearly dependent on car velocity for 100-ton loaded hopper cars. The loading distribution function for tank cars appears more severe than that for hopper cars, and does not obey the same distribution function.

Life prediction diagrams based on crack propagation were prepared to display the general characteristics and major sensitivities of the method.

The SLC crack prediction model was specifically applied to 100-ton capacity hopper car side frames. The application was demonstrative (as opposed to definitive); significant data were either unavailable or tentative. Estimation and bounding were thus employed to overcome these uncertainties. Consequently, exact values used in actual guidelines would be premature.

8.4 CONCLUSIONS BASED ON SIDE FRAME ANALYSIS

Periodic visual inspection was considered. The crack detection limit of "adequate periodic inspection" remained consistent with an assurance of many thousands of miles of safe life. The safe life is somewhat decreased under conditions of reduced material fracture toughness (i. e., low temperature), but it is still significant. Periodic visual inspection is a valid mechanism for incremental assurance of safe life, and it becomes increasingly practical and reliable with increased design conservatism.

Nondestructive inspection for flaw detection applied during component acceptance would be a practical approach to ensuring a 20-year safe life of side frames. Current NDI technology appears to have sufficient flaw detection resolution to satisfy the maximum requirements for conservative designs allowable by AAR. For less conservative designs (i.e., when the resulting stress is approximately equal to the maximum AAR allowable stress), NDI technology is insufficient to provide the required flaw free assurance of 0.008 in.

The existing AAR fatigue test (Standard M-203) is somewhat ambiguous. The statistical significance of a test sample of four side frames compared to a field failure rate of a few per thousand is set aside for the purpose of this report.

Interpretation of the fatigue test as an accelerated crack propagation test was attempted. The conclusion was that the AAR (ASF) test requirement could detect initial cracks of approximately the size corresponding to a 20-year safe life. Relatively slight increases in load and/or test duration or reductions in the maximum allowed crack size could produce the desired consistency. Given the uncertain state of the data and the newness of the methodology, modification of the standard is not presently justifiable. Programs and activities leading to standards modification can be identified.

It was also concluded that until proved otherwise, a safety factor should be applied to the safety life-cycle predictions of this report. This safety factor should be applied even though conservatism is implicit in the methodology formulation and data interpretation. It does not affect the basic trends.

Activities were identified that should result in substantial gains in rail safety related to truck component failure. These activities center on verification and modification of the basic safe-life methodology developed in this study. These include:

- Laboratory-scale verification,
- Full-scale test machine correlation,
- Full-scale service testing in the FAST facility,
- Further analytical development, and
- Extension to other components.

The major conclusions reached are limited to 100-ton hopper cars. Specifically, they do not extend to 100-ton tank cars. There are short-term data limitations, but in most senses these same limitations exist for any safe-life methodology. The method currently considers the average crack growth under expected values of random loading and can be extended to cover the joint (rare) occurrence of faster than normal growth coupled to greater than expected (rare) occurrences of loading.

9. REFERENCES

- The Aerospace Corporation. Preliminary Rail Vehicle Safe-Life Technology, ATR-78(3847-01)-4. November 1977.
- Anderson, D.H. and Stephens, R.S. "Fatigue Data Acquisition and Reduction for Cumulative Fatigue Damage Assessment", Society for Experimental Stress Analysis Spring Meeting, May 1974.
- Association of American Railroads, Specifications for Design, Fabrication and Construction of Freight Cars, Vol. 1. March 1976.
- Association of American Railroads, Field Manual of the AAR Interchange Rules. 1977.
- Association of American Railroads, Manual of Standards and Recommended Practices. 1977.
- Association of American Railroads. Research and Test Department. Coupler Steel Study, Report #-107. December 1970.
- Association of American Railroads, Research and Test Department. The Fracture Properties of Two Failed Cast Steel Wheels from the Union Pacific Railroad. Report R-123. May 1973.
- Barsom, J.M. "Fatigue Crack Growth Under Variable-Amplitude Loading in Various Bridge Steels," Fatigue Crack Growth Under Spectrum Loads. ASTM-STP-595, American Society for Testing and Materials, 1976.
- Car and Locomotive Cyclopedia of American Practices, Third Ed. Simmons-Boardman Publishing Corp., New York. 1974.
- Carter, C.S. and R.G. Caton. Fracture Resistance of Railroad Wheels, Report FRA-ORD&D-75-12. Federal Railroad Administration. September 1974.
- Collipriest, J.E. and R.M. Ehret. Computer Modeling of Part Through Crack Growth, Technical Report SD-72-CE-0015. Space Division, Rockwell International Corp. 1972.
- Evans, R.A. and M.R. Johnson. "Analysis of Environmental Truck Component Load and Bolster Fatigue Test Data." Interim Report AAR Research and Test Report, R-246. September 1976.
- Federal Railroad Administration. Freight Car Safety Regulations. 1974.
- Federal Railroad Association Accident Bulletin #134-143 DOT FRA, ORS, 1975.

Forman, R.G., V.E. Kearney, and R.M. Engle. "Numerical Analysis of Crack Propagation in Cyclic-Loaded Structures," J. Basic Engr., Transactions of the ASME, Vol. 89. September 1967.

Johnson, M. R. "Development of Fatigue Standards for Freight Car Truck Components and Wheels." ASME Paper 74-RT-4. April 1974.

Johnson, M. R., "Analysis of Railroad Car Truck and Wheel Fatigue, Part 1: Service Load Data and Procedures for the Development of Fatigue Performance Criteria." Report FRA-ORD&D-75-68. May 1975.

Johnson, M. R., "Structural Adequacy of Freight Car Castings and Wheels," Unnumbered AAR Technical Report. October 1976.

Miner, M. A. "Cumulative Damage in Fatigue." J. Appl. Mech. September 1945.

Packman, P. F., et al. "Reliability of Flaw Detection by Nondestructive Inspection." ASM Metals Handbook, Vol. 11. 1974.

Paris, P. and R. A. Erdogan. "A Critical Analysis of Crack Propagation Laws," J. Basic Engr., Transactions of ASME. December 1963.

Pellini, W. C. "Principles of Fracture-Safe Design," Adams Lecture, Welding Journal. 1971.

Rolfe, S. T. and J. M. Barsom. Fracture and Fatigue Control in Structures: Applications of Fracture Mechanics. Prentice-Hall, Inc., Inglewood Cliffs, New Jersey. 1977.

Sharkey, R. L. and D. H. Stone. "A Comparison of Charpy V-notch Impact Transition Temperature Curves for AAR Grades of Cast Steel." ASME Paper 75-RT-1. 1975.

Shigley, J. E. Mechanical Engineering Designs. McGraw-Hill. 1977.

Yen, C. Y. "Interpretation of Fatigue Data," Metal Fatigue: Theory and Design. ed. A. F. Madayag, John Wiley and Sons, Inc., New York. 1969.

APPENDIX A
RANDOM LOAD DISTRIBUTION FUNCTIONS

Several random load distribution functions are described in this appendix. These functions can be used to describe the loading spectra found in service.

A.1 UNIFORM LOADING DISTRIBUTION

The mathematical form of the uniform load distribution is given by

$$p(\Delta\sigma) = \begin{cases} 1/(\Delta\sigma_{\max}) & 0 < \Delta\sigma < \Delta\sigma_{\max} \\ 0 & \text{otherwise} \end{cases}$$

The magnitude of the cyclic load is positive and bounded, and all intermediate cyclic loads are equally probable. The mean cyclic load is $\Delta\sigma_{\text{mean}} = (\Delta\sigma_{\max})/2$. The roots of the various moments are given by

$$\left[\overline{(\Delta\sigma)^m} \right]^{1/m} = (\Delta\sigma)_{\max} \left\{ (1+m)^{-1/m} \right\}$$

(see Figure A-1). For our purposes here, the mth power of the moment is taken to coincide with the crack growth exponent m.

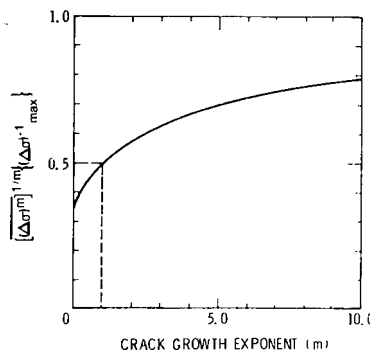


Figure A-1. Statistically Significant Loading Index for Uniform Random Loading Distribution

A.2 GAUSSIAN LOADING DISTRIBUTION

The mathematical form of the Gaussian distribution for positive load cycles is given by

$$P(\Delta\sigma) = \begin{cases} \frac{\sqrt{2/\pi}}{S} \exp\left(-\frac{(\Delta\sigma)^2}{2S^2}\right) & (\Delta\sigma > 0) \\ 0 & (\Delta\sigma < 0) \end{cases}$$

where S is the standard deviation of the symmetric distribution. This is shown in Figure A-2a and compared with the uniform distribution function given in Section A.1. The m th root of the mean of the m th power, where $\Gamma(m)$ denotes the gamma function is given by Figure A-2b.

$$\left[\overline{(\Delta\sigma)^m} \right]^{1/m} = \sqrt{2} S \left[\frac{\Gamma\left(\frac{m+1}{2}\right)}{\sqrt{\pi}} \right]^{1/m}$$

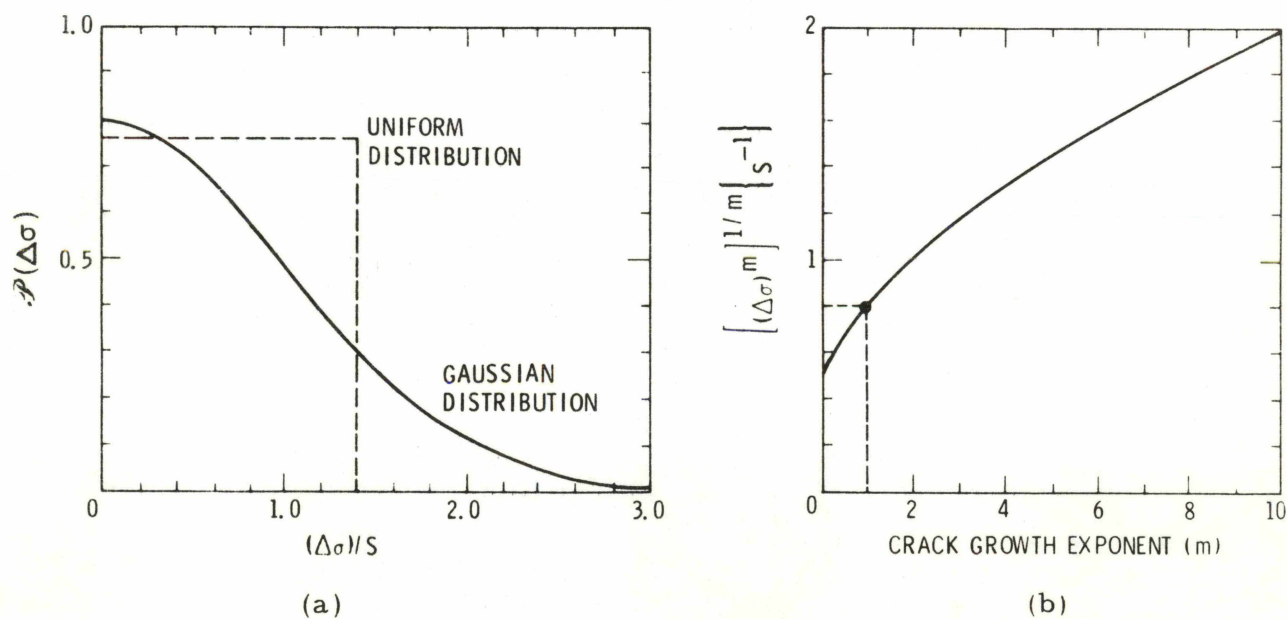


Figure A-2. Uniform and Gaussian Random Loading Distributions and Significant Statistical Index of Random Loading

A. 3 RAYLEIGH LOADING DISTRIBUTION

The general form of the Rayleigh distribution is given in Figure A-3.

Its mathematical form is

$$f(\Delta\sigma) = \begin{cases} \frac{\Delta\sigma}{\alpha^2} \exp\left[-1/2\left(\frac{\Delta\sigma}{\alpha}\right)^2\right] & \Delta\sigma > 0 \\ 0 & \Delta\sigma < 0 \end{cases}$$

For the random loading crack growth problem, the appropriate statistic (Figure A-3) is

$$\left[\overline{(\Delta\sigma)^m} \right]^{1/m} = \sqrt{2} \alpha \left\{ \Gamma(m/2 + 1) \right\}^{1/m}$$

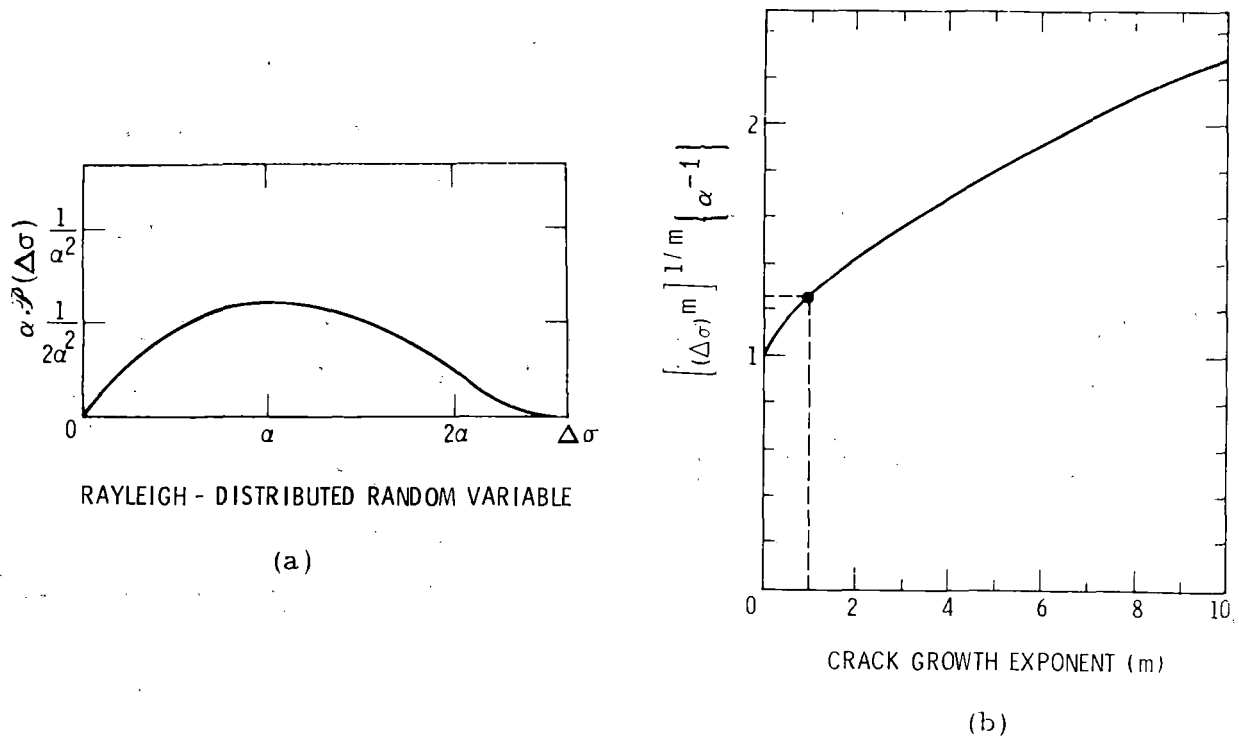


Figure A-3. Rayleigh Distribution and Significant Statistical Index of Random Loading

A.4 GAMMA LOADING DISTRIBUTION

The gamma probability distribution contains two characteristic parameters, in contrast with the previous examples, which contained only single parameters. The behavior is therefore more general. The gamma distribution (Figure A-4a) is defined as

$$p(\Delta\sigma) = \begin{cases} \frac{(\Delta\sigma)^\alpha \exp[-(\Delta\sigma)/\beta]}{\beta^{\alpha+1} \Gamma(\alpha+1)} & \Delta\sigma, \alpha, \text{ and } \beta > 0 \\ 0 & \text{otherwise} \end{cases}$$

The statistic appropriate to the crack growth hypothesis is

$$\left[\overline{(\Delta\sigma)^m} \right]^{1/m} = \beta \left\{ \frac{\Gamma(\alpha + m + 1)}{\Gamma(\alpha + 1)} \right\}^{1/m}$$

This relationship is plotted in Figure A-4b.

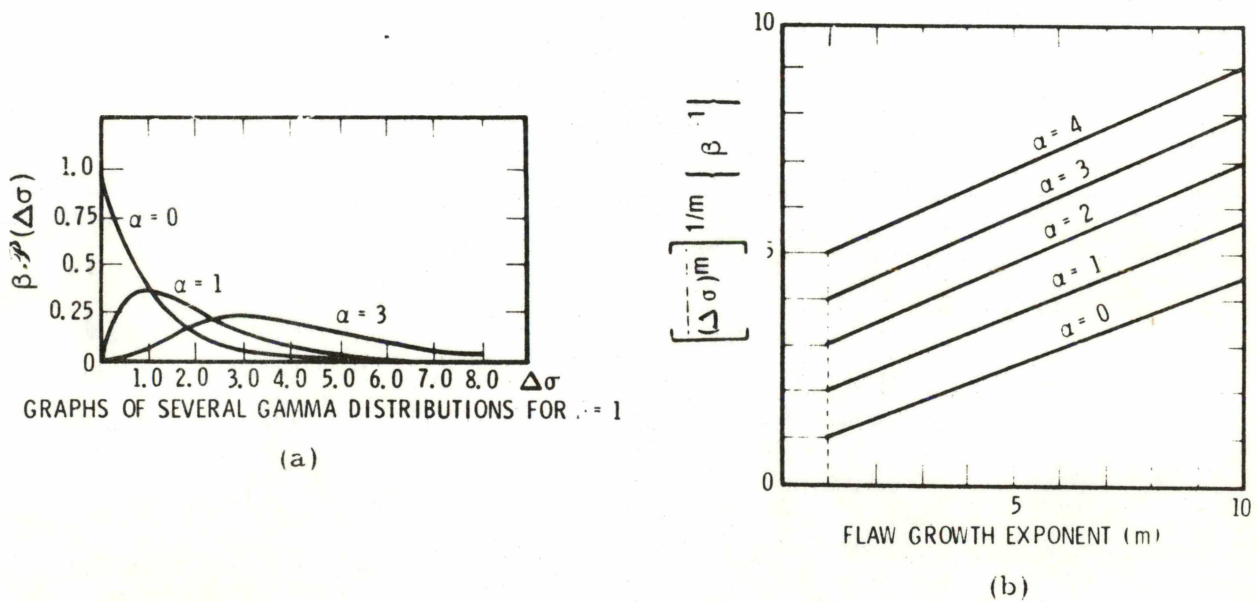


Figure A-4. Gamma Distribution and Significant Statistical Index of Random Loading

A. 5 BETA LOADING DISTRIBUTION

The beta distribution is another two-parameter distribution function. This distribution is bounded somewhat similarly to the uniform distribution, in contrast to most of the other distributions discussed (i. e. Rayleigh, Gaussian, and gamma). The formal definition is given by

$$P(\Delta\sigma) = \begin{cases} \frac{(\alpha + \beta + 1)!}{\alpha! \beta!} \left(\frac{\Delta\sigma}{\Delta\sigma_{\max}}\right)^\alpha \left(1 - \frac{\Delta\sigma}{\Delta\sigma_{\max}}\right)^\beta & 0 \leq \frac{\Delta\sigma}{\Delta\sigma_{\max}} \leq 1 \\ 0 & \text{otherwise} \end{cases}$$

Examples are given in Figure A-5a. For the random loading crack growth problem, the relevant statistic is

$$\left[\overline{(\Delta\sigma)^m}\right]^{1/m} = (\Delta\sigma)_{\max} \left\{ \frac{(\alpha + \beta + 1)! (\alpha + m)!}{(\alpha + \beta + 1 + m)! \alpha!} \right\}^{1/m}$$

This relationship is shown in Figure A-5b.

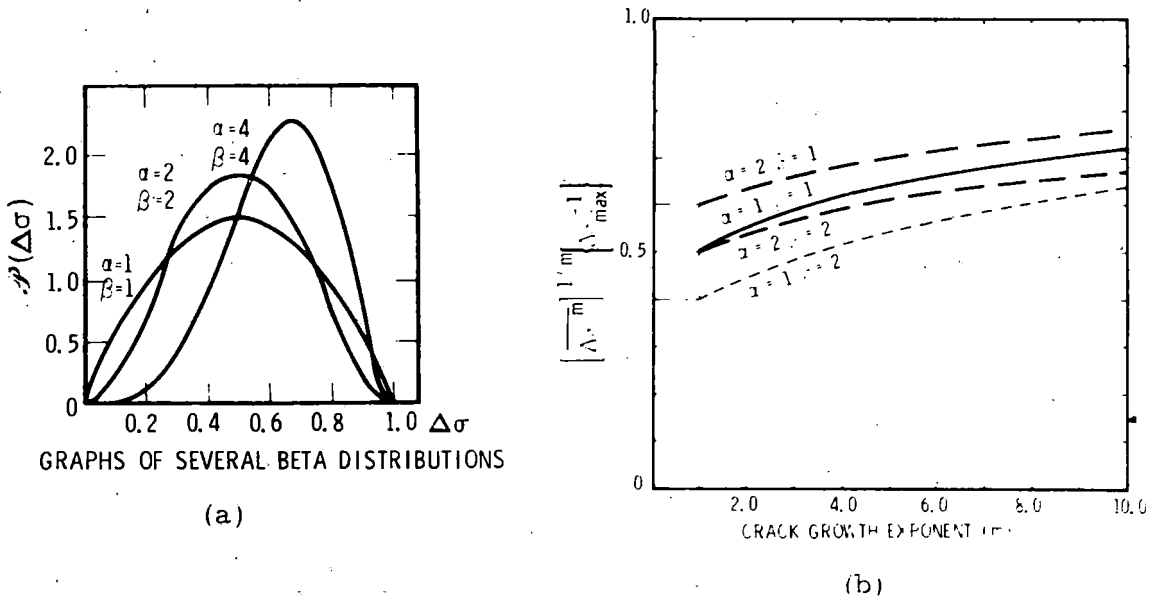


Figure A-5. Beta Distributions and Significant Indices of Random Loading

APPENDIX B

EVALUATION OF A RELATED THEORETICAL MODEL

The closest related work on crack propagation under spectrum loading is Barsom's 1976 study. The materials investigated were typical bridge steels, and the load spectrum utilized was a Rayleigh distribution. The major conclusion reached was that spectrum loading on crack growth could be fairly well correlated with the Paris empirical relation.

The Barsom Model:

$$\frac{da}{dN} = A \left[(\Delta K)_{\text{rms}} \right]^m$$

where:

$$(\Delta K)_{\text{rms}} = \text{root mean square stress intensity fluctuation}$$

$$= \sqrt{(\Delta K)^2}$$

Two circumstances contribute to this apparently good correlation. First, the crack growth exponent for the materials investigated was $m \cong 2.59$ (i. e., a close approximation to $m = 2$). The average growth per cycle should depend approximately on the square of the cyclic stress intensity. Second, the properties of the Rayleigh distribution function are such that the statistical indices for various moments do not depend strongly on the order of the moment. Thus,

$$\overline{\Delta\sigma} = 1.26 \alpha = 0.89(\Delta\sigma)_{\text{rms}}$$

$$\sqrt[2]{\overline{(\Delta\sigma)^2}} = 1.41 \alpha = 1.00(\Delta\sigma)_{\text{rms}}$$

$$\overline{[(\Delta\sigma)^{2.59}]^{1/2.59}} = 1.50 \alpha = 1.06(\Delta\sigma)_{\text{rms}}$$

$$\overline{[(\Delta\sigma)^4]^{1/4}} = 1.68 \alpha = 1.19(\Delta\sigma)_{\text{rms}}$$

The Rayleigh loading distribution is a particularly poor distribution for the investigation of significant statistical loading indices.

The effective stress statistical indices given above are not very different. The scatter in crack growth data is substantial. The combination of the experimental scatter plus the small variation in significant statistics of the indices of Rayleigh-distributed random loading lead to inconclusive discrimination between mean stress, root mean square stress, and fourth-root of fourth-power mean stress as the driving variable for crack propagation.

Barsom's results are not inconsistent with the present hypothesis, and the data are not sufficient to discriminate. The Barsom hypothesis is incorporated in the results on probability distributions (i. e., assume that $m = 2$ for the estimation of the significant loading statistic). The life estimation charts are presented independently of any statistical hypotheses and may be used with either the present or the Barsom model.

APPENDIX C

GLOSSARY OF ABBREVIATIONS AND TERMS

AAR	Association of American Railroads
AASHTO	American Association of State Highway and Transportation Officials
ASF	American Steel Foundry
ASTM	American Society for Testing and Materials
Component strength	The load-carrying capacity of an entire component.
CVN	Charpy V-notch. An impact test specimen used to measure the energy absorbed during fracture under impact loading (ASTM Standard E23-72).
Damage tolerance	The maximum amount of damage in the form of cracks that a stressed component can sustain without failing.
Durability	The ability of a system or component to resist cracking, corrosion, thermal degradation, delamination, wear, and foreign object damage for a specified period of time.
Durability limit	Economic life. Repair and maintenance cost exceeds new vehicle cost.
DT	Dynamic Tear Test (Proposed Method for 5/8-in. Dynamic Tear Test of Metallic Materials, Vol. 10, ASTM Book of Standards).
Factor of Safety	The ratio of the yield strength to the design maximum allowable stress.
Fail safe	A design approach in which safeguards are incorporated into the design of a structure so that even if local failure occurs, the structure is safe.
FAST	Facility for Accelerated Service Testing
FRA	Federal Railroad Administration
Fracture mechanics	The study of material response to stress in the presence of a crack.

Fracture toughness	The ability of a material to resist flaw propagation, K_{Ic} . A measure of the amount of energy a material can absorb before fracturing.
Hardenability	The depth of hardening under given cooling conditions, not to be confused with hardness.
Hardness	Resistance of a material to penetration.
Jominy Test	A test for determining the relative hardenability of steels in which one end of a heated cylindrical specimen is quenched; the resulting hardness decreases towards the unquenched end.
K	Stress Intensity Factor
K_{Ic}	Critical stress intensity factor under mode I loading conditions (displacement normal to crack surfaces). Fracture toughness per ASTM Standard E399.
K_{Id}	Dynamic fracture toughness. The critical stress intensity factor measured at a high strain rate.
Ladle analysis	A method of chemical analysis in which samples of the molten steel stream are taken in a steel spoon (ladle) during the pouring of the heat.
LAST	Lowest Anticipated Service Temperature
Magnetic Particle Inspection	A nondestructive means of detecting surface discontinuities.
Margin of safety	Factor of safety minus one.
Miner's Rule	Miner-Palmgren cycle-ratio summation theory. If a component is loaded at stress level S_i for n_i cycles and N_i = the total number of cycles of life the component has at stress level S_i , then no more component life remains when $\sum \frac{n_i}{N_i} = 1$

NDI	Nondestructive Inspection
NDT	Nil Ductility Transition (temperature). Often used to delineate the temperature regions of brittle and ductile fracture behavior; measured as specified in ASTM Standard E208-69.
Pagoda roof	Rain flow. A counting technique for grouping random loads according to their magnitude.
QC	Quality Control
RAD	Ratio Analysis Diagram. A graph on which fracture toughness is plotted versus yield strength in order to group materials according to a ratio of toughness to yield strength, which is an index of critical crack size or damage tolerance.
RT	Room Temperature
Safe life	A design approach in which a safe service life, in numbers of cycles of operation or time, is established, and the component is inspected or removed from service at some fraction of its predicted life.
SIP	Structural Integrity Program
SLC	Safety life-cycle. That period during which a system or component functions properly without endangering safety of service operation or degrading performance of the rail vehicle.
Structural integrity	The ability of a structure to perform its design function under dynamic and static loads and environment (including temperature) for its expected design life.
Toughness	A measure of ductility or energy absorbed during fracture. Fracture toughness, reduction of area, and elongation of a tensile coupon or Charpy impact energy are generally used.

UTS

Ultimate Tensile Strength

Ultrasonic
Inspection

A nondestructive means of detecting and locating internal
discontinuities.

w/o

Percent of Weight

PROPERTY OF FRA
RESEARCH & DEVELOPMENT
LIBRARY

Task 6 Railroad Structural Integrity Criteria
Analysis-Final Report, 1978, L. Raymond, J. Buch,
C. Zilliagus, The Aerospace Corporation, US DOT,
03-Rail Vehicles & Components